2015

Properties of Forced Convection experimental with Silicon Carbide based Nano-Fluids

Abhinay Soanker
Lehigh University

Properties of Forced Convection experimental with Silicon Carbide based Nano-Fluids

by

Abhinay Soanker

A Thesis

Presented to the Graduate and Research Committee

of Lehigh University

in Candidacy for the Degree of

Master of Science

in

Mechanical Engineering and Mechanics

Lehigh University

(August 2015)

This thesis is accepted and approved in partial fulfillment of the requirements for the Master of Science.

_____
Date

_____
Dr. Sudhakar Neti, Thesis Advisor

_____
Dr. Alparslan Oztekin, Co-Advisor

_____
D. Gary Harlow, Chairperson

Mechanical Engineering and Mechanics

ACKNOWLEDGMENTS

I would like to thank my thesis advisors, Professors Sudhakar Neti and Alparslan Oztekin. They gave me valuable technical information as well as a moral support all through my research work. I would like to extend my gratitude towards Dr. Satish Mohapatra, President and CEO, Dynalene .Inc, Allentown for allowing me to run my experiments at their facility and also for providing a constant technical input all through my research. I would take this opportunity to specially thank Dr. Dileep Singh, Scientist, Argonne National Laboratory for providing us with SiC nano-fluid and was very supportive by providing us all the necessary technical data throughout my work. In addition, I would sincerely thank K Hari Krishna, Kevin Coscia, Boji, Shreya, Becky, Lauren, George for providing me the technical support to conduct my experiments at Dynelene .Inc.

My heartfelt, thanks to my dear friends Rinosh P, Rajani K, Pawan A, Rahul R, and Midhun Joy for their moral support all through my graduate studies here at Lehigh University. In addition, I would like to thank my fellow graduate students Nipun Goel and Laura Solomon for their help. A special thanks to JoAnn Casiano for being very helpful at every stage of my graduate studies at Lehigh University.

My acknowledgement section would only be incomplete without thanking my parents and family. My parents were always there to support me during adversities. I could not thank them enough for the care and strength they provided me all through my life. This would not have been possible without the support of my brother Ashish Soanker and my Sister in law Bhavana Gangam. I would sincerely thank both of them

for keeping trust in me and support. I thank my Grandparents for their love and support. Last but not the least; I would like to give a special mention about my lovely pet Bruno, who just keeps inspiring me with its unconditional love.

Table of Contents

LIST OF TABLES

LIST OF FIGURES

ABSTRACT

With the advent of nanotechnology, many fields of Engineering and Science took a leap to the next level of advancements. The broad scope of nanotechnology initiated many studies of heat transfer and thermal engineering. Nano-fluids are one such technology and can be thought of as engineered colloidal fluids with nano-sized colloidal particles. There are different types of nano-fluids based on the colloidal particle and base fluids. Nano-fluids can primarily be categorized into metallic, ceramics, oxide, magnetic and carbon based. The present work is a part of investigation of the thermal and rheological properties of ceramic based nano-fluids. α-Silicon Carbide based nano-fluid with Ethylene Glycol and water mixture 50-50% volume concentration was used as the base fluid here. This work is divided into three parts; Theoretical modelling of effective thermal conductivity (ETC) of colloidal fluids, study of Thermal and Rheological properties of α-SiC nano-fluids, and determining the Heat Transfer properties of α-SiC nano-fluids.

In the first part of this work, a theoretical model for effective thermal conductivity (ETC) of static based colloidal fluids was formulated based on the particle size, shape (spherical), thermal conductivity of base fluid and that of the colloidal particle, along with the particle distribution pattern in the fluid. A MATLAB program is generated to calculate the details of this model. The model is specifically derived for least and maximum ETC enhancement possible and thereby the lower and upper bounds was determined. In addition, ETC is also calculated for uniform colloidal distribution pattern. Effect of volume concentration on ETC was studied. No

effect of particle size was observed for particle sizes below a certain value. Results of this model were compared with Wiener bounds and Hashin- Shtrikman bounds.

The second part of this work is a study of thermal and rheological properties of α-Silicon Carbide based nano-fluids. The nano-fluid properties were tested at three different volume concentrations; 0.55%, 1% and 1.6%. Thermal conductivity was measured for the three-volume concentration as function of temperature. Thermal conductivity enhancement increased with the temperature and may be attributed to increased Brownian motion of colloidal particles at higher temperatures. Measured thermal conductivity values are compared with results obtained by theoretical model derived in this work. Effect of temperature and volume concentration on viscosity was also measured and reported. Viscosity increase and related consequences are important issues for the use of nano-fluids.

Extensive measurements of heat transfer and pressure drop for forced convection in circular pipes with nano-fluids was also conducted. Parameters such as heat transfer coefficient, Nusselt number, pressure drop and a thermal hydraulic performance factor that takes into account the gains made by increase in thermal conductivity as well as penalties related to increase in pressure drop are evaluated for laminar and transition flow regimes. No significant improvement in heat transfer (Nusselt number) compared to its based fluid was observed. It is also observed that the values evaluated for the thermal-hydraulic performance factor (change in heat transfer/change in pressure drop) was under unity for many flow conditions indicating poor overall applicability of SiC based nano-fluids.

CHAPTER 1: INTRODUCTION TO NANO-FLUIDS

1.1 Introduction

Development of new and efficient materials plays a significant role which contributes to the advancement of technology. Major research is being carried out across the globe to develop such materials which has superior mechanical and thermal properties. Composite materials are one such material, which has very high strength to weight ratio. These materials have strength comparable to some of the hard metals while weighing less than them. Similarly, there is a huge interest amongst the scientific community for the development of high performing heat transfer fluid. In the quest to find an efficient heat transfer fluid; scientists have developed new fluids called Nano-Fluids. These can be classified as colloidal substances where the colloidal particle sizes are at Nano scale and hence called Nano-fluids.

1.2 Nano-Fluids

The word “colloid” was coined by the chemist Thomas Graham in mid-19th century to describe the suspended particles in the liquids. It came to the interest of scientific community only in early-20th century when they found applications in the many industrial processes. One of the important parameters for an effective colloidal fluid is the stability of the colloidal particles in the fluid. Since, almost always the density of colloidal particle is greater than the liquid, the suspended particles tend to settle down with the time. Addressing this issue of settling is a major challenge to the scientific community. After more than ten decades after this field came into existence, researchers have come up with the new approach of preparing the colloidal fluids which is by replacing micron level colloidal particles with nano-level particles. This

addition of Nano-particles to the fluid was termed as Nano-fluids and Choi (1995) from Argonne national laboratory was the first to introduce this term to scientific community. Nano particles as said are at nanoscale which are close to the size of atomic level and at this level the viscous forces and Brownian motion of the particles are very prominent which helps in counteracting the gravitational effects. Hence, nano-particles have better stability than the particles at micron level. Even though nano-fluids have better stability than larger colloidal fluids, the stability level is still not sufficient to be used for commercial purposes. This is because, nano-fluids have a great attraction forces which makes them susceptible to agglomeration and this results in larger particles. To address this issue various techniques have been introduced which inhibits the agglomerations and details are discussed in the later chapters.

1.3 Nano-Fluids in Heat Exchangers

Though the Nano-fluids find applications in varied fields, primary interest is to use them for heat transfer applications. In many cases such as for cooling in thermal power plants, automotive radiators, electronic equipment etc., liquids are used. Fluids in these applications are typically water or ethylene glycol based, which have poor thermal conductivity. By using Nano fluids, with suspended particles whose thermal conductivity is high, it is expected that resultant colloidal fluid would have an enhanced thermal conductivity than its base fluid.

For example, a study reveals that a 14% enhancement of thermal conductivity was observed for graphene based nano-fluids with a volume concentration as low as

0.056% at 25 ^{o}C and of 86% enhancement at 50 ^{o}C [1].Thermal conductivities values for the investigation are shown in Figure 1

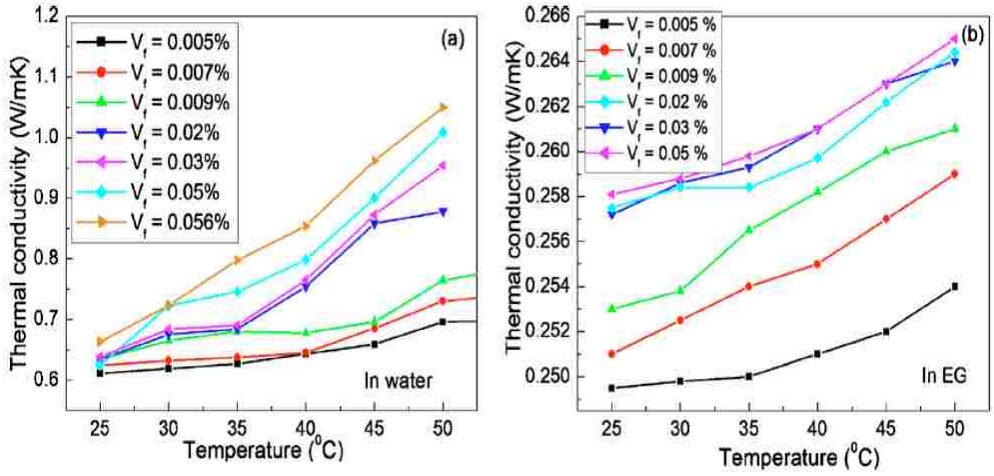

Figure 1: graphs shows the enhanced thermal conductivity values that are achieved for graphene based nanofluids with ethylene glycol(left) and water (right) as base fluids at different volume concentrations [1**]**

1.4 Thermal Conductivity of Nano Fluids

As discussed earlier, enhancement of thermal conductivity is observed in nano-fluids through many experimental works that was carried out in the past. From these published papers, an inconsistency in effective thermal conductivity values for same nano-fluid and at same concentration can very well be observed. This is because, effective thermal conductivity is affected by several factors including the surface chemistry of the nano particles, stabilizers used, shapes of nano particles, agglomerations size, stability etc. [2, 3, 4]. Many models have been surfaced in the past few decades that can predict approximate thermal conductivity enhancement of

these nano-fluids. Some of them are based on the static models, while some are based on dynamic modelling.

1.5 Commercialization of Nano-Fluids

Though the Current research shows a promising future for nano-fluids used in heat transfer applications, there are some hurdles that need to be addressed before they can be commercialized. For instance, nano-fluids tend to show higher viscosity compared to the base fluids which in turn increases the pumping power required, thereby decreasing the effectiveness of these colloidal fluids. Settling is another important issue which makes these fluids unsuitable for commercialization. Settling of particles results in change in thermal properties with time and result in non-uniform properties. This may also result in clogging of the pipe lines when used in heat exchangers. In some cases cost of these fluids are too high to be useful for commercial purposes.

1.6 Scope of Work

The current work is primarily focused on Silicon carbide (SiC) based nano-fluids for heat transfer applications. This research is divided into three parts, first being the theoretical modelling of the Thermal conductivity enhancement of nano-fluids. Later work is focused on experimentally measuring the thermo-physical properties of SiC nano-fluid that is obtained from Argonne National Laboratory. In subsequent chapters forced convention properties and pressure drop measurements are discussed.

Theoretical modelling and prediction of effective thermal conductivity

Extensive work has been carried out to derive a model which can predict the possible upper and lower bounds of effective thermal conductivity of nano-fluids. The prediction is based on the thermal properties of particle and base fluid, and the volume concentration. Additionally, modelling is done for the uniform colloidal distribution pattern. In this work, a static model is assumed i.e. there is no Brownian motion component that is added. This model can predict the thermal conductivity pattern based the particle size and volume concentration for a given nano-fluid. Further, obtained upper and lower bounds is compared to some of the existing models like wiener bound and H-S bounds.

Experimental determination of Thermo-physical properties of SiC nanofluids

In this section, experiments have been conducted to find the thermal conductivity and rheological properties of SiC nano-fluid and compare them to that of base fluid. Base fluid used here is Ethylene glycol and Water with 50-50% volume concentration. Experiments measurements have been made for base fluid, 0.55%, 1% and 1.6% volume concentration of SiC nano particles.

Forced convection properties and pressure drop measurements

A heat transfer test section built at the Dynalene, Inc., was used to conduct the forced convection measurements. Experiments were conducted by supplying constant heat flux to a straight horizontal pipe with testing fluid flowing inside the pipe. With temperature and flow data, parameters like Nusselt number and heat transfer

coefficient are determined at various Reynolds number. Convection data presented here pertains only for the laminar and transient regions.

Comparison of these values for base fluid, with 0.55%, 1%, and 1.6% volume fraction of SiC particles are presented. Pressure drop measurements are also made using a differential pressure transducer across the test section and based on this data, the effectiveness of SiC nano-fluids are calculated.

CHAPTER 2: REVIEW ON NANO-FLUIDS

2.1. Introduction

Though the research on nano-fluids only started in late 20th century, there was a rapid development in this field in the past decade with exponential increase in number of research published every year. Contribution of nano-fluids as heat transfer fluid is estimated to be over 2 billion dollars per year [26]. This chapter gives a brief review of pervious work on nano-fluids that is available in literature.

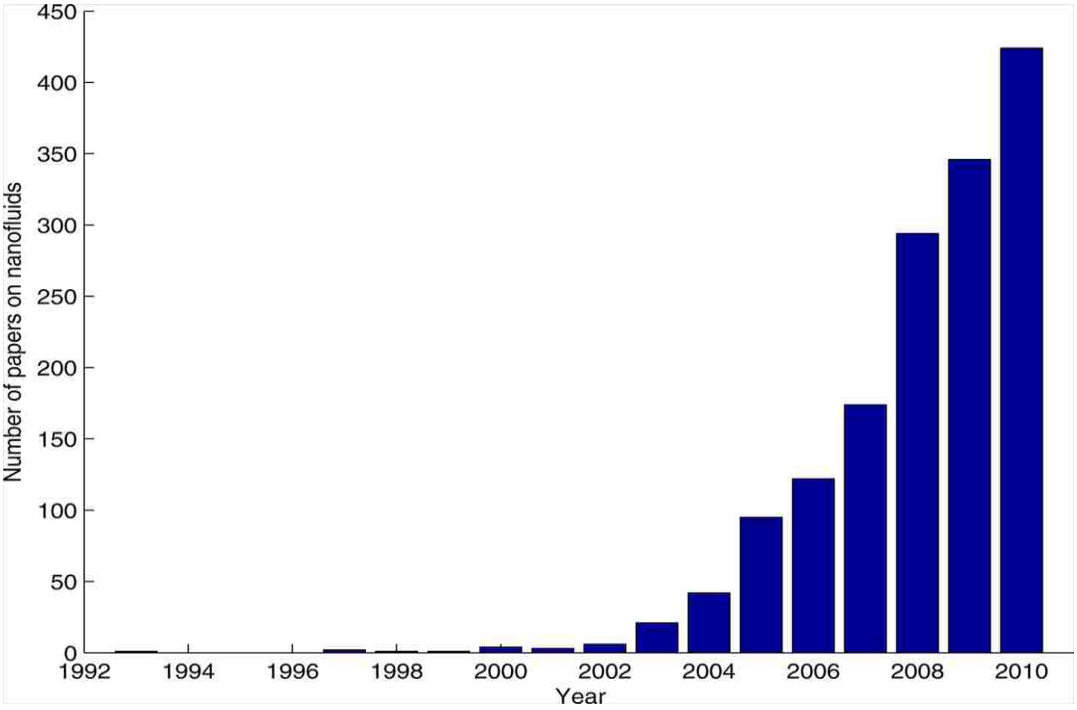

Figure 2: Trends in nano-fluid research papers for over a decade [26]

2.2. Stability of Nano-fluids

One of the primary requirements to make an effective nano-fluid is the stability. While density is attributed for the sedimentation, at nano level, it's the agglomeration that amplifies the density effects [27]. Particle size, zeta potential, pH and the physical observation are the methods that was carried by Sergio [27] to evaluate the stability of

water based nano fluids. Further, dispersant such as sodium n-dodecyl sulphate (SDS) and polyethylene glycol (PEG) were added to single wall carbon nano-horn and TiO2 nano-fluids respectively to increase the stability [27]. Sergio [27] also demonstrated the influence of preparation techniques on the stability of the nano-fluids. Mingyuan [25] observed an increase in Zeta potential of SiC nano-fluid with increase in pH and tend to decrease after pH 10. It also studied the effect of pH and Tetramethyl ammonium hydroxide as dispersant on Zeta potential and found that 0.6% Wt dispersant enhanced Zeta potential than without dispersant [25].

2.3. Experimental Thermal Conductivity of nano-fluids

Effective thermal conductivity measurement of nano-fluids is an important parameter to be determined. There is a large uncertainty in thermal conductivity values amongst published papers. Various measurement techniques were adopted to measure the effective thermal conductivity of nano-fluids, transient hot wire method, steady state parallel plate technique, Temperature and oscillation technique were used by some researchers as consolidated in a review article by Xiang-Qi [2]. Vasudeva Rao [28] studied the Thermal conductivity of TiO_2 based nano-fluids with change in volume concentrations (0.2 -1%), temperatures (30 ^{0}C to 70^{0}C) and base fluids. In this paper, Enhancement of Thermal conductivity for Water based TiO_2 nano-fluid displayed an increase from 0.649% to 5% when Volume concentration changed from 0.2% to 1% at 30^{0}C and. Enhancement recorded were higher at 10.64 to 14.2 % when vol. conc. changed from 0.2 to 1% volume concentration and 50/50% volume conc. Ethylene glycol and water was used as base fluid at 30^{0}C [28].

Timofeeva [29] studied effect of shape on the thermal conductivity of nano-fluid. They considered Alumina nano-particle with platelets, blades, cylinders, and brick and found that the thermal conductivity start to decrease below sphericity of 0.6 [29]. Results obtained in this paper as shown in the Figure 3.

Timofeeva [18] measured thermal conductivity of α-SiC based nano-fluids for different particle size and concluded that the effective thermal conductivity increases with the increase in the size of the particle [18]. Figure 4 shows the results presented in paper.

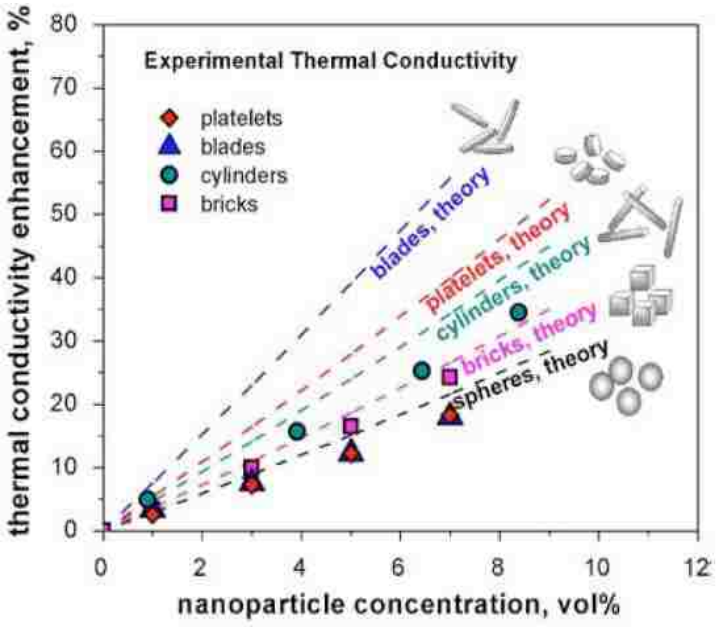

Figure 3: Effect of particle size on thermal conductivity of Alumina nano-fluid as reported by Elena Timofeeva [29] compared with Hamilton Crosser model (dashed lines in the graph)

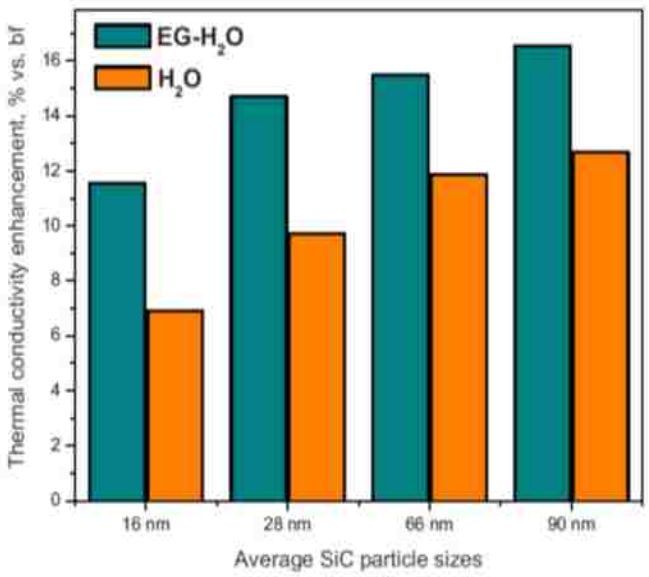

Figure 4: Effect of particle size on Thermal conductivity was presented by Timofeeva [18] for α-SiC nano-fluid.

Michael P. Beck [30] studied the effect of particle size on alumina nano particles. They considered particles size ranging from 8 to 282 nm diameter and concluded that the thermal conductivity enhancement decreases with decrease in particle size when the size falls below 50nm [30].

While most research support increase in particle size increase the enhancement, some research findings support exact the opposite trend. M. Chopkar [31] measure the thermal conductivity of Al_2Cu nanfluid with different particle size and found that thermal conductivity of nano-fluids decreased with increase in particle size [31].

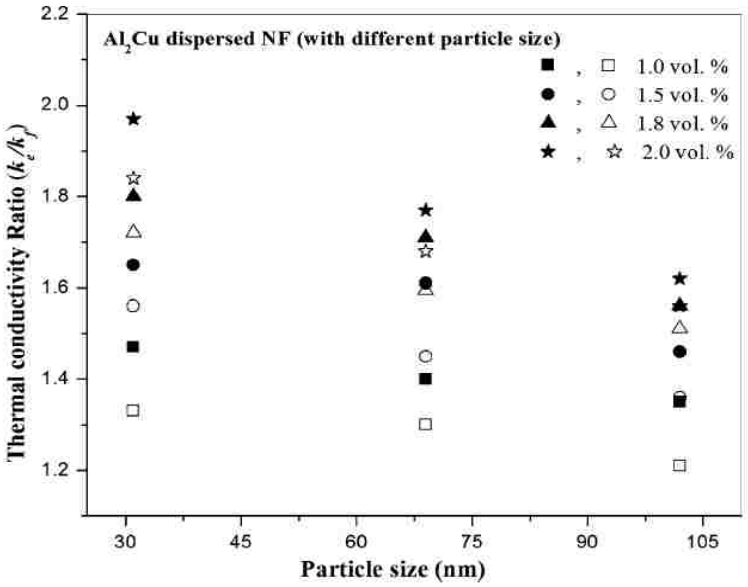

Figure 5: Effect of particle size on Al_2Cu based nano-fluid presented by M. Chopkar [31]

2.4. Theoretical models on Effective Thermal Conductivity of Nano fluids

Based on the approach, various models were proposed to calculate the effective thermal conductivity (ETC) of colloidal fluids. They are categorized into static models and dynamic models.

In static models, thermal conductivity of the colloidal fluid is modelled considering no motion of particulate suspensions in the base fluid. This makes the system similar to solid composite materials. On contrary, dynamic models calculate the thermal conductivity which also includes the random motion of colloidal particles which are caused by Brownian effect [3]. Some of these models predict the upper and lower bounds of ETC enhancement and most other predicts it for uniformly distributed colloidal fluids.

Static Models

The Effective Thermal conductivity model developed in this work is based on the static model and hence basic static models that are extensively used in the literature are discussed in the following section.

Wiener Bounds (Parallel and Series Model)

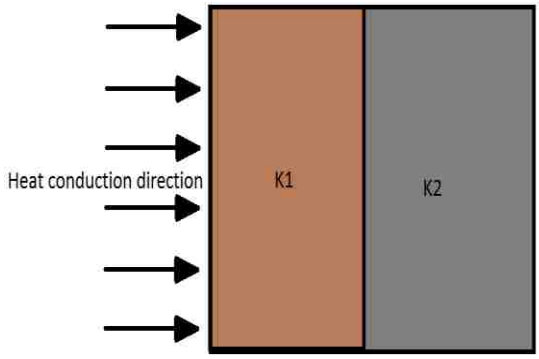

Figure 6: Series Bound or Wiener Lower bound Model

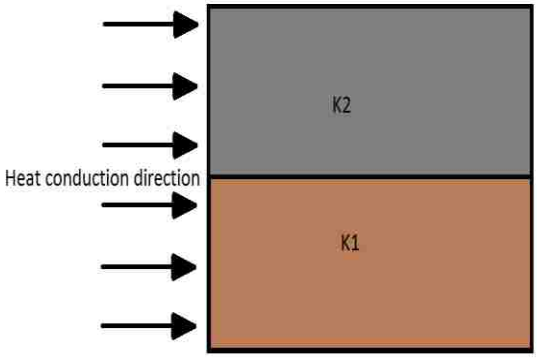

Figure 7: Parallel bound or Wiener Upper bound Model

Wiener bounds a calculated based on the thermal resistance method and can be applied for two or more composite materials system. This model is the basic model which is used to predict the upper and lower bounds of possible thermal enhancement at a particular volume concentration. In static model, this bound is considered to be the least restrictive bound [5]. Upper and lower bounds for Wiener are also called as parallel and series bound respectively.

Wiener model, as shown in Figure 6 & Figure 7 assumes that composite materials are slab or stripe like arrangement. Hence, the application of this model for composites with different shapes inclusions may not give the accurate values. The

Wiener upper and lower limits for two phase material are dependent on the Thermal conductivity of base fluid, thermal conductivity of particulate inclusions and the volume concentrations.

Wiener limits for effective thermal conductivity are calculated as follows [6] using Equation **(1)** & **(2)**

Lower Wiener bound

$$\mathbf{K_{eff}^{Series}} = \frac{(\mathbf{1}-\emptyset)}{\mathbf{K_f}} + \frac{\emptyset}{\mathbf{K_p}} \qquad (1)$$

Upper Wiener bound

$$\frac{\mathbf{1}}{\mathbf{K_{eff}^{Parallel}}} = (\mathbf{1}-\emptyset) \times \mathbf{K_f} + \emptyset \times \mathbf{K_p} \qquad (2)$$

H-S Bounds

Hashin and Shtrikman bounds are derived based on the effective medium theory [8]. This model is considered to have bounds narrow than the Wiener bounds [7] as shown in Figure 8. H-S bounds can be calculated using the Equation **(3)** given below when thermal conductivity of the two materials and volume concentration are known [8]

$$\mathbf{K_f} \times \left(\mathbf{1} + \frac{\mathbf{3}\times\boldsymbol{\varphi}\times(\mathbf{K_p}-\mathbf{K_f})}{\mathbf{3}\times\mathbf{K_f}+(\mathbf{1}-\boldsymbol{\varphi})\times(\mathbf{K_p}-\mathbf{K_f})}\right) \leq \mathbf{K_{eff}} \leq \left(\mathbf{1} - \frac{\mathbf{3}\times(\mathbf{1}-\boldsymbol{\varphi})\times(\mathbf{K_p}-\mathbf{K_f})}{\mathbf{3}\times\mathbf{K_p}-(\boldsymbol{\varphi})\times(\mathbf{K_p}-\mathbf{K_f})}\right) \times \mathbf{K_p} \quad (3)$$

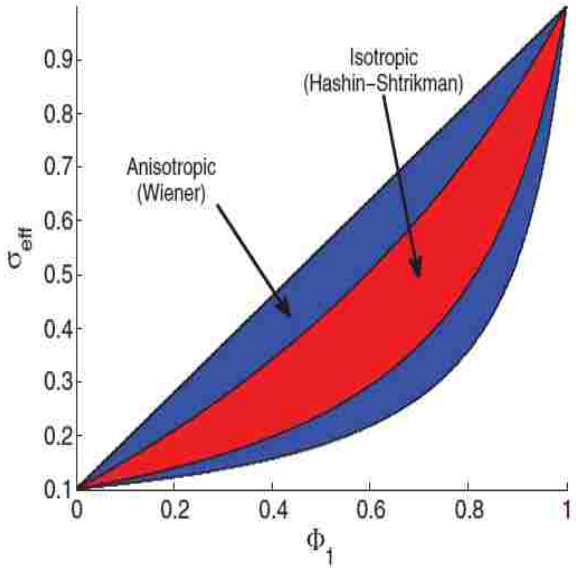

Figure 8. Comparison of Wiener and H-S bounds for different volume concentrations[7]

Maxwell

Maxwell model is a prominent static model which uses effective medium theory approach to calculate the effective thermal conductivity. Here in this model, a uniform distribution of non-interacting colloidal particles is considered. Since this model is valid only for non-interacting particles, it is accurate at low volume concentrations. Maxwell effective thermal conductivity equation is same as the H-S lower bound.

2.5. Viscosity of Nano-fluids

Viscosity of nano-fluids has direct effect on the pressure drop and pumping power requirement [32] when used for forced convection applications. Many of the previous research works studied on the effect of size and shape of particle,

temperature, additives and pH on the viscosity of nano-fluid [32]. Like Thermal conductivity, findings on effect of particle size on viscosity of nano-fluids contradict each other. Yulong [33] worked on the water based TiO_2 nano-fluids and found that viscosity of nano-fluids increased with increase of particular size [33].

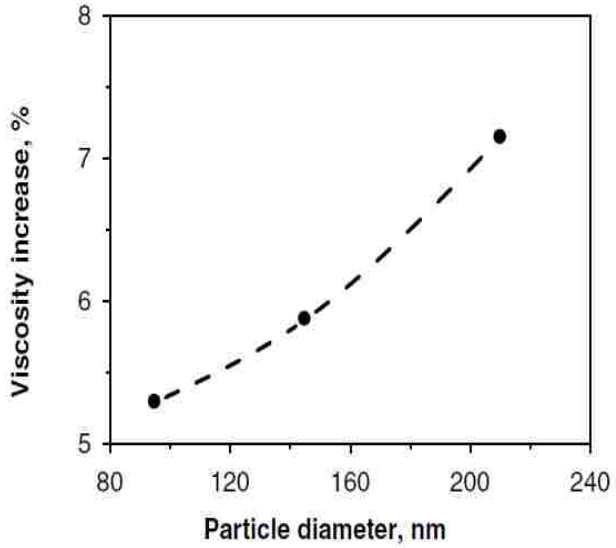

Figure 9: Results presented by Yulong [33] on aqueous TiO_2 nano-fluid

Timofeeva [18] studied viscosity of water based and aqueous Ethylene glycol based SiC nano-fluids and concluded that viscosity of SiC nano-fluids decreases with the increase of particle size [18].

Effect of temperature on water based SiO_2 nano-fluid was measured by Tavman [34] and found that the viscosity of nano-fluid decreases with increase of temperature [34] as shown in the Figure 10.

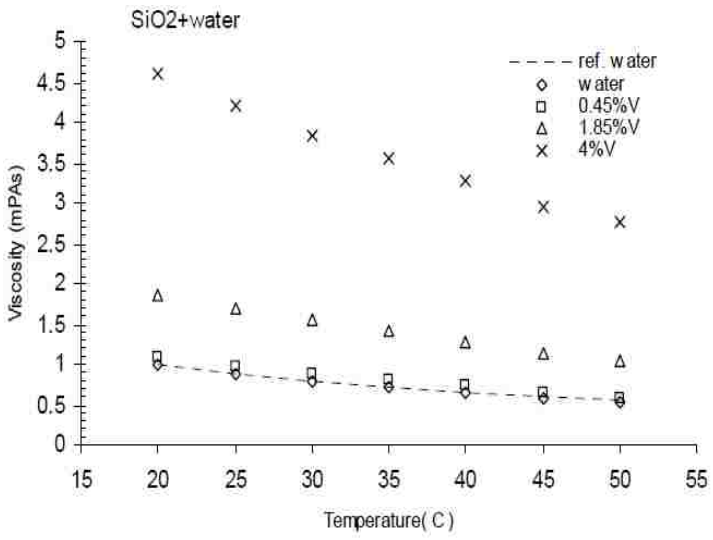

Figure 10: Effect of temperature on SiO_2 nano-fluids by Tavman [34]

2.6. Forced convection

There are many research publications on Forced convection properties of nano-fluids. Some of the important parameters are Nusselt number, Heat transfer coefficient, pressure drop, friction factor and Thermal-Hydraulic Performance factor or Merit factor.

Timofeeva [18] studied change of Heat transfer coefficient, Nusselt number of SiC nano-fluids with velocity of flow and found that both heat transfer coefficient and Nusselt number increased linearly [18]. The same work also outlines the effect of particle size on above parameters as shown in Figure 11.

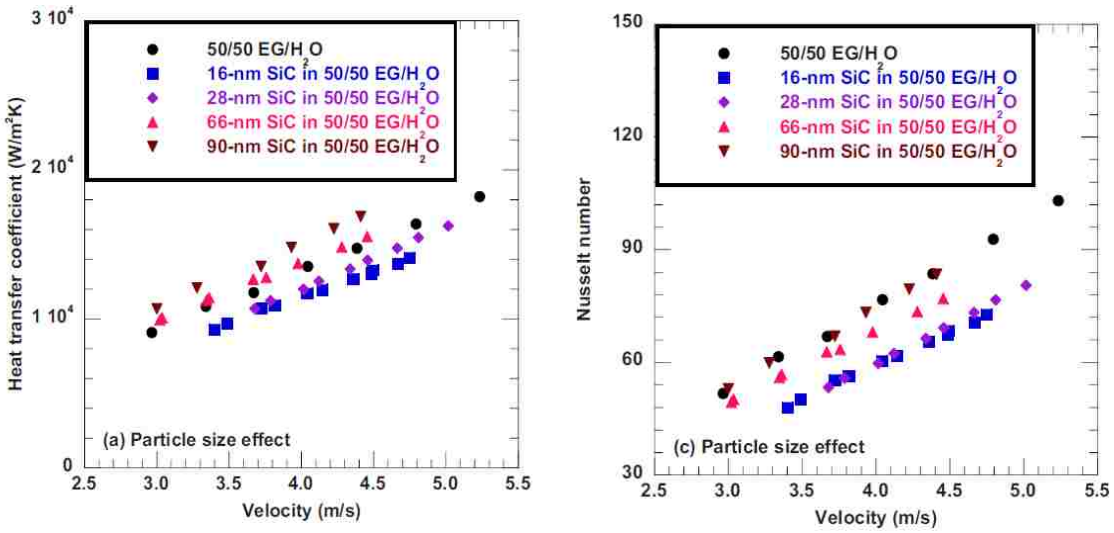

Figure 11: Timofeeva [18] SiC nanofluid data on change of Heat transfer coefficient and Nusselt number with velocity of flow and for different particle size [18]

Wenhua [17] used merit factor which is defined as ratio of Heat transfer coefficient enhancement to Increase in pumping power [17]. Parameter calculated for water based SiC nano-fluids is shown in the Figure 12

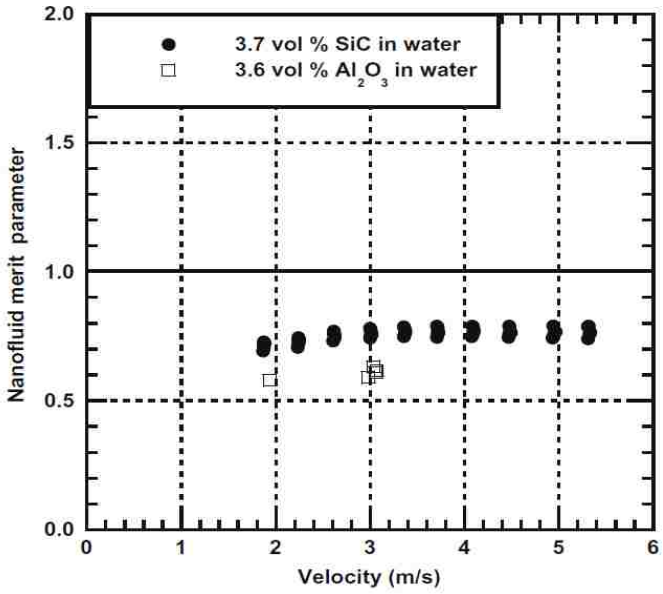

Figure 12: Wenhua [17] show merit parameter for SiC and Al_2O_3 nano-fluids as a function of velocity

CHAPTER 3 THEORETICAL MODEL FOR EFFECTIVE THERMAL CONDUCTIVITY OF COLLOIDAL-FLUIDS

3.1 Introduction

Effective Thermal conductivity (ETC) of colloidal particles plays an important role in determining the effectiveness of colloidal fluid systems, especially when these fluids are used for heat transfer applications. Apart from the experimental method, ETC can be calculated based on theoretical models which are discussed in Section 2.4.

3.2 Current Theoretical Model Description

As discussed earlier, one of the primary properties of nano-fluid is that majority of these fluids display higher effective thermal conductivity (ETC) than its base fluid. Hence, measuring the ETC is very crucial to determine the effectiveness of the nano-fluids for heat transfer applications. Measuring the thermal conductivity of fluids is very challenging as the measured values often carry an error due to convection of fluid. Convection may occur due to temperature gradients within the testing fluid and disturbances in the environment. Even a minor disturbance in the environment may distort the results.

To predict enhancements of colloidal fluids, we have different theoretical and empirical relations as discussed in the Section 2.4. In this work, a static theoretical model has been developed based on the thermal conductivity of base fluid and particle, particle size, shapes, colloidal distribution pattern and volume concentrations. ETC is derived based on thermal resistance of the system. This model is solved by generating a Matlab program and is based on certain type of colloidal distribution pattern and shape of particle as described in the following Sections 3.3. & 3.4.

Initially, we are considering a distribution pattern which gives the one of the least enhancements of thermal conductivity. This was further developed to predict the maximum thermal conductivity enhancement possible. Effective thermal conductivity for a uniformly distributed pattern is also modelled. Estimating the maximum and minimum enhancement possible for a given colloidal fluid may provide some guidelines while experimentally measuring the thermal conductivities.

3.3. Shape of the Colloidal Particle Considered

As we know that the shape of the particle plays a crucial role in determining the effective thermal conductivity of these colloidal fluids, it is important to include the shape factor while formulating theoretical model. When dealing with the colloidal fluids, spherical particles are frequently used to disperse in the fluid medium. Hence, a model is specifically developed by considering the uniformly sized spherical shaped particle inclusions.

3.4. Dispersion Pattern Considered for Current Model

From the previous literature, it is evident that the thermal conductivity of colloidal fluids is dependent on colloid structuring [20&21] and packing in the matrix [20 & 22]. From the wiener model explained in the Section 2.4, we can see that arrangement pattern of the material with respective to heat conduction direction affected the ETC of the system. Wiener bounds are specifically modelled for slab or stripes like arrangements shown in Figure 6 & Figure 7. A similar arrangement is made for spherical colloidal particles.

Lower Bound Arrangement (Series arrangement)

Model considered here is a cuboid system which is assigned the base fluid properties and colloidal particle properties are assigned to spherical shaped inclusions. Heat is conducted only in one direction i.e. direction perpendicular to y-z plane as shown in Figure 13 the Based on the diameter of the colloidal particle, volume concentrations and volume of the cuboid system considered we calculate the number of particles. Once we know the number of particles, we need to arrange these particles into the cuboid system in the plane (y-z) perpendicular to the heat conduction as show in the Figure 13.

Filling of particles in each plane should be done in an order. For example, we should start filling second plane only after first plane reaches the maximum packing density (discussed in the following section). This process is continued till all the spheres are arranged into the cuboid system.

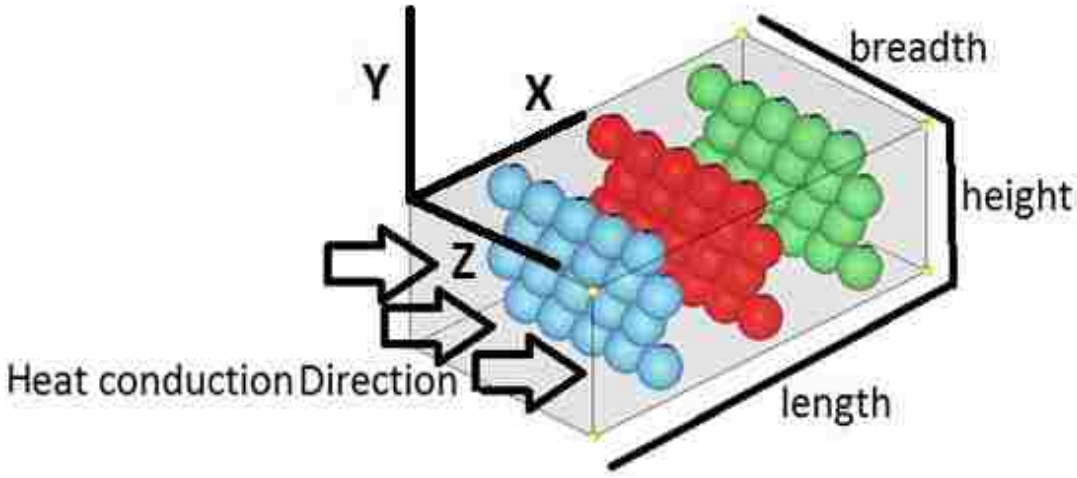

Figure 13: Series arrangement within a cuboid system

Maximum packing density calculations

Each plane should be filled with the maximum possible spherical particles to get least ETC value as discussed. Considering two types of packing, square lattice arrangement and hexagonal lattice arrangement, Gauss proved that the hexagonal lattice shown in Figure 14: Hexagonal Arrangement is the densest for any plane lattice packing [9], and it was further verified by Fejes Tóth. The packing density that can be achieved by hexagonal lattice is shown in Equation **(4**)

$$\eta_h = \frac{\pi \times \sqrt{3}}{6} = 0.9068996821 \qquad (4)$$

This implies that maximum of 90.68 percent of area can be utilized in a plane by circular shaped objects. By considering the hexagonal packing in the plane, we get the approximate highest thermal resistance possible and the least thermal conductivity enhancement.

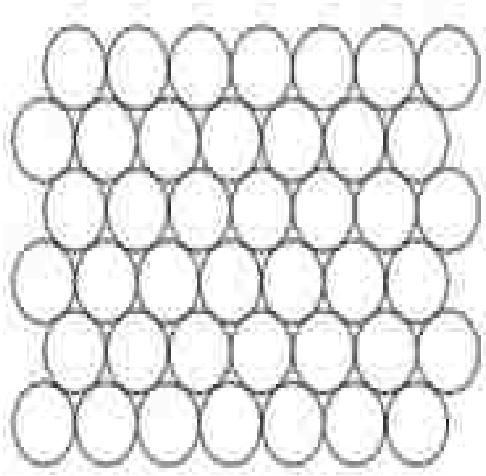

Figure 14: Hexagonal Arrangement[42]

Since, the highest packing density cannot be achieved all conditions, number of spheres that can be arranged in each plane along breadth b and height h in hexagonal lattice arrangement is calculated based on the formula given by Equation (5)& (6)

Number of particles that can be arranged along the breadth (refer Figure 13 & 15) in each plane y-z considered is $\left(\frac{b-R}{2\times R}\right)$ (5)

where b= breadth of cuboid system considered; R= Radius of the spherical particle

Here AC = $\sqrt{(AB^2-BC^2)}$ (from Figure 15: Hexa packing Calculation)

AC= $\sqrt{3}$ R (R = radius of sphere)

Number of such rows that can be fixed along the height (refer Figure 13& 15) in each plane considered $\left(\frac{h}{1.732\times R}\right) - \left(\frac{0.268}{1.732}\right)$ (6)

Where, h= height of cuboid system considered; R= Radius of the sphere particle

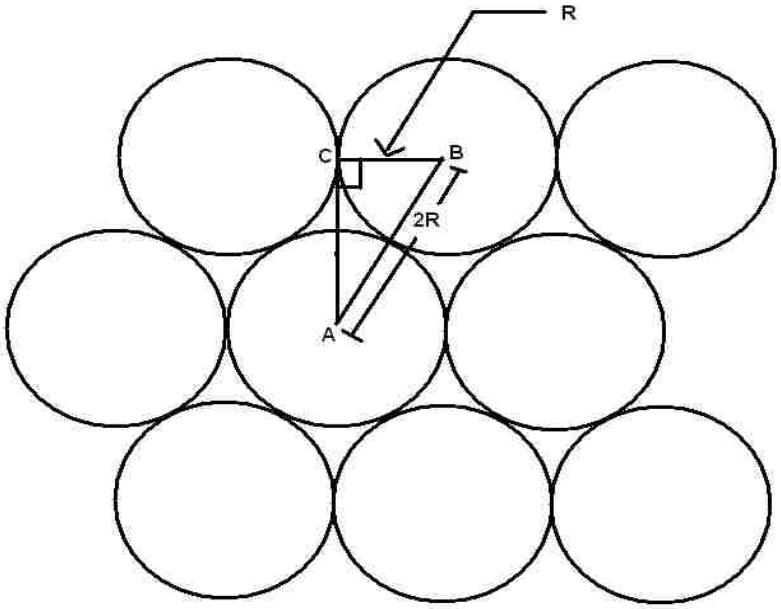

Figure 15: Hexa packing Calculation

Upper Bound Arrangement (Parallel arrangement)

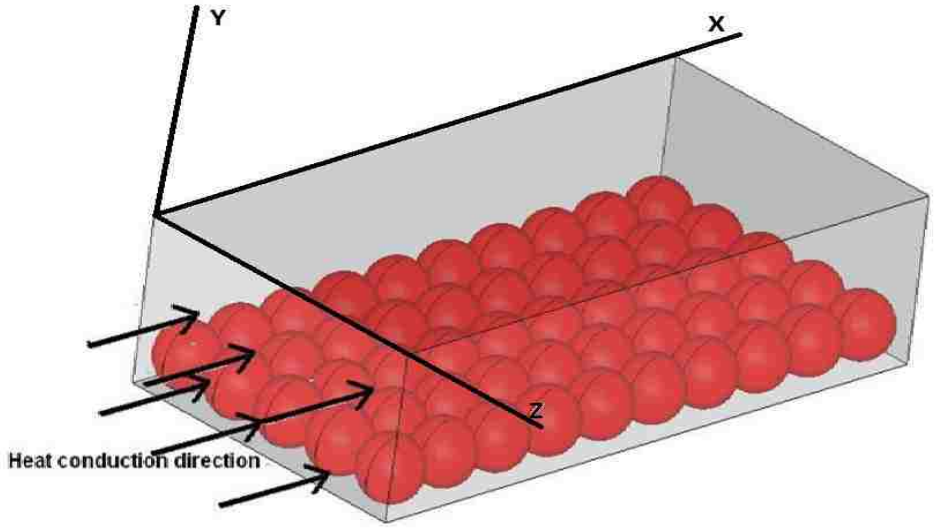

Figure 16: Parallel arrangement within the cuboid

Here we have a similar cuboid system with spherical particles, but the spherical particles are filled in plane parallel to the direction of heat conduction (x-z plane) as shown in the Figure 16. Unlike in series arrangement, here square packing as shown in Figure 17 is used to get the maximum thermal conductivity enhancement.

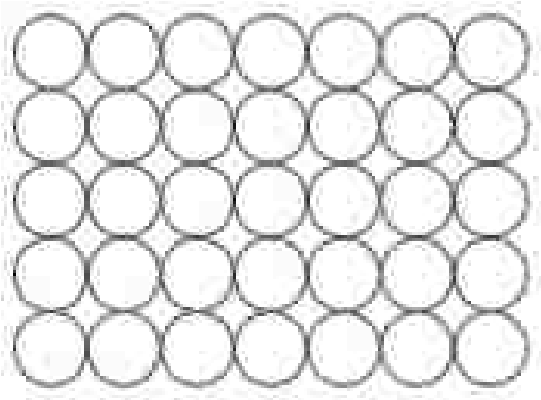

Figure 17: square packing[42]

3.5. Effective Thermal Resistance (ETR) of the System

To calculate the ETC, we need to evaluate the effective thermal resistance (ETR) of the system. This can be done by finding the thermal resistance of spherical particle. Further, using this expression we can calculate the ETR of the entire system. There are various ways to calculate the thermal resistance of the system one of which is discussed in the following section.

Theoretical Calculation for Thermal Resistance of Sphere shaped Particle

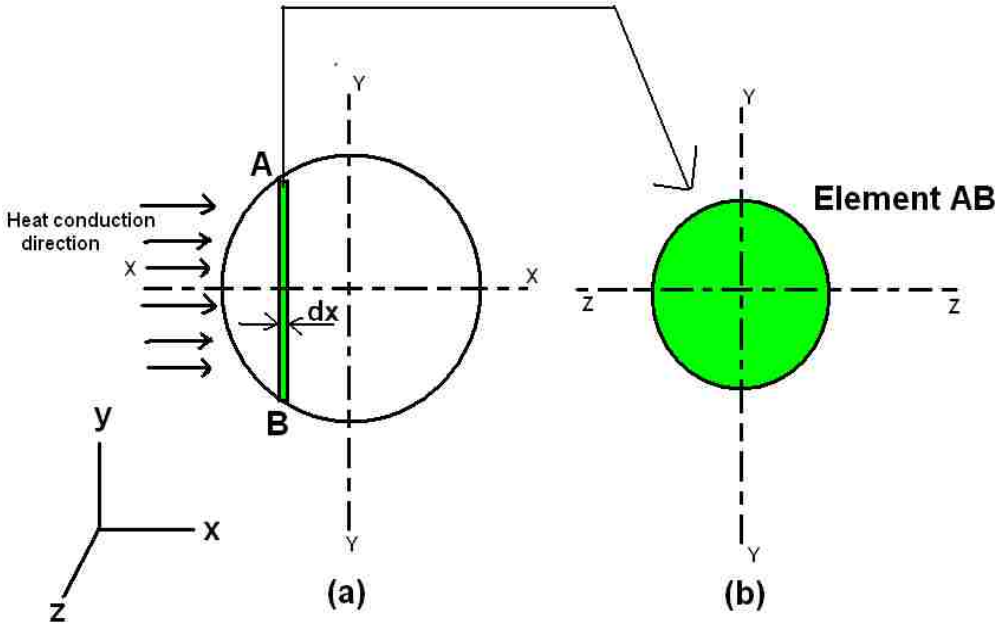

Figure 18: Geometry of the Spherical particle

Consider a sphere of radius ‘R’, origin at the center of the sphere and heat is conducted only in x direction as shown in the left side of Figure 18

To solve this ETC and ETR, we first need to calculate the thermal resistance of element AB shown in the left side of Figure 18 and integrating the result will give the thermal resistance of entire sphere.

Considering element of thickness dx as shown in the left side of Figure 18

Radius of the element AB = y

'y' changes as the function of 'x' (where 'x' varies from –R to R)

Where $\mathbf{x^2 + y^2 = R^2}$;

$$\mathbf{y^2 = R^2 - x^2} \text{ (From Figure 18)} \quad (7)$$

Thermal resistance of element 'AB' is

$$\text{Thermal Resistance} = \frac{\boldsymbol{dx}}{(\boldsymbol{K} * \boldsymbol{A})} \quad (8)$$

A= surface area perpendicular to the direction of heat flux

K= Thermal conductivity

Area of element 'AB' normal to the heat conduction direction is

$$A = \pi y^2 = R^2 - x^2 \text{ (from Equation (7))} \quad (9)$$

Substituting A from equation (9) in equation (8)

$$\text{Elemental Thermal Resistance} = \frac{dx}{K * \pi * (R^2 - x^2)} \quad (10)$$

$$\text{Total thermal resistance} = \int_{-R}^{R} \frac{dx}{K * \pi * (R^2 - x^2)} \quad (11)$$

By solving above equation we get

$$\text{Thermal resistance of sphere} = \frac{\left(\ln\left|\frac{x+R}{x-R}\right|\right)}{(2*K*\pi*R)} \text{ with limits -R to R} \qquad (12)$$

Note: substitution of limit (-R to R) will make the Thermal resistance of sphere infinity to avoid this, limits should be adjusted with a small value δR such that δR<<1 and δR>0

Therefore adjusted limits should be {-R+δR to R-δR}

$$\text{Effective area of each sphere is} \quad \frac{4\times\pi\times R^2}{\ln\frac{x+R}{x-R}} \qquad (13)$$

Once we calculate the ETR of the sphere and effective area of sphere which is perpendicular to the direction of heat conduction, it can be solved as simple one directional heat transfer problem applied for composite materials. A MATLAB code has been generated to calculate the ETC.

3.6. Influence of system dimensions on Effective thermal conductivity

Though it is expected that the Effective thermal conductivity of the colloidal fluid is independent of dimensions of the system, it is observed that ETC value is influenced when the radius of the colloidal particle is comparable to the dimension of the cuboid system. This means changing the dimensions of the cuboid has an effect on the ETC value.

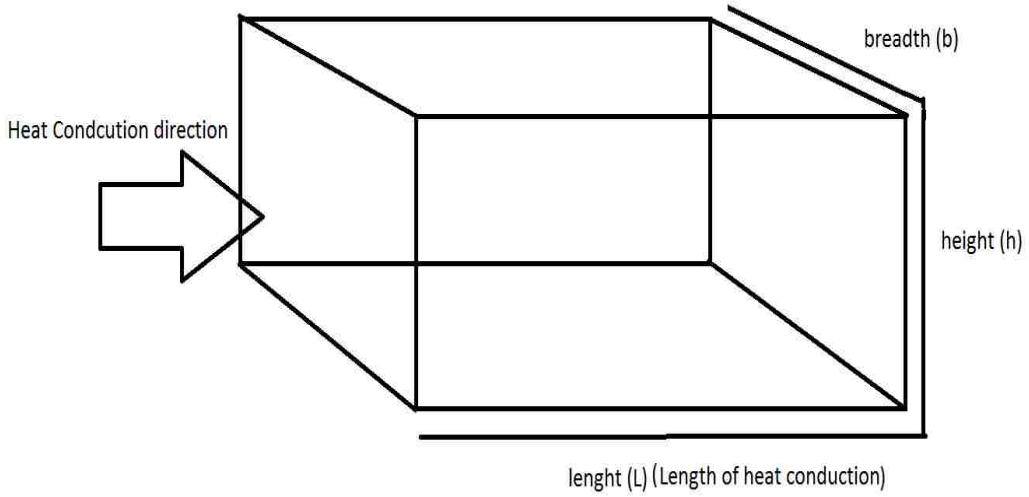

Figure 19: Cuboid system

A new parameter, Dimensional ratio is defined in this work to account for this effect. It is defined as ratio of radius of the particle to the length of heat conduction shown in Figure 19.

$$\textbf{Dimensional ratio } (\dot{q}) = \frac{\textbf{Radius of the colliodal particle}}{\textbf{Lenght of heat conduction (L)}} \qquad (14)$$

For same volume concentration, Thermal conductivity ratio (K_p/K_f), ETC value does not change as long as the Dimensional Ratio ($\dot{q}$) is constant. Nevertheless, when the Dimensional ratio falls below a certain value all the different cases converge to a value as shown in Figure 20 & Figure 21**.** Convergence basically was dependent more on the number of particles present in the system than the particle size. It is observed that all the cases to converged to a single ETC when considering a million or more particles in the system.

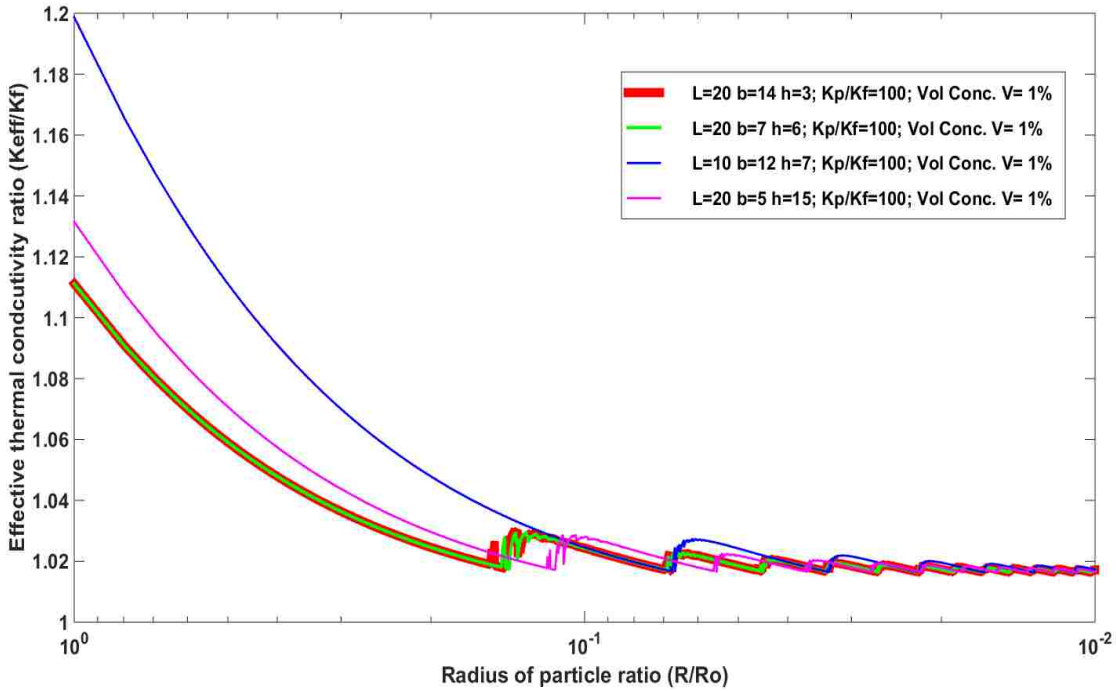

Figure 20:Variation of ETC with radius of particle ratio for lower bound

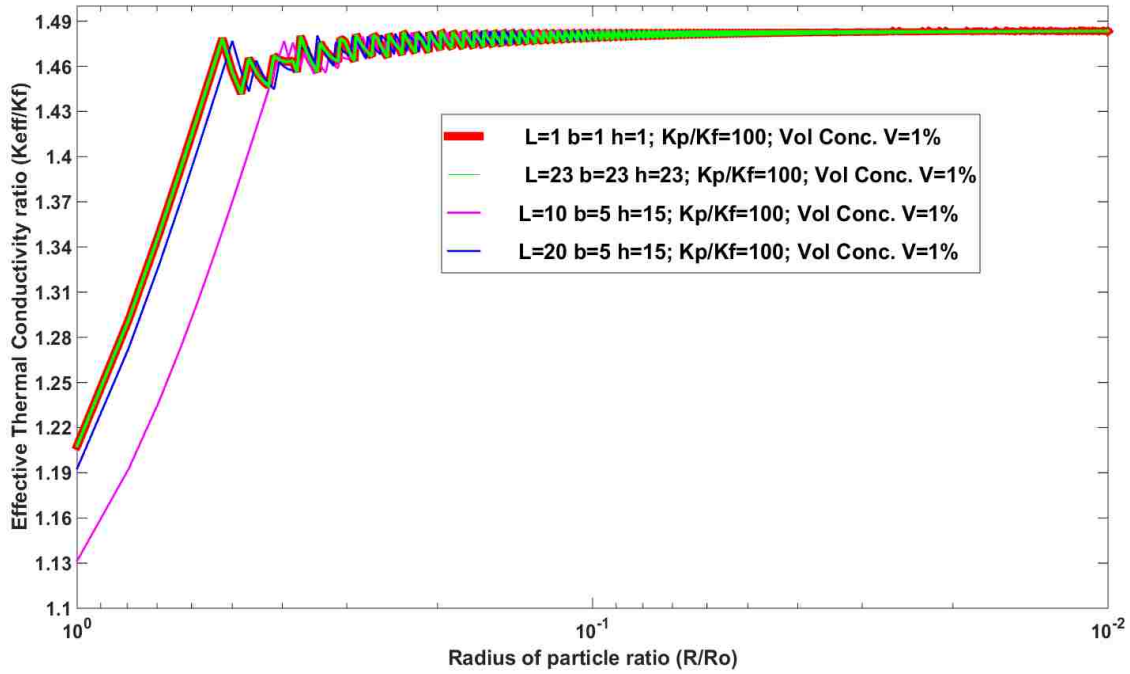

Figure 21: Variation of ETC with radius of particle ratio for upper bound

Number of particle at (R/Ro) $=10^{-2}$ is one million

Ro=Radius of particle when whole volume concentration is attributed by single particle

3.7. Effective Thermal conductivity (ETC) Value

Change in ETC value was observed as the size of the colloidal particle is decreasing. Change is noticed only initially when the size of the particle is large and comparable to the dimension of the system. ETC becomes constant when the radius of particle falls below a certain value.

Though there is a change in the ETC for upper bound and lower bound models as shown in the with the particle size, it is primarily due to physical dimensions of the system and change is not evident at very low particle radius. Though it is very difficult to locate the exact radius at which the system ETC converges to the final ETC value, it can be defined in terms of number of particles. From observations, the ETC values turns fairly constant beyond one million particle system.

We can also observe a large fluctuations in the ETC before these fluctuations are dampened at lower particle size. This is primarily attributed by change in maximum packing density efficiency, which is affected by the plane area (y-z plane refer Figure 13 & x-y plane refer Figure 16) and particle size. This in turn affects the particle arrangement in plane in consideration. There by causing the fluctuations and this influence is minimized as the particle size drops.

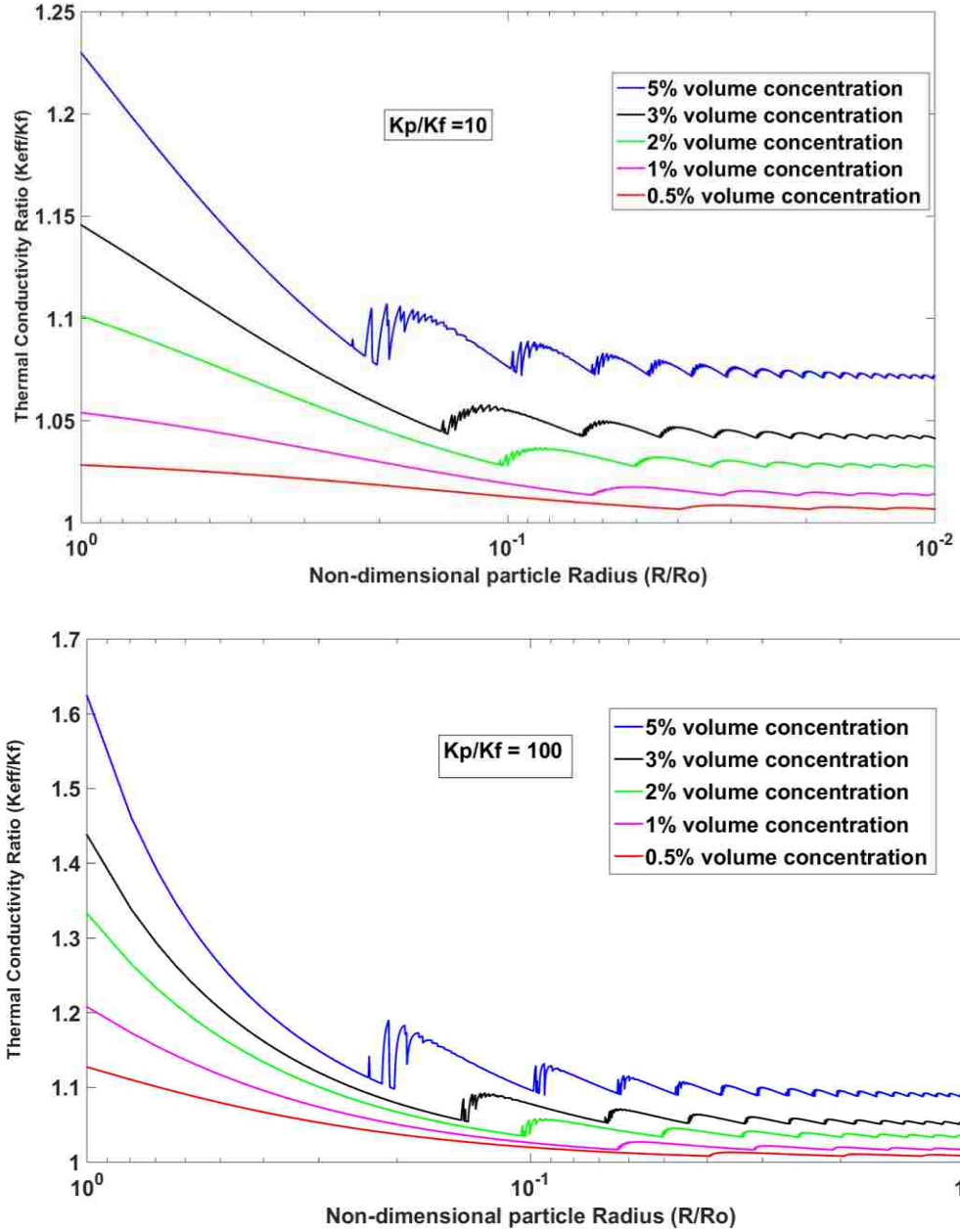

Figure 22 : Above graphs represents the change in Effective thermal conductivity ratio with respective to the particle size in terms of non-dimensional radius and at constant volume concentrations of 0.5%,1%, 2%, 3%, 4%, 5%. This is based on the lower bound arrangement discussed in the Section 3.4.

Number of particle at (R/Ro) $=10^{-2}$ is one million

Ro=Radius of particle when whole volume concentration is attributed by single particle

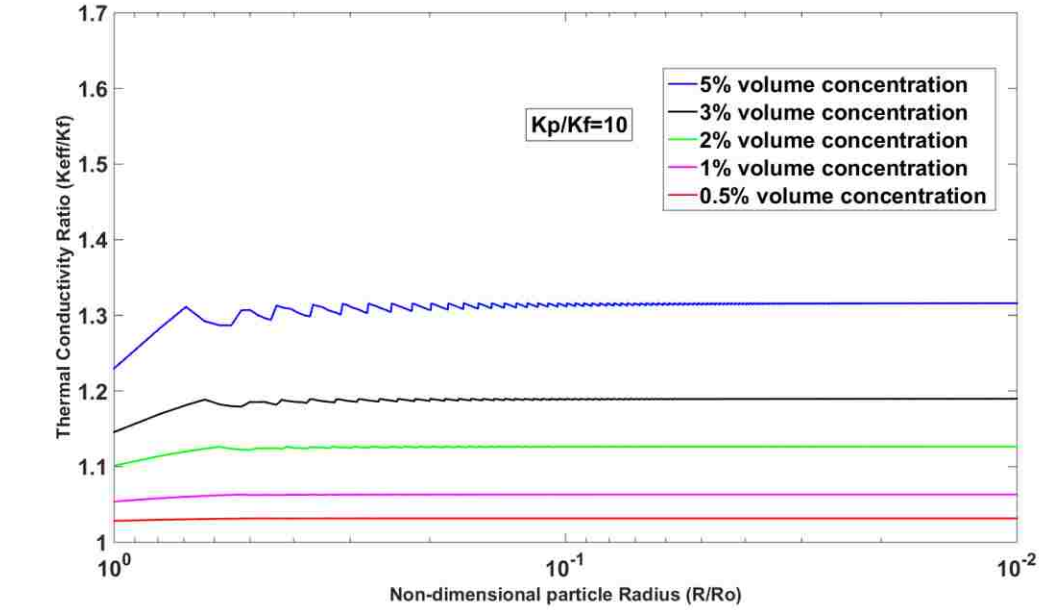

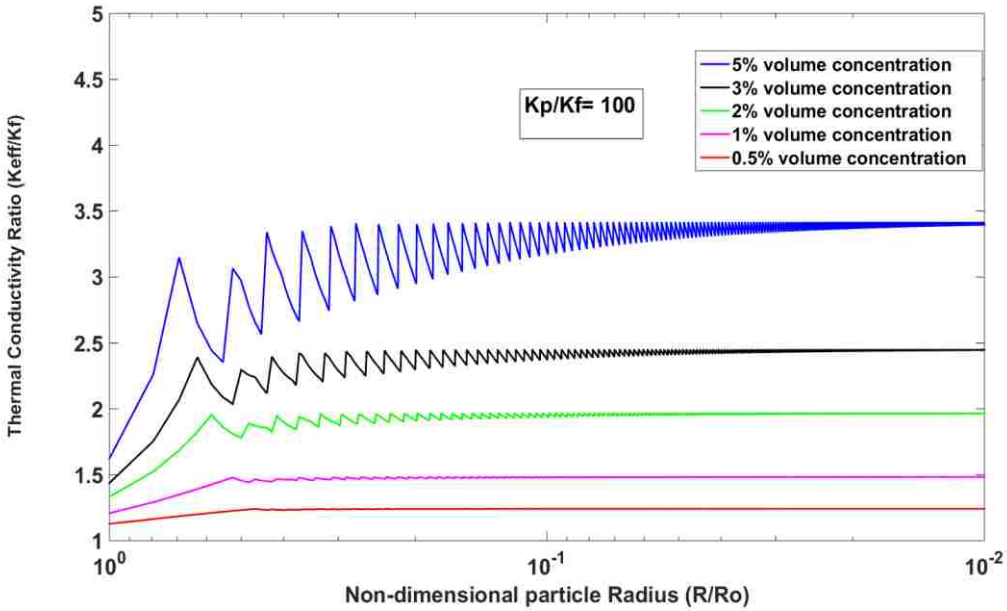

Figure 23 : Above graphs represents the change in thermal conductivity ratio with respective to the particle size in terms of non-dimensional radius and at constant volume concentrations of 0.5%, 1%, 2%, 3%, 4%, 5%. This is based on the upper bound arrangement discussed in the Section 3.4.

Number of particle at (R/Ro) $=10^{-2}$ is one million

Ro=Radius of particle when whole volume concentration is attributed by single particle

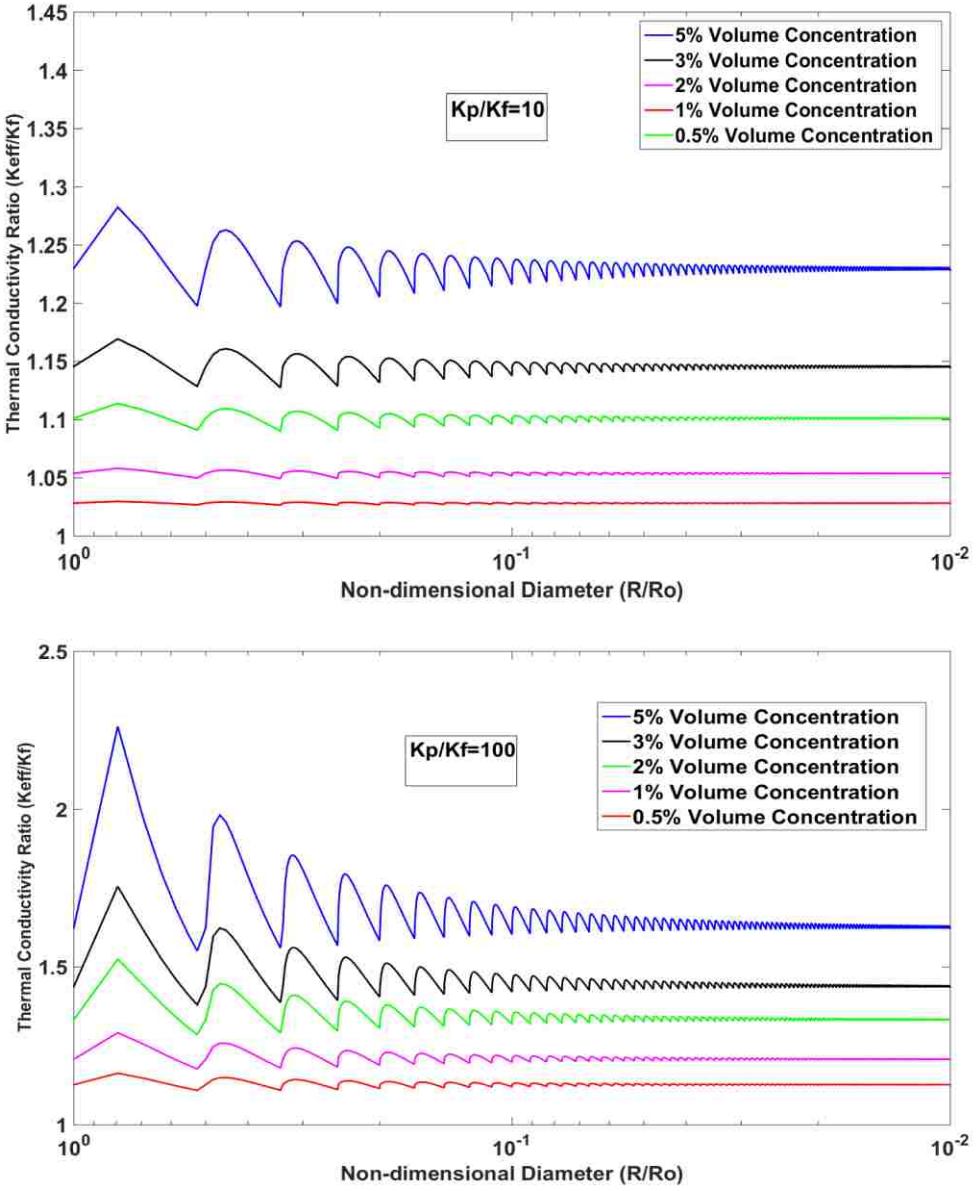

Figure 24 : Above graphs represents the change in thermal conductivity ratio with respective to the particle size in terms of non-dimensional radius and at constant volume concentrations of 0.5%,1%, 2%, 3%, 4%, 5% based on the uniform distribution arrangement.

Number of particle at (R/Ro) $=10^{-2}$ is one million

Ro=Radius of particle when whole volume concentration is attributed by single Particle

3.8. Effect of volume concentration on effective Thermal conductivity

Theoretical model that was derived in this work was used to generate the upper and lower bound of effective thermal conductivity of the colloidal fluid as a function of volume concentration. From Section 3.7. we can see that the thermal conductivity values changes with particle size for both upper and lower bound arrangements. Hence, we are considering the ETC at the colloidal size where the value is stabilized. Thermal conductivity trend with volume concentration is calculated for two different K_p/K_f ratio.

Further obtained graphs as shown in Figure 25 & Figure 26 are compared to the wiener and H-S bounds. We can observe that upper bound for current model is always less than both wiener and H-S upper bounds. While, the lower bound for the current model is less than the H-S lower bound and is always greater than wiener lower bound. As expected in both cases, upper and lower bounds of the current model has ETC within the limits of wiener bounds.

This model cannot predict ETC at very high volume concentrations, as we know that spheres cannot occupy complete volume of a cuboid and hence, graphs were plotted only certain small volume concentration.

Since, in most cases, the volume concentrations do not exceed 10 percent, graph as shown in Figure 26 is generated to give a clear view of effect of volume concentration only up to 10 percent.

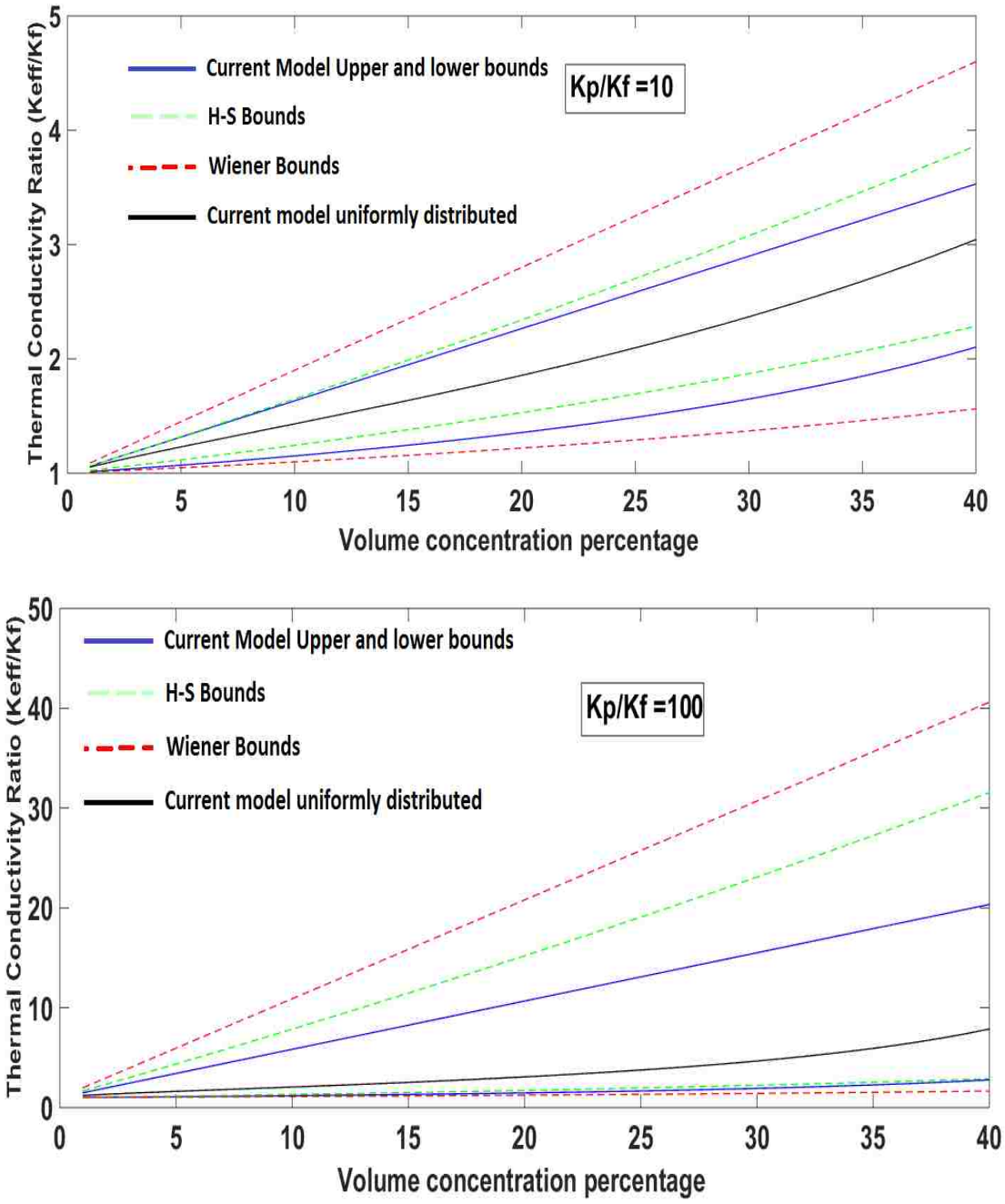

Figure 25 : Above graphs represents change in Thermal conductivity ratio with change in volume concentrations up to 40%. Comparison of Current model with other static models is made for K_p/K_f at 10 and 100.

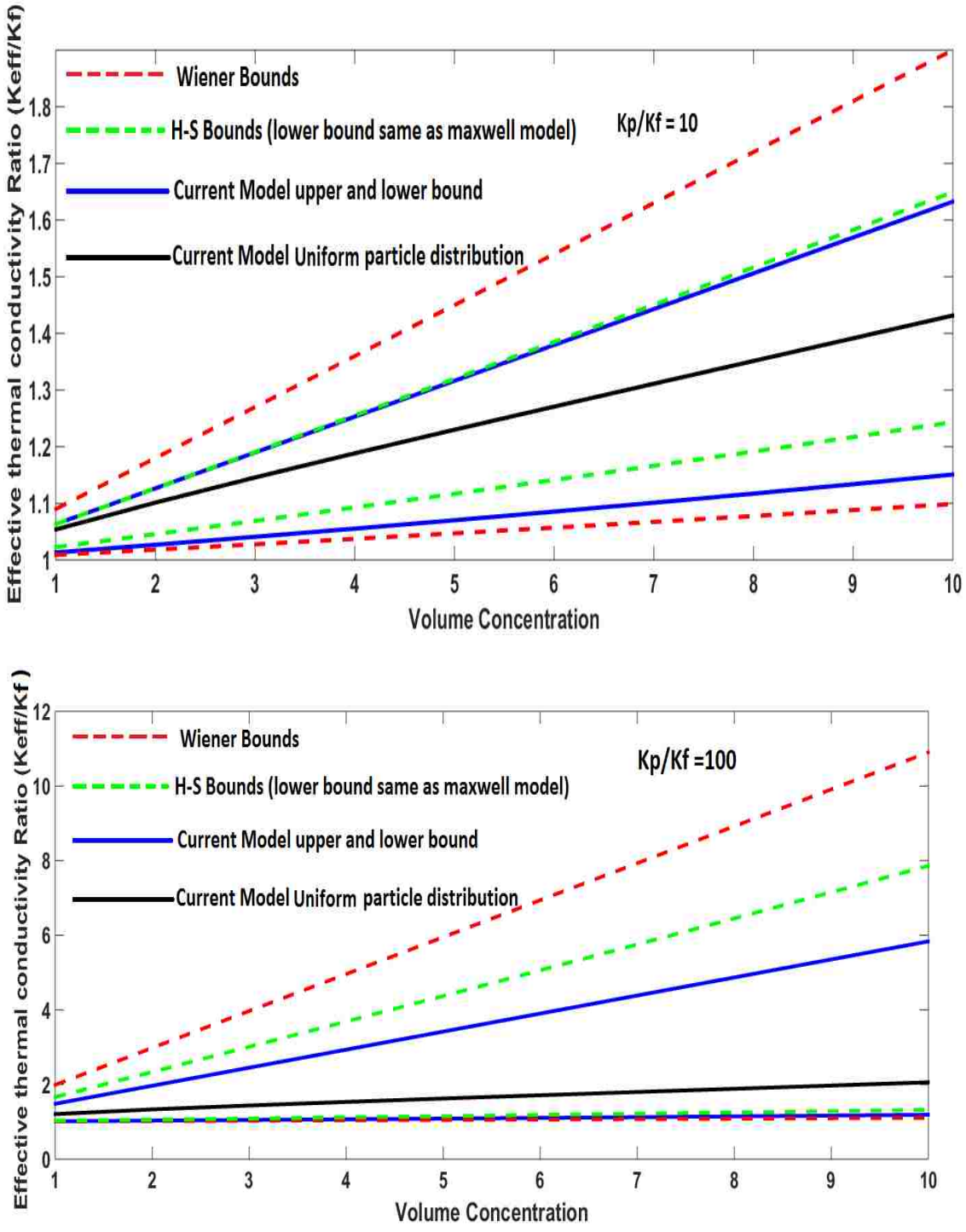

Figure 26: Above graphs represents change in Effective Thermal conductivity ratio with change in volume concentrations up to 10%. Comparison of Current model with other static models is made for K_p/K_f at 10 and 100.

To get effective bounds, it is very important for upper and lower bounds to be as close as possible. At higher K_p/K_f, current model has successfully generated bounds which is narrower than the Wiener and H-S bounds shown in Figure 25 &Figure 26. Further current model can also predicted effective thermal conductivity ratio for uniformly distributed particles which can be considered as most of colloidal fluids are tested for uniform distribution condition.

CHAPTER 4: THERMO-PHYSICAL MEASUREMENT OF SIC NANO-FLUID

4.1. Introduction

This chapter summarizes the different physical and chemical properties of current nano-fluid that were used as a part of research. This section also presents the results of thermal conductivity and viscosity measurement that were carried out.

4.2. Composition of SiC Nano-fluid

Silicon Carbide nano-fluid that was obtained from the Argonne National Laboratory contained Ethylene glycol and water mixture as a base-fluid with 4% volume concentration α-SiC nano particles. This nano-fluid was procured from Saint Gobain .Inc as water based suspension by Argonne National Laboratory. The average particle size was reported to be at 90nm. Received fluid was further diluted to three different concentrations of 0.55%, 1% and 1.6% volume concentrations and thermo-physical properties were determined.

Base fluid

Ethylene-glycol and water mixtures are commonly used as a heat transfer fluid for various applications. Addition of Ethylene glycol to water helps in increasing the boiling point of the fluid and as well as decreases the freezing point. This shifting of boiling and freezing points are very critical for high temperature application and for conditions where the temperature drops below 0 0C. Freezing point and boiling point and of 50.6% aqueous ethylene glycol is -37.9 and 107.8 ^{o}C respectively [24]. Hence, the base fluid considered here is a mixture of ethylene-glycol and water mixture with 50-50% volume concentration.

Properties of nano-particles

Silicon carbide is categorized under the family of ceramics and is extensively used in the industry for various applications. Its availability in nature is very rare, but can be produced artificially. It is also considered as one of the very hard ceramics and retains it even at high temperatures [25]. Commonly available polymorphs of SiC are Hexagonal and cubic structures. Cubic structure is referred as β-SiC and Hexagonal lattice structure is referred as α-SiC [23]. Most commonly available α-SiC is 6H-SiC [23].

Density of bulk α-SiC

Density of SiC varies based on the lattice structure. It could be anywhere between 3166 to 3248.78 kg/m^3 depending on the type of SiC [23]. For 6H-SiC, the density at 300K is 3211 kg/m^3[23].

Thermal Conductivity of bulk α-SiC

Thermal conductivity of SiC also depends on the lattice structure and temperature. For 6H-SiC, the thermal conductivity at 293K is 360 W/mK [23].

Additives in Nano-fluid

Nano-fluids cannot be commercialized just by achieving higher thermal properties; it is also necessary to produce a stable colloidal suspension. Uniformity and Stability will ensure the homogeneous distribution of thermal and physical properties. Stability increases as the colloidal particle size decreases, but decrease in size would also increases the attraction forces between particles and result in

agglomeration. This would result in settling of nano-particles due to gravity. To avoid agglomeration, various techniques like prolonged ultrasound sonication, surface modification, addition of surfactants, increasing Zeta potential by changing PH value etc. can be used.

For the current α-SiC or 6H-SiC based nano-fluid, stability is increased by changing the Zeta potential by increasing the pH of the fluid with Ammonium Hydroxide (NH_4OH). Increasing the Zeta potential would result in maintaining the difference in charge between bulk dispersion medium and the fluid layer just surrounding the colloidal particle. Zeta potential value can be positive or negative based on the pH. Typical variation of Zeta potential with pH is shown in the Figure 27. The isoelectric point is the point when the Zeta potential is zero. The stability of colloidal fluid will increase as the value moves away from isoelectric point. It is anticipated that Zeta potential should at least be ±30 for a colloidal suspension to be stable.

For the nano-fluids used here, to help increase the zeta potential and thus stability, pH is maintained at 9.5±0.3 [18] by adding NH_4OH. Weak base such as Ammonium Hydroxide is preferred over other strong base material since it has better buffering effect around pH of 9.4. Aqueous Ethylene glycol tends to produce acidicdity with time and this would result in decrease of pH over time. Only disassociated base will contribute to the pH of the solution. NH_4OH as a weak base does not disassociate completely at this pH and will only disassociate as and when the acidic compounds neutralizes the disassociated base keeping the pH of nano-fluid constant for long

period. Ammonium Hydroxide has a disadvantage that it has a low boiling point (low vapor pressure) and would tend to evaporate over time, which can affect the pH of fluid

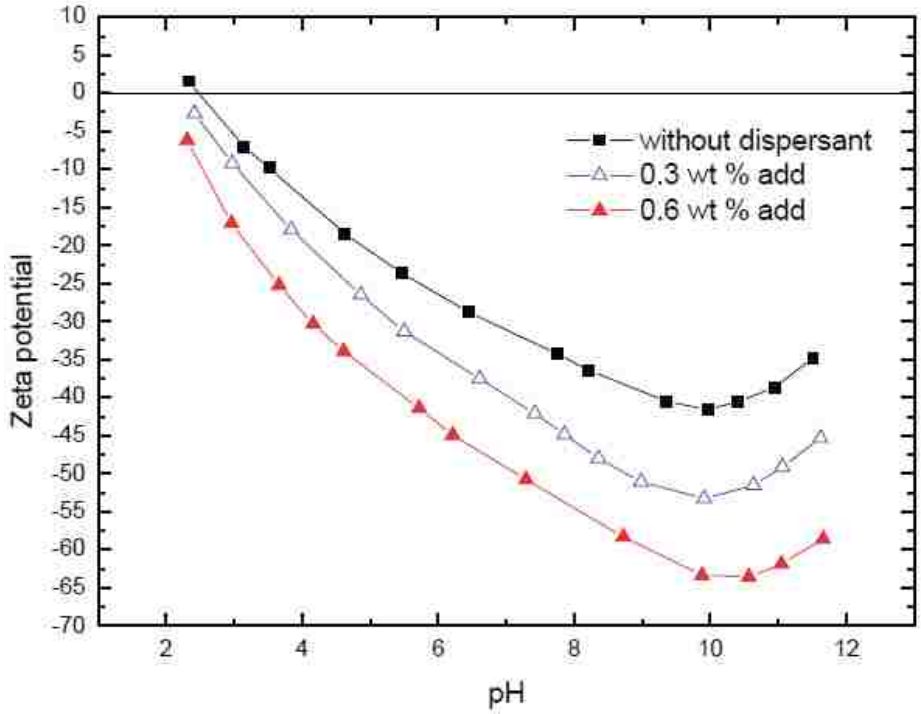

Figure 27: Graph shows the variation of Zeta potential with change in pH for SiC[25].

4.3. Experimental Measurement of Thermal conductivity

Thermal conductivity measurements are carried out using KD2Pro thermal conductivity meter which uses transient heat conduction method for measuring the thermal conductivity of fluids. This meter has three different types of probes to measure thermal conductivity of solids and liquids. These probes themselves act as a sensor as well as the heat source. Probe that is designated for fluid thermal Conductivity measurement is inserted into the fluid to be tested. As the heat causes

convections in the fluids, it is important to adjust the power settings and heat pulse duration to the lowest point possible on KD2Pro. This will ensure minimizing the natural convections that may be caused due to thermal gradients. Measurements were carried out in a very still (motionless, non-vibratory) environment to avoid convection due to external disturbances. Thermal conductivity data for SiC nano-fluids and base-fluid were measured at different temperatures.

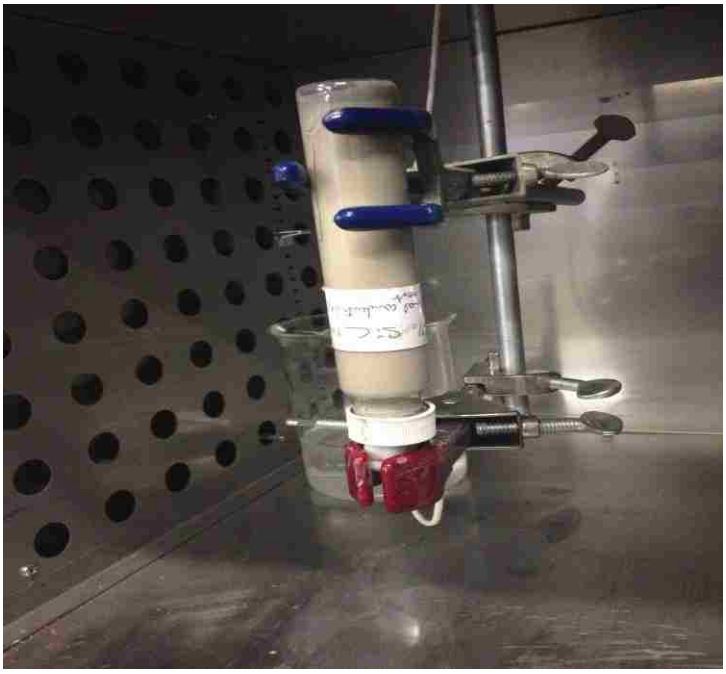

Figure 28: Arrangement of testing fluid for thermal conductivity measurement

Thermal Conductivity of base-fluid

Before measuring the Thermal conductivity of SiC nano-fluid, it is necessary to measure and establish the thermal conductivity of base fluid to ensure that the values obtained are the matching with the values obtained from the literature. Thermal conductivity of base fluid is measured at different temperatures and is plotted as

shown in the Figure 29. Deviation is compared with ASHRAE data and average deviation observed is around 6.5%.

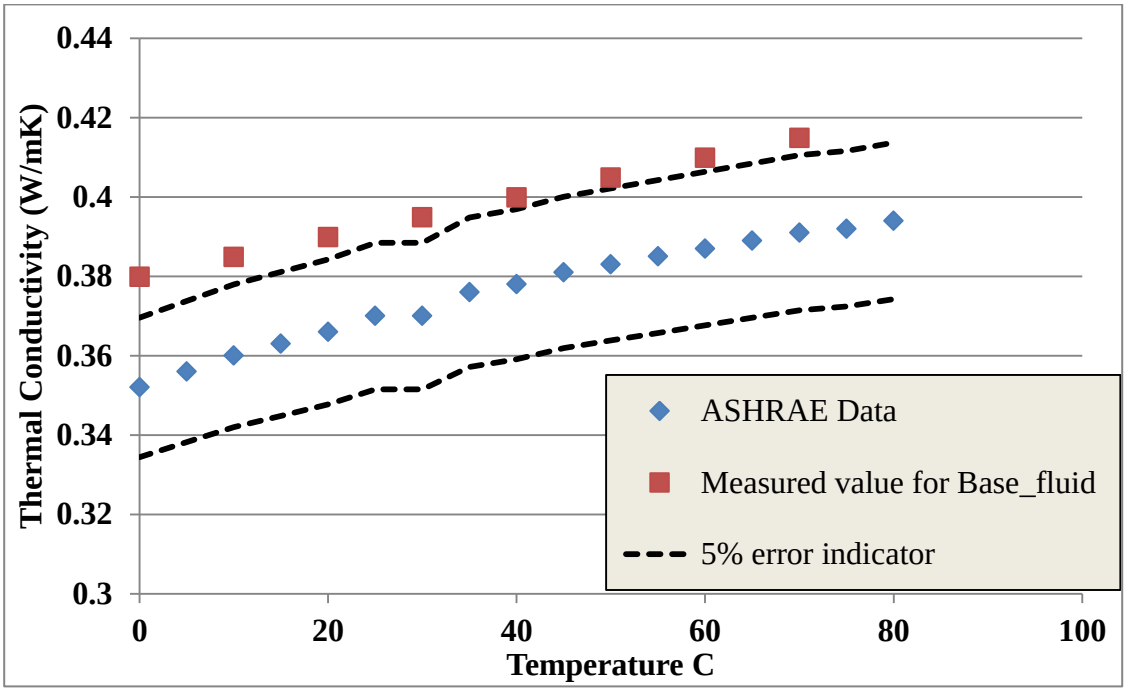

Figure 29: Graph indicating Thermal conductivity as a function of temperature and comparing the measured Thermal conductivity data of Base fluid (Ethylene Glycol – Water 50-50 Volume %) to standard data from ASHRAE (data represented in W/mK). average deviation observed was less than 6.5 percent. ASHRAE data is known to be +/- 5% uncertainty.

Thermal Conductivity of SiC Nano-fluids

Thermal Conductivity was measured for 0.55%, 1% and 1.6% volume concentrations of SiC nano-fluid with temperature change and compared the same with the base-fluid to determine the enhancement percentage. Variation of nano-fluid thermal conductivity as a function of temperature and volume fraction is shown in the Figure 30

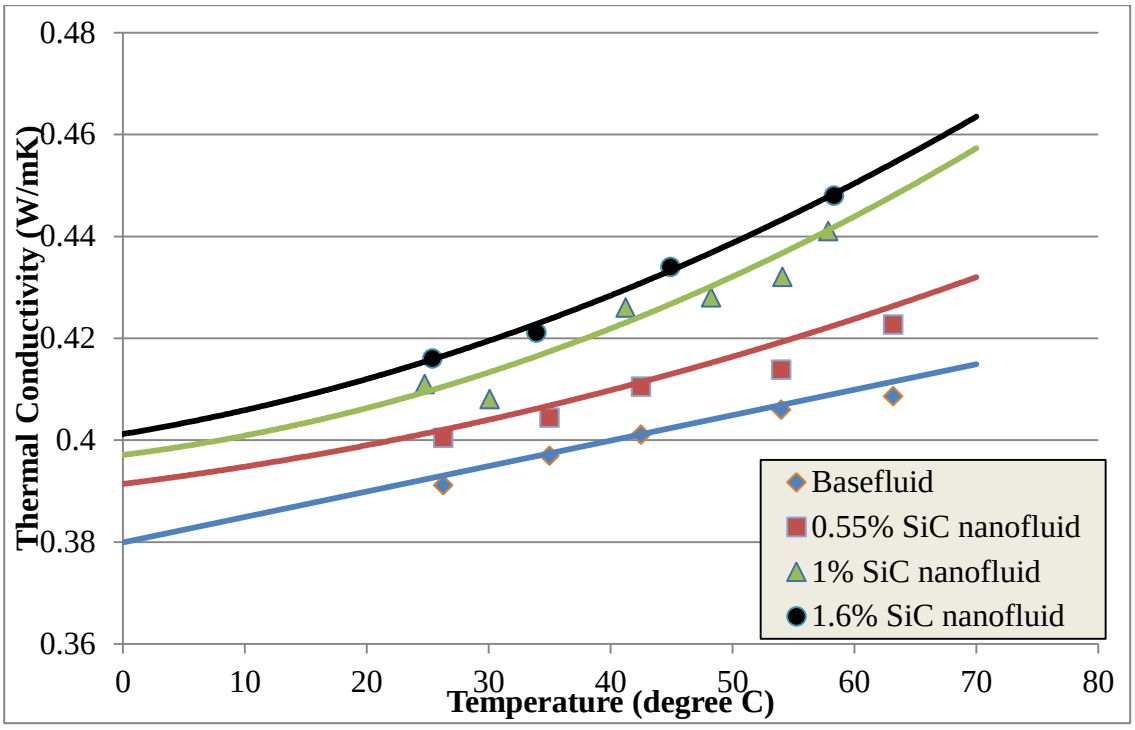

Figure 30: Variation of measured Thermal conductivity of SiC nanofluid (W/m-K) for different volume concentrations with Temperature

	Basefluid	0.55% SiC Nanofluid		1% SiC Nanofluid		1.6% Nanofluid	
Temp (^{o}C)	TC (W/mK)	TC (W/mK)	Enhancement Percentage	TC (W/mK)	Enhancement Percentage	TC (W/mK)	Enhancement Percentage
0	0.379	0.391	2.94	0.397	4.53	0.401	5.61
10	0.384	0.394	2.51	0.400	4.16	0.405	5.46
20	0.389	0.399	2.28	0.406	4.21	0.412	5.67
30	0.394	0.404	2.25	0.413	4.66	0.419	6.23
40	0.399	0.409	2.42	0.421	5.50	0.428	7.13
50	0.404	0.416	2.76	0.432	6.72	0.438	8.35
60	0.409	0.423	3.28	0.443	8.29	0.450	9.88
70	0.4149	0.432	3.96	0.457	10.22	0.463	11.71

Table 1: Thermal conductivity obtained by curve fitting of Measured values

From Figure 30 and Table 1**,** it is seen that all the three volume concentrations of SiC nano-fluids show enhancement in thermal conductivity compared to its base-fluid. On an average, 2.8%, 6%, and 7.5% enhancement was recorded for 0.55%, 1% and 1.6% SiC nano-fluids respectively.

Comparison of Measured Thermal conductivity with the current model

Thermal conductivity values obtained from the measurements are compared with the theoretical model that was developed as part of this work. Comparison is made for all the three volume concentrations at 20^{o}C. Theoretical model calculations are based on the thermal conductivity value of 360W/mK 6H-SiC at 20 ^{o}C and Ethylene Glycol and water mixture thermal conductivity value at 20 ^{o}C is taken from Table 1.

From Figure 31 we can observe that measured values are well within the upper and lower bounds of theoretical model. Measured values obtained are close to the lower bound with average deviation of 2.3%. We can conveniently limit the uniform distribution as higher bound, as deviation of upper bound is very high.

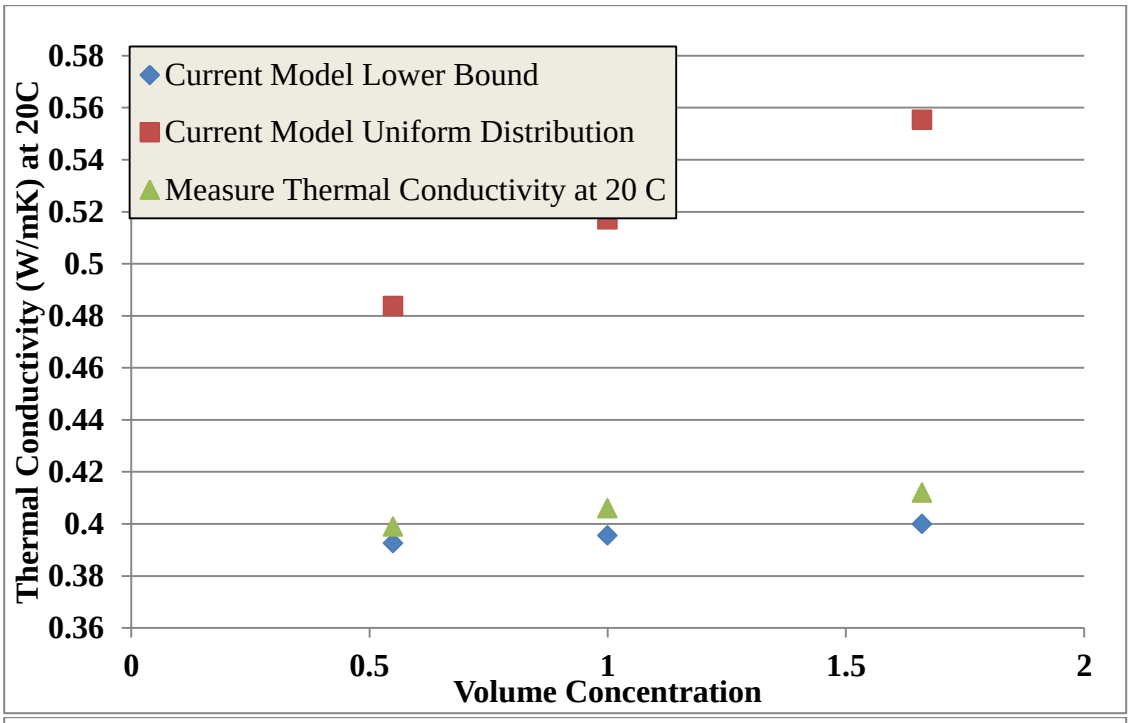

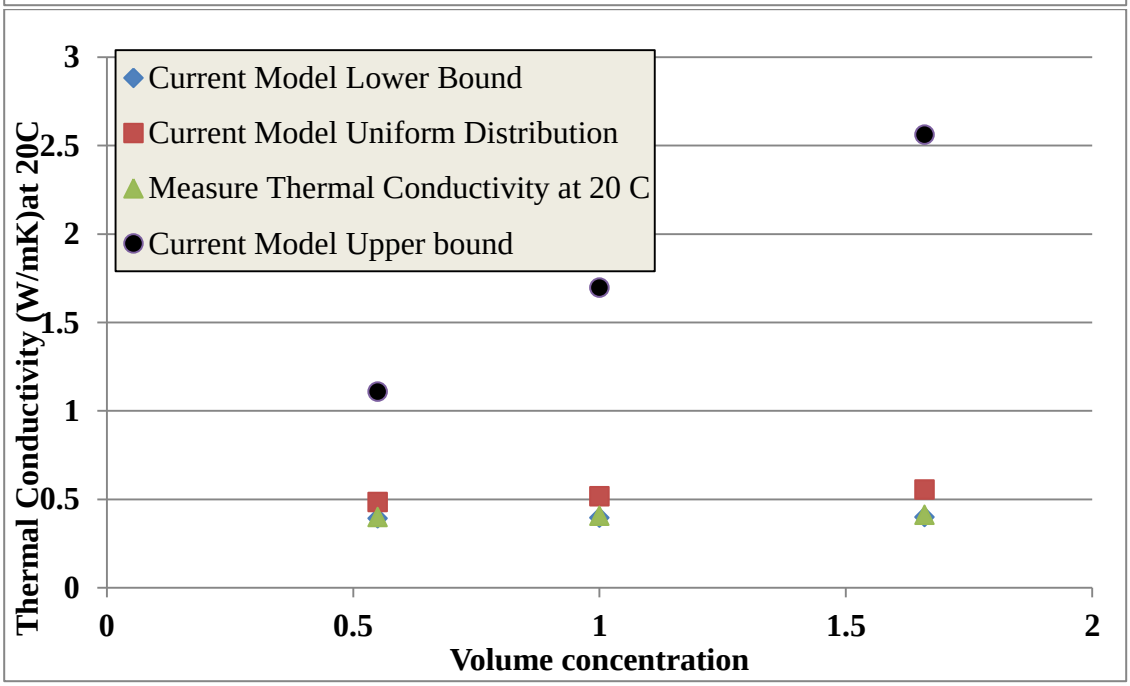

Figure 31: Graphs showing variation Thermal conductivity with volume concentration at 20 ^{o}C and comparison is made with the derived Theoretical model explained in chapter . 3

4.4. Viscosity of SiC Nano-fluid

Addition of nano particles tends to increase the viscosity when compared to its base-fluid and hence it is important to measure the viscosity of the nano-fluids to determine the actual effectiveness. Measurements were carried out to determine the viscosity of the testing fluids at different temperatures using TA instrument made AR-G2 Magnetic Bearing Rheometer. This instrument is facilitated with temperature control unit which maintains the testing fluid at a desired temperature all through the experiment. Viscosity is measured from 0 to 50^{o}C and values for remaining temperatures in Figure 32: Variation of Viscosity with temperature were extrapolated using curve fitting. Viscosity is measured at different shear rates at each temperature and an average viscosity value for testing fluid in consideration is presented.

From Figure 32: Variation of Viscosity with temperature, it is evident that as the temperature is increasing the difference between the base-fluid and nano-fluids viscosity values tend to decrease. But from Table 2, we can notice that as the temperature is increasing, percentage increases of viscosity values are increasing. On an average, 7.9%, 14.49% and 24.37% increase was recorded for 0.55%, 1% and 1.6% SiC nano-fluid respectively.

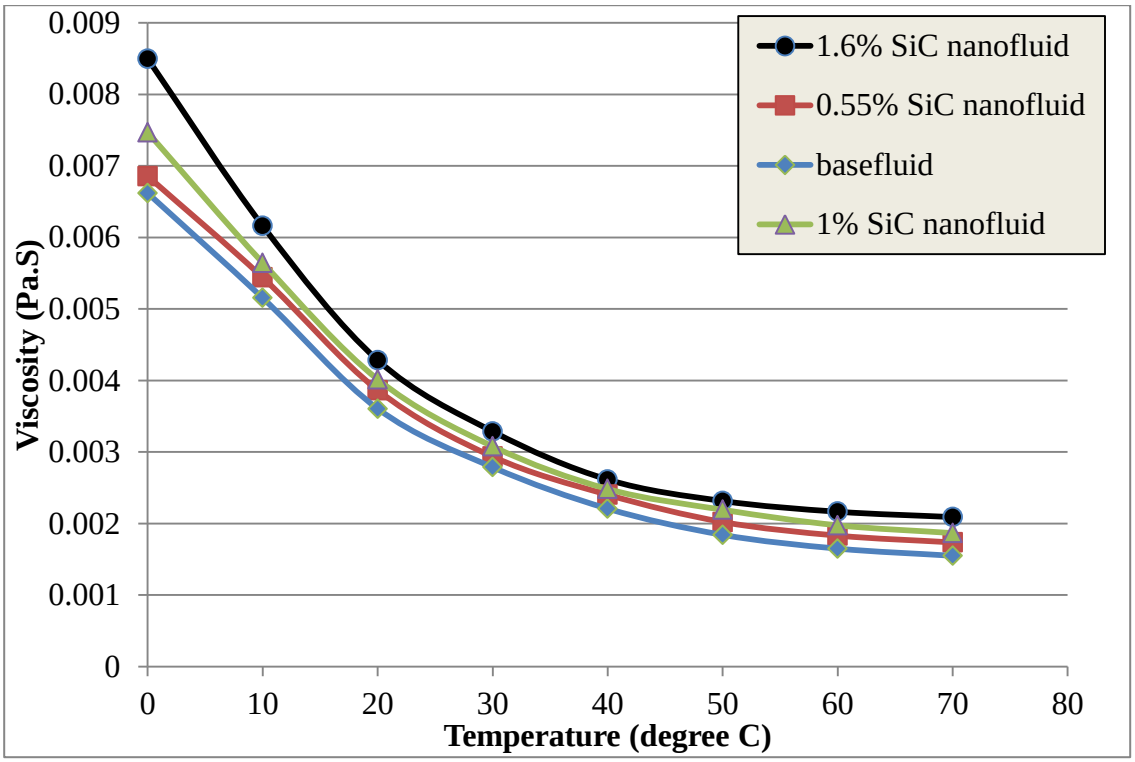

Figure 32: Variation of Viscosity with temperature

Temp (^oC)	Base Fluid	0.55% SiC Nano fluid		1% SiC Nano fluid		0.55% SiC Nano fluid	
	Viscosity (Pa.S)	Viscosity (Pa.S)	% Increase	Viscosity (Pa.S)	% Increase	Viscosity (Pa.S)	% Increase
0	0.00662	0.00686	3.58	0.00747	12.84	0.0085	28.38
10	0.00515	0.00544	5.55	0.00565	9.54	0.00616	19.56
20	0.00361	0.00387	7.18	0.00402	11.37	0.00428	18.81
30	0.00279	0.00294	5.33	0.00308	10.47	0.00329	17.95
40	0.00221	0.0024	8.83	0.00248	12.45	0.00262	18.42
50	0.00184	0.00202	9.77	0.00219	19.06	0.00232	25.69
60	0.00165	0.00183	11.01	0.00198	19.75	0.00217	31.25
70	0.00155	0.00174	12.03	0.00187	20.46	0.00209	34.90

Table 2: Viscosity obtained by curve fitting of Measured values

4.5. Results and Discussion

It is evident that the thermal conductivity of SiC based nano-fluid for 0.55%, 1% and 1.6% volume concentration displayed an enhancement when compared to its base fluid. As proposed by Keblinski, thermal conductivity enhancement in nano-fluids is primarily driven by four mechanisms; Brownian motion of the nanoparticles, liquid layering, the nature of heat transport in the nanoparticles, and the effects of nanoparticle clustering [37]. Brownian motion is the random movement of the suspended particle in the base fluid which results in collision of particles and thereby increasing the heat transfer between particles [5, 36]. Some research suggests that heat transfer by particle collision is negligible and predicts that convection of surrounding base fluid due to Brownian motion would create higher heat transport [5]. It is proposed that the base fluid immediately surrounding the nanoparticle forms a nano layer which adheres to the nanoparticle and is considered to have higher thermal conductivity than the base fluid. This could contribute to the higher thermal conductivity of nano-fluids. Apart from this, a simple explanation could be addition of very high thermal conductive particles itself may assist in enhancement of ETC.

Further, it is observed that there is an increase in percentage enhancement with temperature. This could be due to the Brownian motion since Brownian motion increases with the temperature.

Viscosity of the nano-fluid is dependent on many factors such as volume concentration of nano particle, temperature, pH of fluid, particle size etc. In the current work, we have observed that the viscosity of the nano-fluid tends to increase with the

increase in volume concentration and decrease with the increase in temperature. The possible reason for increase in viscosity with volume concentration is that, as the volume concentration increases the particle interaction increases and this interaction could result interaction induced viscosity [38]. This also give us an explanation of how the particle size effects the viscosity, for a volume concentration, larger particle Fluid system have less number of particles and hence minimum particle interaction interactions and lower viscosity. Viscosity dependency on temperature can easily be explained by the fact that the viscosity of base fluid decreases with the temperature and hence would effectively decreases the viscosity of nano-fluid.

CHAPTER 5: FORCED CONVECTION EXPERIMENTAL RESULTS

5.1. Introduction

Heat exchangers are one of the primary systems used in heat transfer applications. Convection is the basic phenomena by which the heat transfer takes place in these heat exchangers. As nano-fluids are to replace current heat exchanger fluids, forced convection properties is required to evaluated and compare them with the base-fluid and determine the effectiveness of the current nano-fluids.

As discussed earlier in the chapter 1, though nano-fluids tend to increase the heat transfer properties, it is also accompanied by the increase in the viscosity and pressure drop values when compared to its base fluid. This would result in increase in the pumping power requirements for the heat exchangers. Hence, measuring the heat transfer as well as pressure drop properties of the nano-fluid under consideration is necessary to determine the actual effectiveness and presumed advantage of nano-fluids.

5.2. Forced convection properties

One of the important forced convection properties that is required to determined heat transfer and the related non-dimensional heat transfer coefficient. Nusselt number is directly proportional to the heat transfer coefficient and inversely proportional to the thermal conductivity of the fluid in consideration. From Chapter 4, it is observed that thermal conductivity of the nano-fluids are higher and thereby it is important to note that a marginal increase in heat transfer coefficient of nano-fluids would not result in appreciable increase in Nusselt number.

In this experiment, Nusselt number has been calculated based on the measured temperature dependent thermal conductivity and heat transfer coefficient values. These values are compared to the empirical relations based on the Reynolds and Prandtl number which is a material property of the medium. Following are the correlations from the literature that were used to compare with measured heat transfer data.

5.3. Correlations for Nusselt number

Laminar Correlations

Shah and London correlation for laminar flow with hydrodynamically fully developed and thermally developing flow for a constant heat flux[13].

$$\mathrm{Nu}_0 = \begin{cases} 1.953 \times \left(\left(\mathrm{Re} \times \mathrm{Pr} \times \frac{\mathrm{D}}{\mathrm{L}}\right)^{1/3}\right) & \text{when } \left(\mathrm{Re} \times \mathrm{Pr} \times \frac{\mathrm{D}}{\mathrm{L}}\right) \geq 33.3 \\ 4.364 + 0.0722 \times \left(\mathrm{Re} \times \mathrm{Pr} \times \frac{\mathrm{D}}{\mathrm{L}}\right) & \text{when } \left(\mathrm{Re} \times \mathrm{Pr} \times \frac{\mathrm{D}}{\mathrm{L}}\right) < 33.3 \end{cases} \quad \textbf{(}15\textbf{)}$$

Churchill and Ozoe proposed a correlation for hydrodynamically and thermally developing flow in circular ducts with uniform heat flux [14]

$$\frac{\mathrm{Nu_x}}{\left(5.364\left[1+\left(\frac{\mathrm{Gz}}{55}\right)^{\frac{10}{9}}\right]^{\frac{8}{10}}\right)} = \left\{1+\left(\frac{\frac{\mathrm{Gz}}{28.8}}{\left[1+\left(\frac{\mathrm{Pr}}{0.0207}\right)^{2/3}\right]^{\frac{1}{2}}\times\left[1+\left(\frac{\mathrm{Gz}}{55}\right)^{\frac{10}{9}}\right]^{\frac{3}{5}}}\right)^{10/6}\right\}^{\frac{3}{10}} \quad (16\textbf{)}$$

Where Gz= $\frac{D\times Re\times Pr}{L}$ (Graetz number)

Transition and Turbulence Correlations

Gnielinski Correlation used for turbulent and transition flow in tubes [10, 12]

$$Nu_D = \frac{\left(\frac{f}{2}\right)\times(Re_D-1000)\times Pr}{1+12.7\times\left(\frac{f}{2}\right)^{\frac{1}{2}}\times\left(\left(Pr^{\frac{2}{3}}\right)-1\right)} \qquad \begin{matrix}0.5\leq Pr\leq 2000\\ 2300\leq Re_D\leq 5\times 10^6\end{matrix} \qquad \textbf{(17)}$$

Where $f = (1.58 \times \ln(Re) - 3.28)^{-2}$

Dittus- Boelter Correlation used for turbulent flow [16]

$$Nu_D = 0.0023 \times Re_D^{\frac{4}{5}} \times Pr^n \qquad (18)$$

when $0.7 \leq Pr \leq 160$ $\qquad 2500 > Re_D > 1.24 \times 10^5$

D is the inside diameter of the circular duct; Pr is the Prandtl number;

n=0.4 for heating of the fluid; n=0.3 for cooling of the fluid

Taborek (1990) is valid only in transition region [16]

$$Nu = \emptyset \times Nu_{lam} + (1 - \emptyset) \times Nu_{turb} \qquad (19)$$

where $\emptyset = 1.33 - \left(\frac{Re}{6000}\right)$ $\quad 2000 < Re < 8000$

5.4. Experimental setup Description

A test section for the heat transfer experiments was designed and constructed at Dynalene. Inc. to measure the forced convection thermal properties of nano-fluids, The experimental setup shown in the Figure 33 consists of thin walled mild steel and copper tubing, fluid reservoir, pump, flow control valves, Temperature sensors (13 RTD's), Pressure drop measurement device, cooling system and regulated DC power source for heating. The test rig requires one and half gallon of testing fluid. The test section is made with mild steel tube, which is insulated and the remaining piping is build using copper material. Mass flow rate can be controlled using valves. Test section is properly insulated to decrease the heat losses. Great care has been taken to establish well defined momentum and thermal flow development and overall heat balance.

The fluid to be test is made to pump at desired flow rate by adjusting the valves. Heating of test section is done using regulated power supply and cooling is provided by water cooled heat exchanger. Once the system reaches the steady state, temperature, mass flow rate and pressure drop data are collected to calculate the Nusselt number, Reynolds number and heat transfer coefficients. Important forced convection properties are measured for base-fluid which is Ethylene glycol and water mixture with 50-50% volume concentration and for SiC nano-fluids at 0.55%, 1% and 1.6% concentrations.

Several researchers that have worked with nano-fluid heat transfer present their data in the heat transfer coefficient as a function of independent variables such as flow rate or velocity.

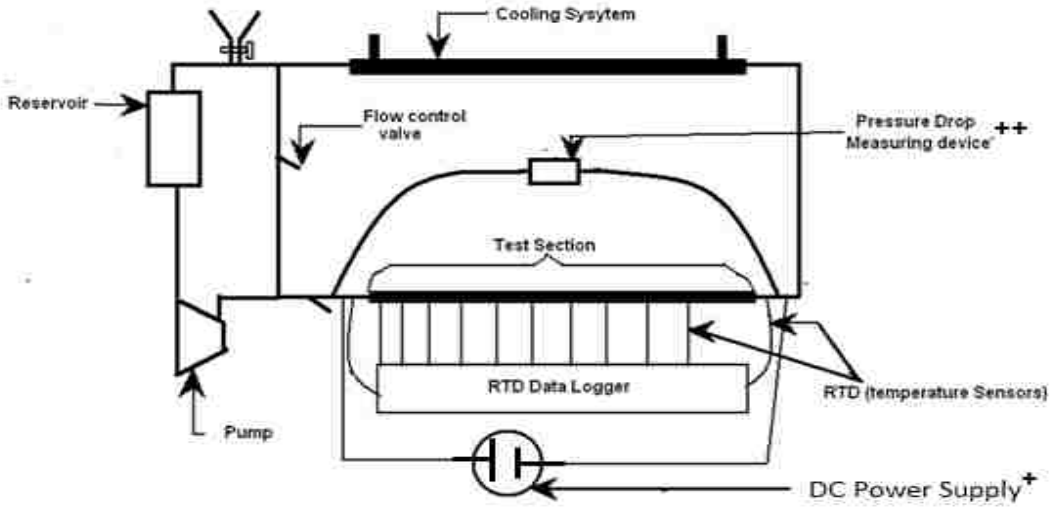

Figure 33: Experimental skid to measure the forced convection properties of fluids
+Power input – 5-110 V and 30-200 Amps (Variable)
++Pressure measurement device – Omega (range 0-10 PSI)

The traditional way of representing heat transfer data Nusselt Vs Reynolds numbers neglects the fact that for the same flow rate, thanks to the increase in the viscosity of the nano-fluid, the Reynolds number decreases. Thus for a given flow rate a spurious increase in the Nusselt number may be noticed as a function of Re, as Re decreases. Possibly due to reasons such as this, some work in the literature is presented in the form of heat transfer coefficient. But presenting data in this (dimensional) manner makes it difficult to compare various sets of measurements from different laboratories. This is particularly true when some of the nano-fluid experiments do not have well established procedures for fully developed flow conditions.

5.5. Comparison of experimental data with Correlations

Some thermal experimental data was collected for base fluid flow to establish the efficacy and accuracy of the experimental system. Figure 34 to Figure 39 below graphically represent some of the measurements made for Nu vs. Re in the laminar and transition regions of flow.

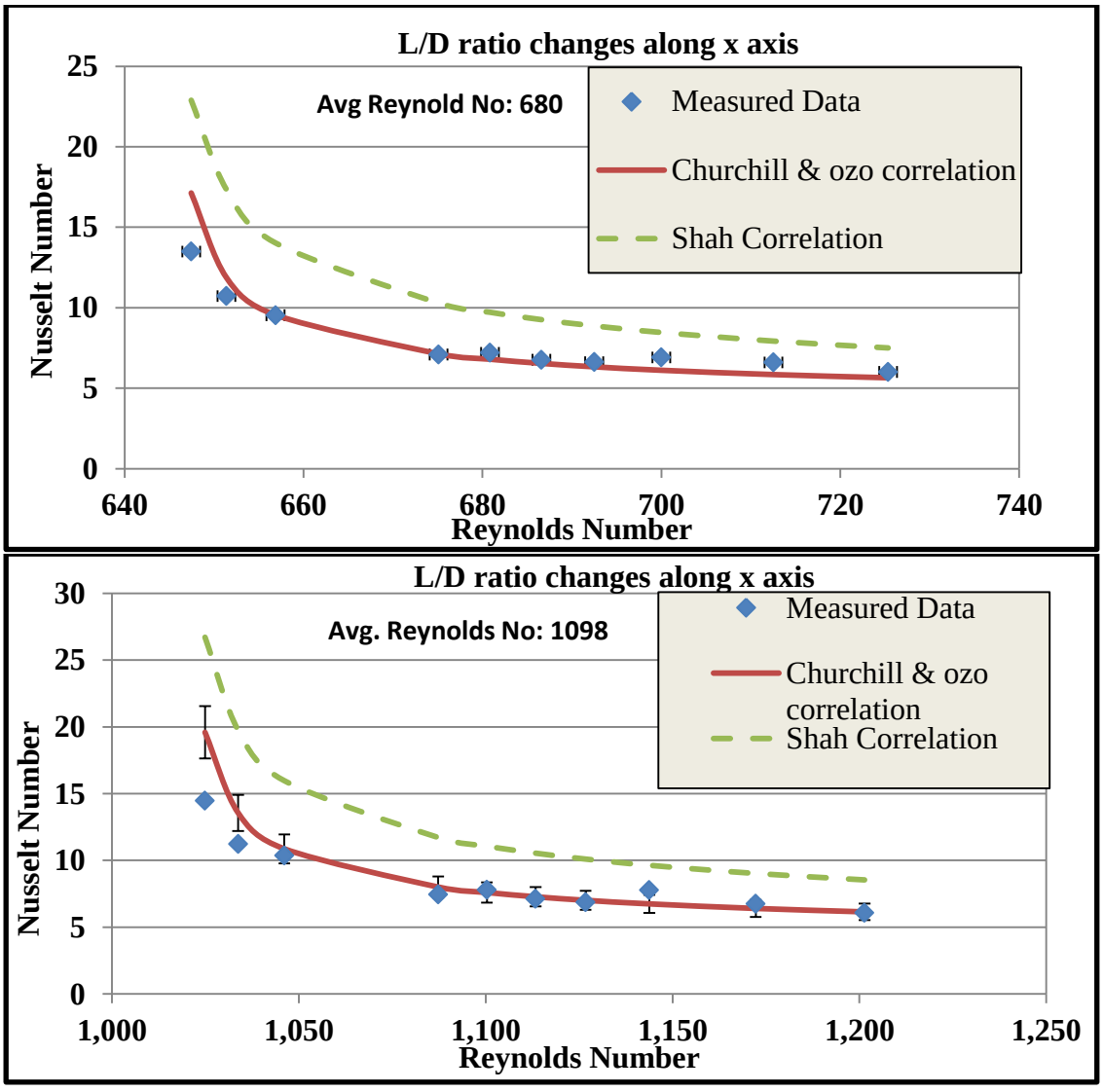

Figure 34: Nusselt number change along test section for Base fluid
Error bar displayed in graph for Churchill & ozoe ±10%

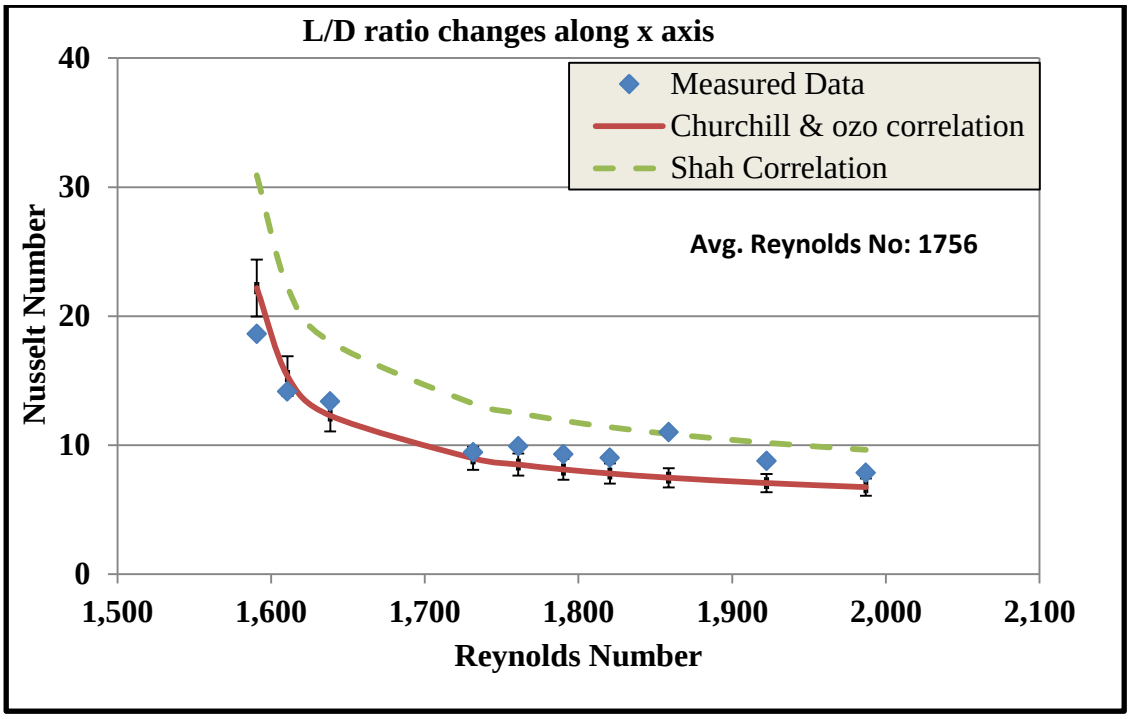

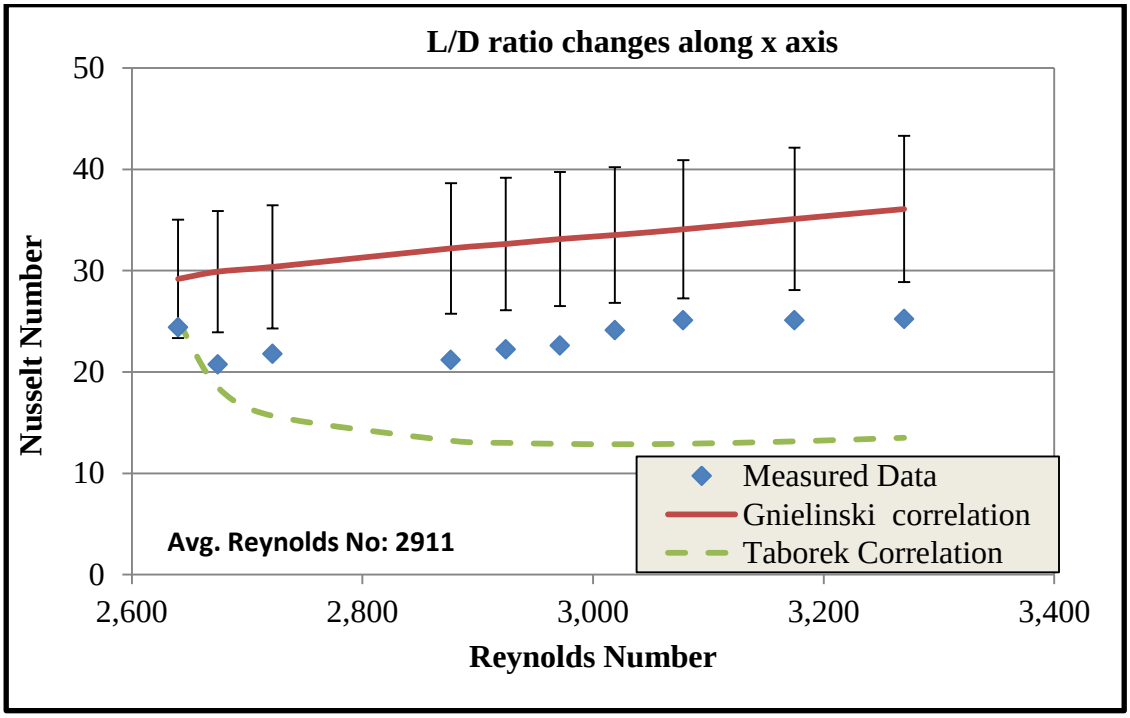

Figure 35: Nusselt number change along test section for Base fluid
Error bar displayed in graph for Gnielinski correlation is ±20% [12]

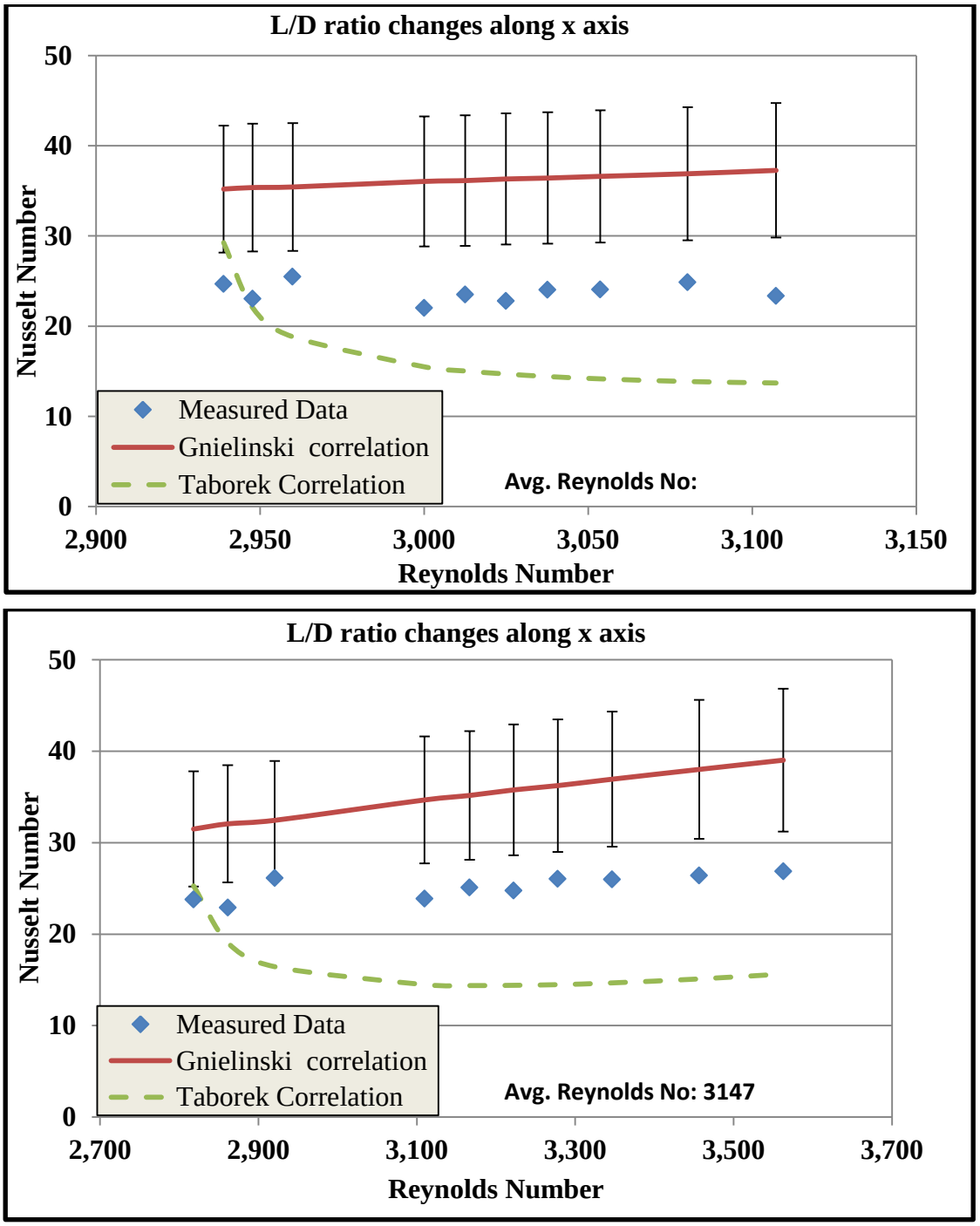

Figure 36: Nusselt number change along test section for Base fluid

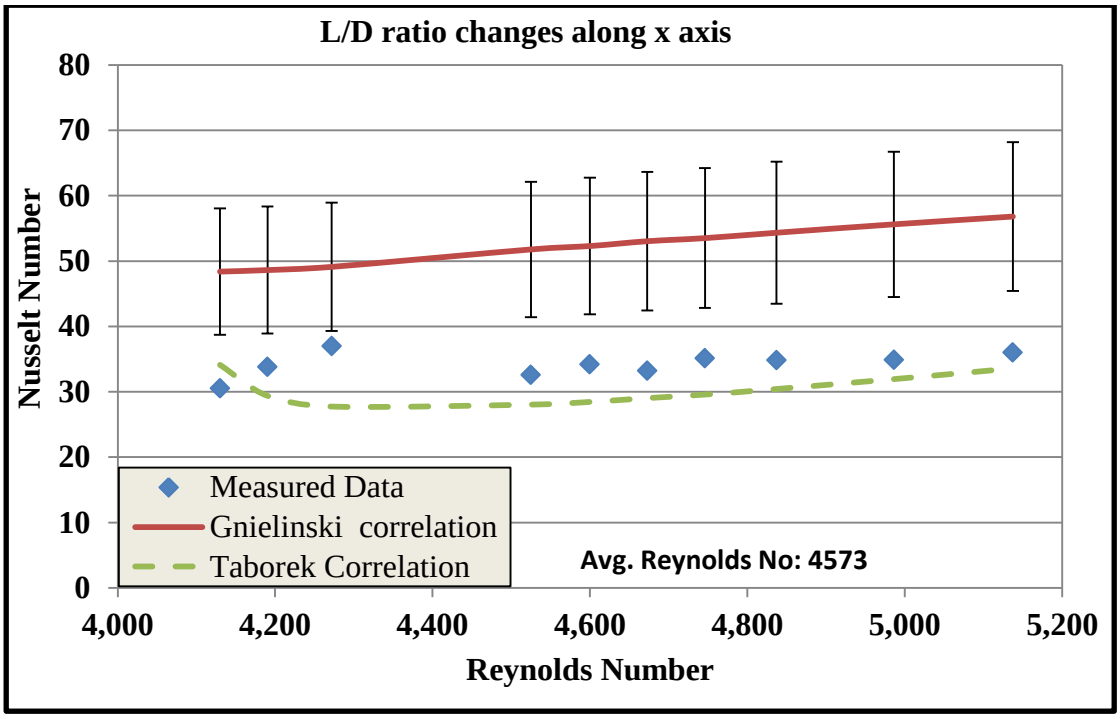

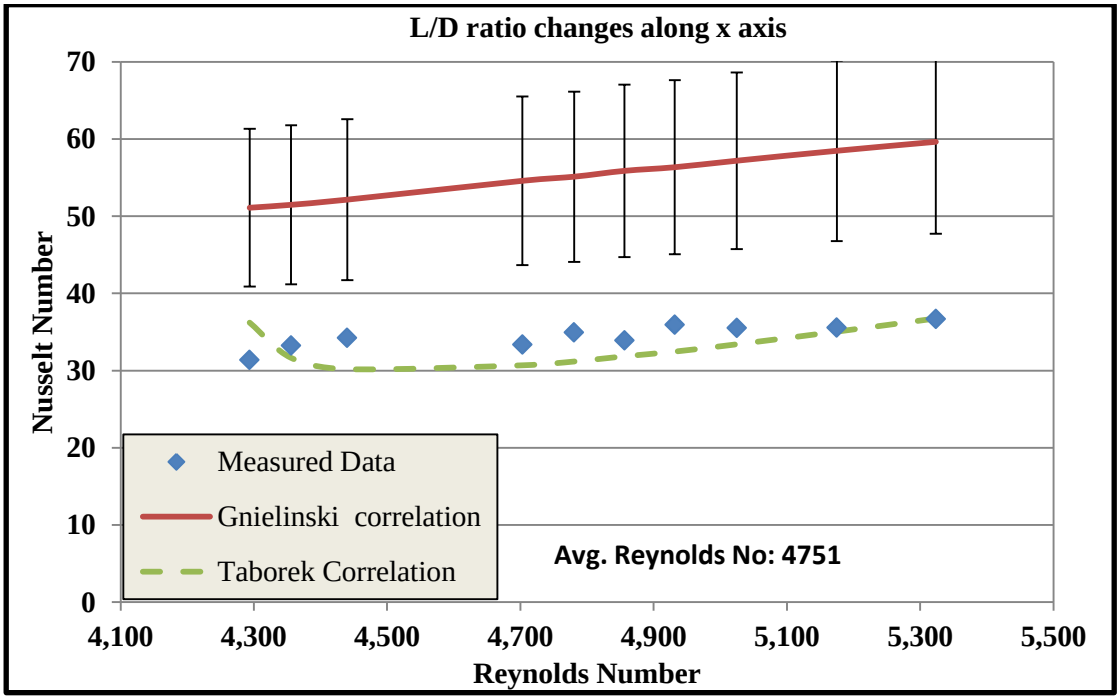

Figure 37: Nusselt number change along test section for Base fluid

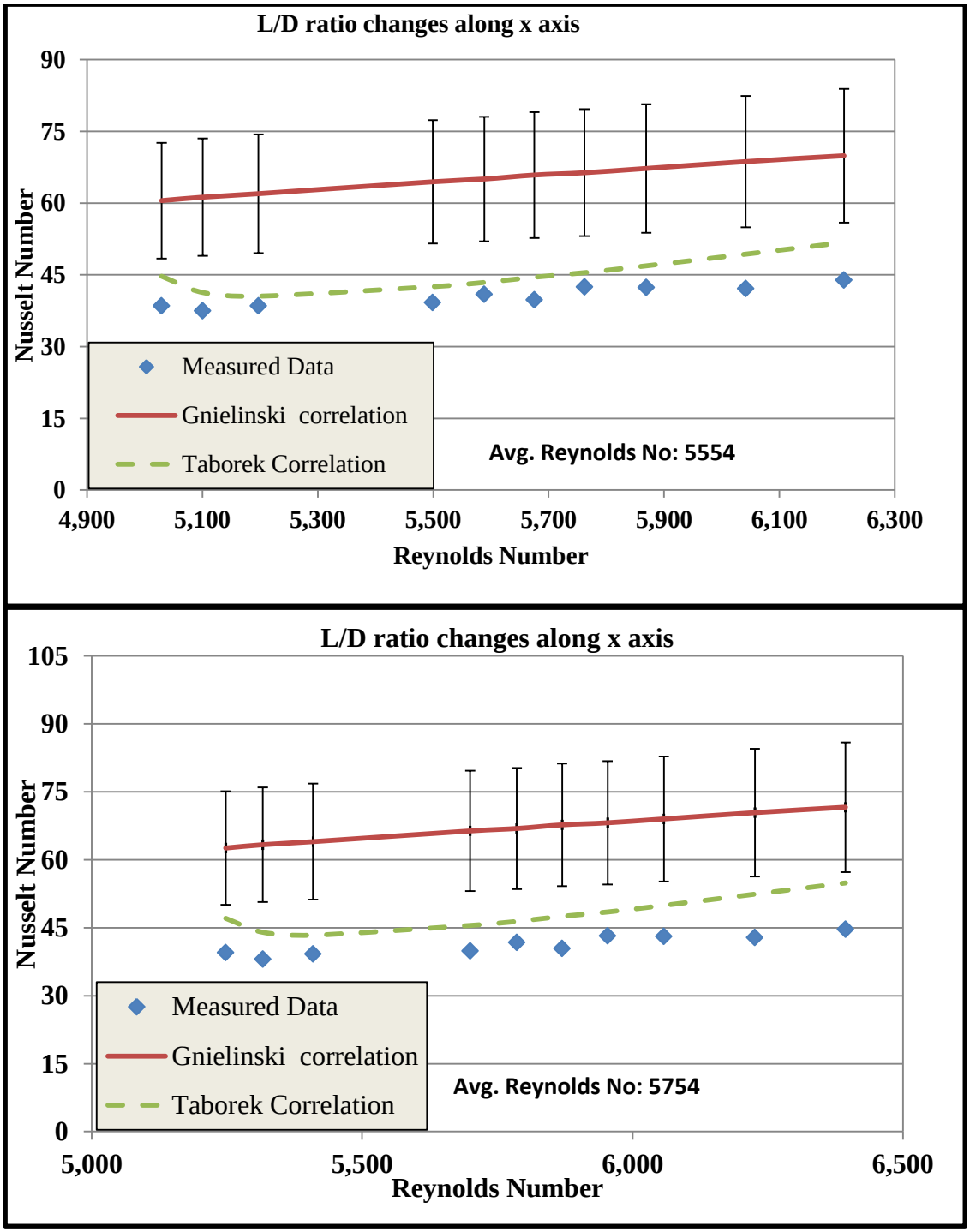

Figure 38: Nusselt number change along test section for Base fluid

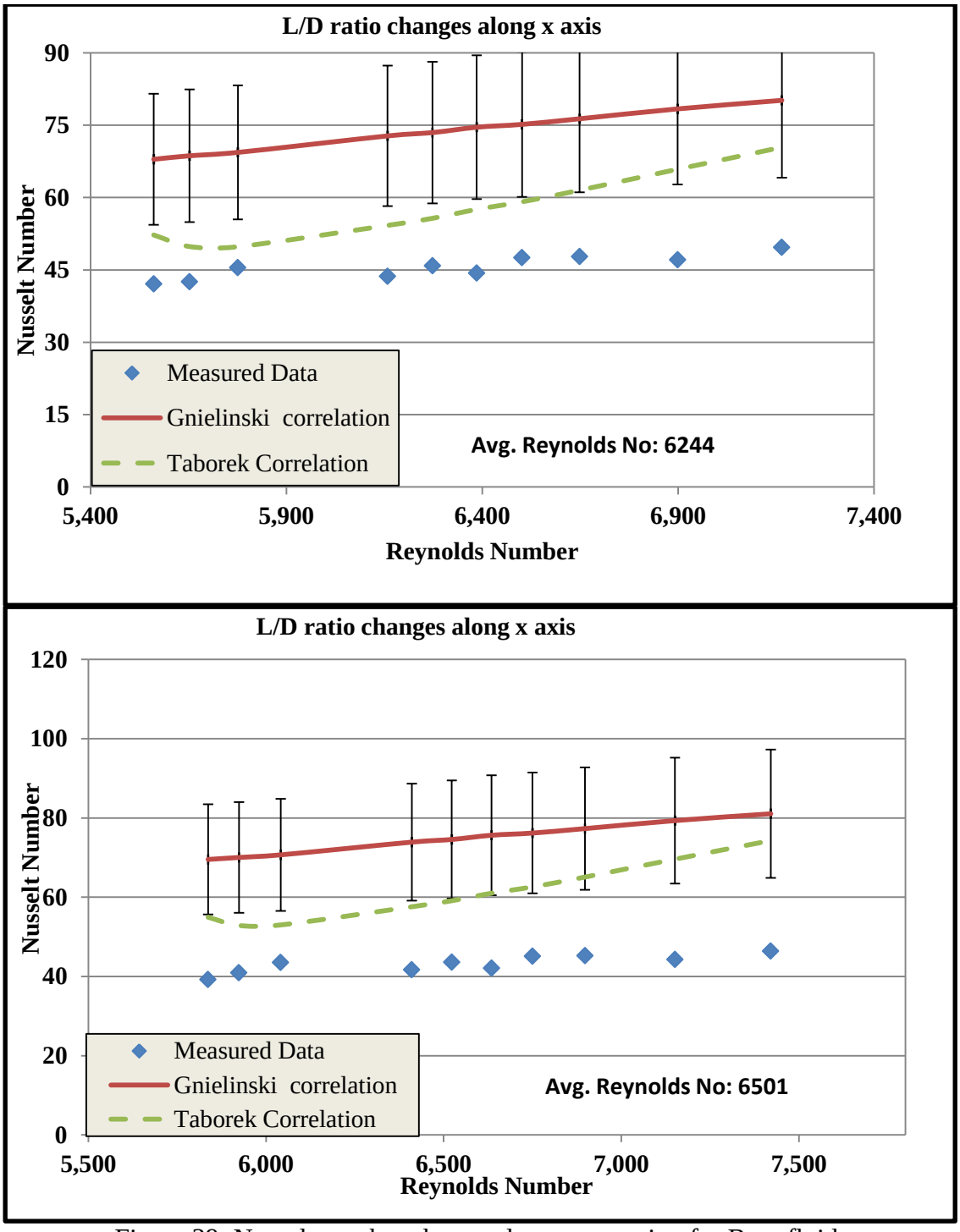

Figure 39: Nusselt number change along test section for Base fluid

Forced convection heat transfer measurements were made with SiC nano-fluids with volume concentrations of 0.55%, 1.0% and 1.6%. Some experimental data collected are presented below starting with 0.55% volume conc. SiC nano-fluid. Figure 40 to Figure 42 data is for 0.55% volume concnetartion. These data also cover the laminar and transition regions of Reynolds number.

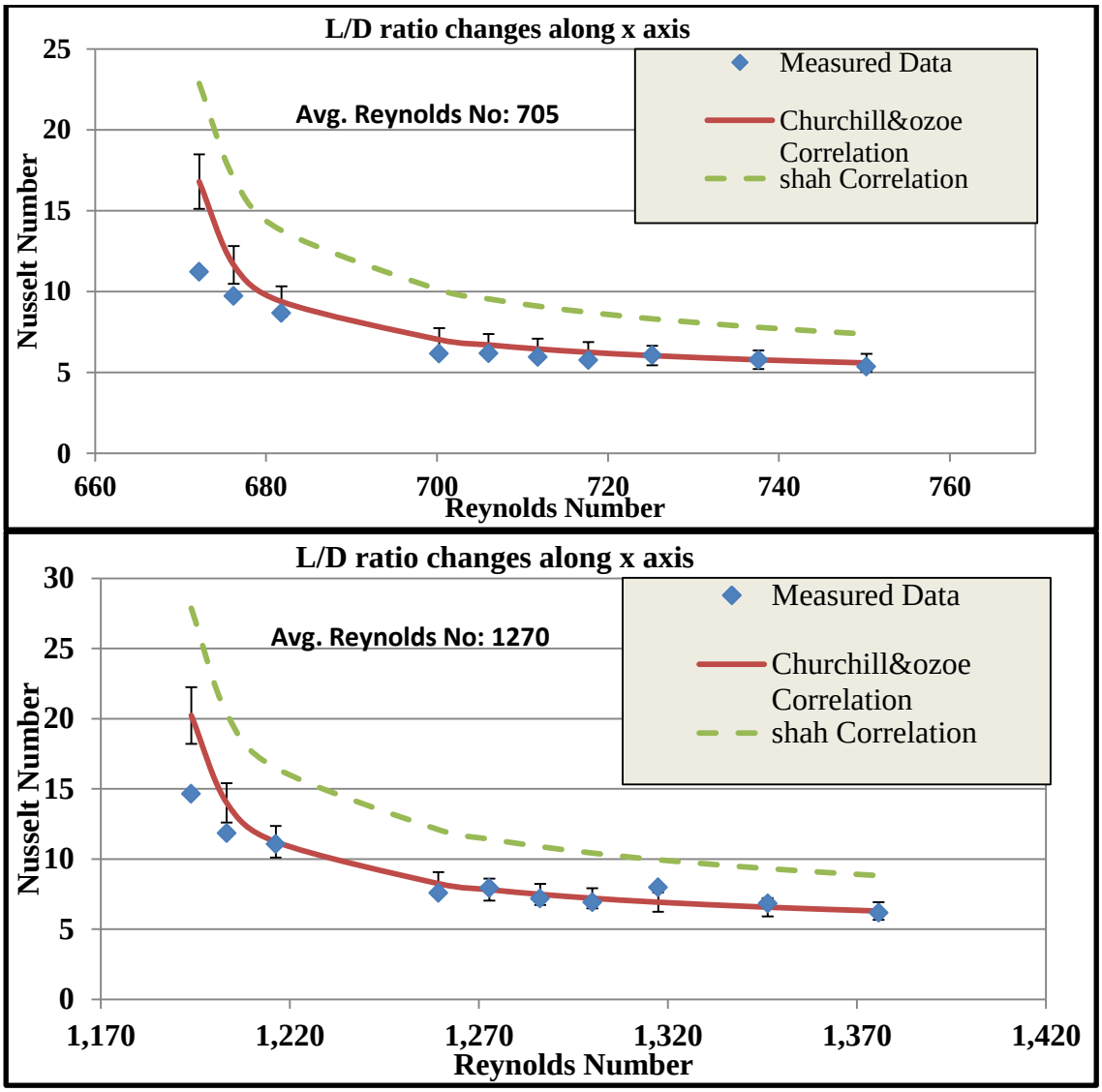

Figure 40: Nusselt number change along test section for 0.55% SiC nanofluid
Error bar displayed in graph for Churchill & ozoe ±10%

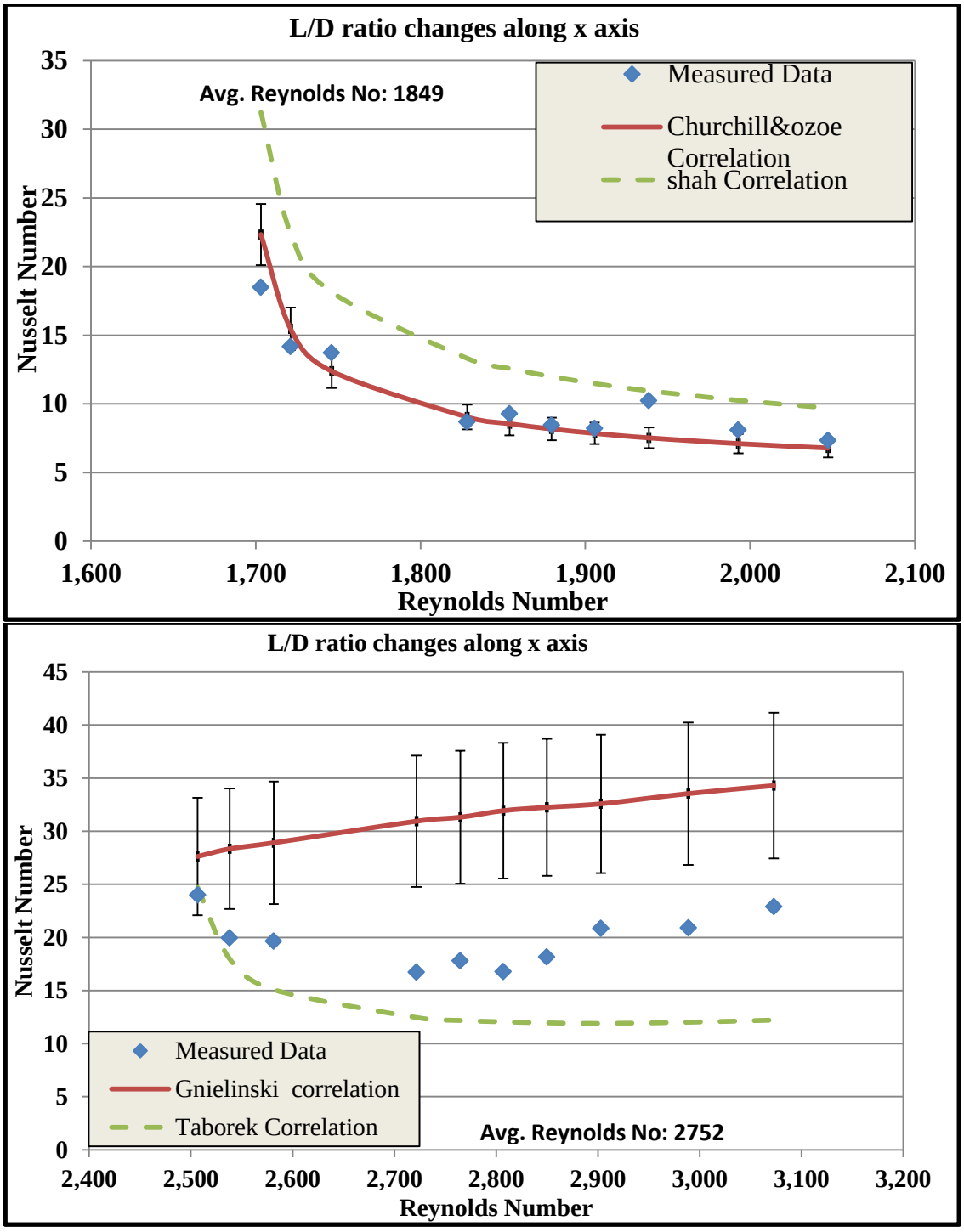

Figure 41: Nusselt number change along test section for 0.55% SiC nano-fluid
Error bar in displayed in graph for Gnielinski correlation is 20% [12]

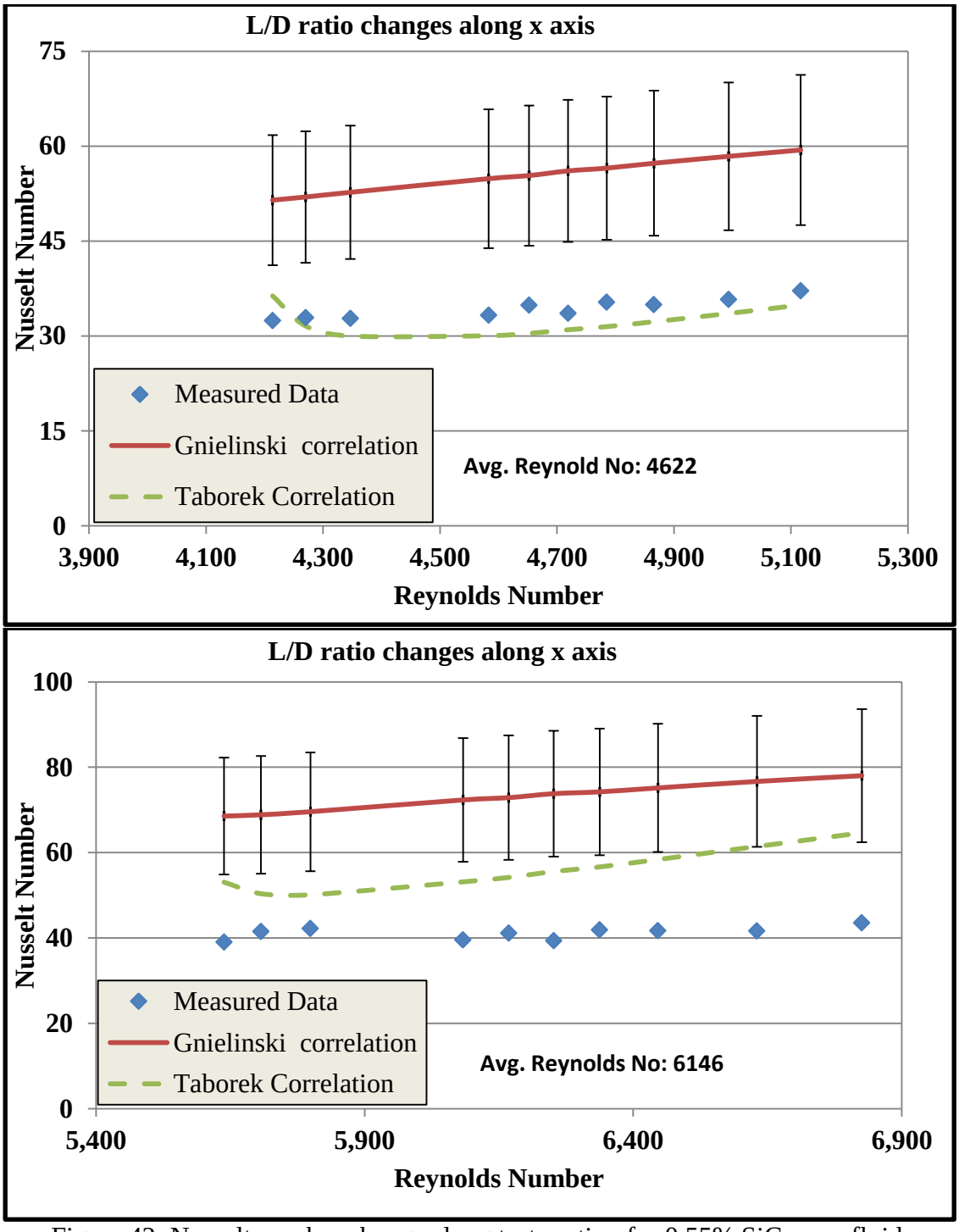

Figure 42: Nusselt number change along test section for 0.55% SiC nano-fluid

Some experimental heat transfer data collected for 1 % volume concentration SiC nano-fluid are presented below shown from Figure 43 & Figure 45 as variations of Nusselt number with Reynolds number.

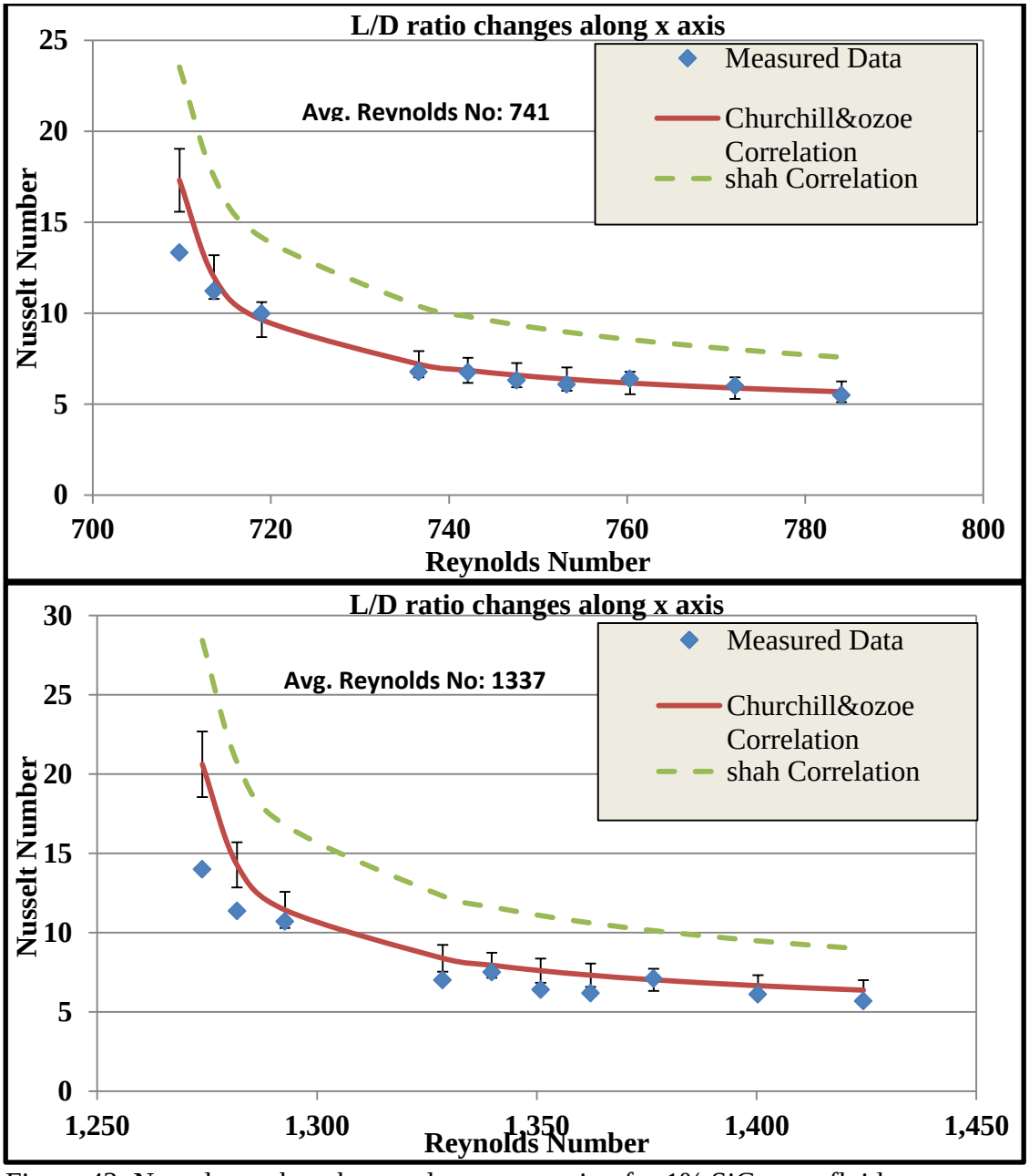

Figure 43: Nusselt number change along test section for 1% SiC nano-fluid
Error bar displayed in graph for Churchill & ozoe ±10%

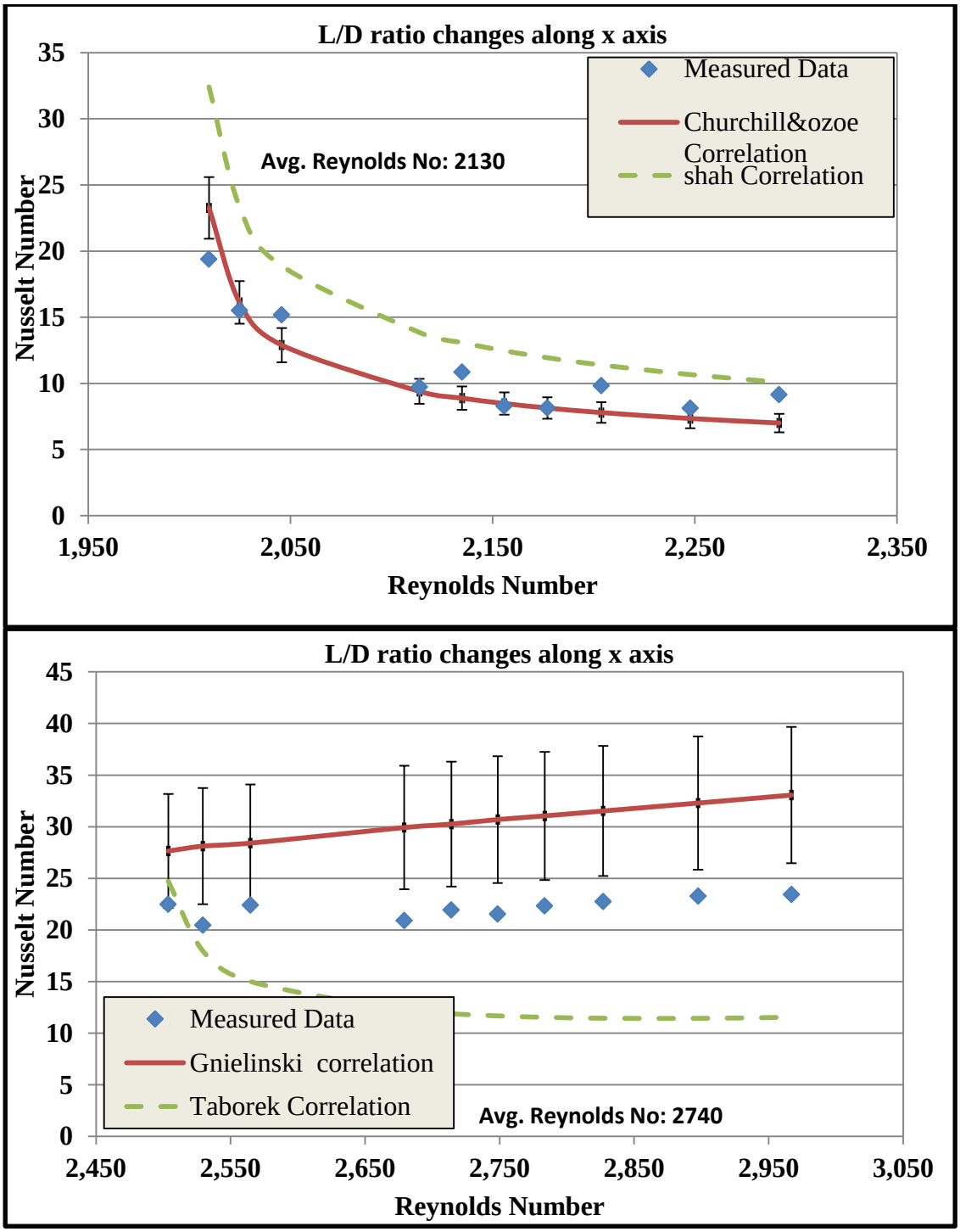

Figure 44: Nusselt number change along test section for 1% SiC nano-fluid
Error bar in displayed in graph for Gnielinski correlation is 20% [12]

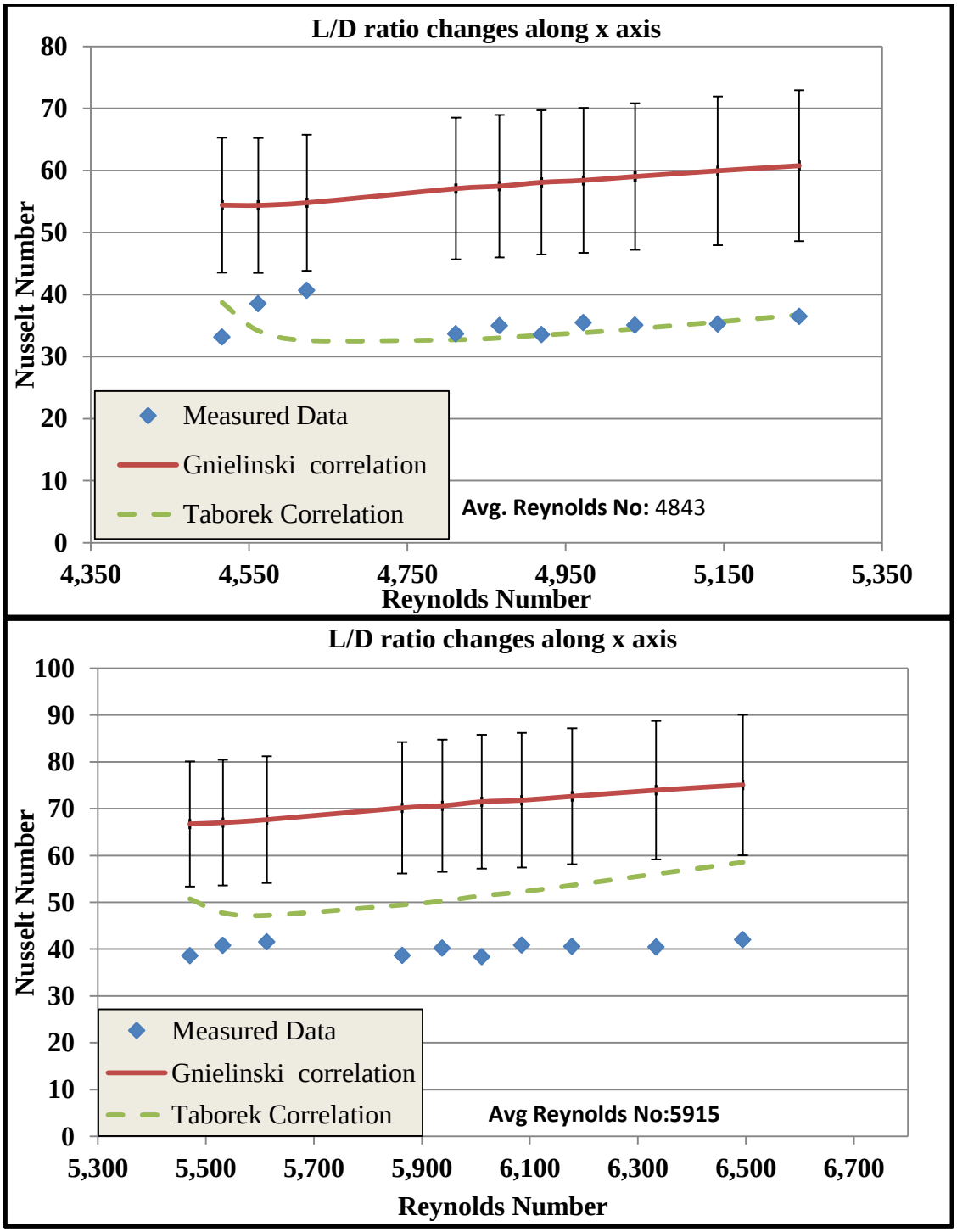

Figure 45: Nusselt number change along test section for 1% SiC nano-fluid

Some experimental heat transfer data collected for 1.6 % volume concentration SiC nano-fluid are presented below shown from Figure 46 & Figure 48 as variations of Nusselt number with Reynolds number.

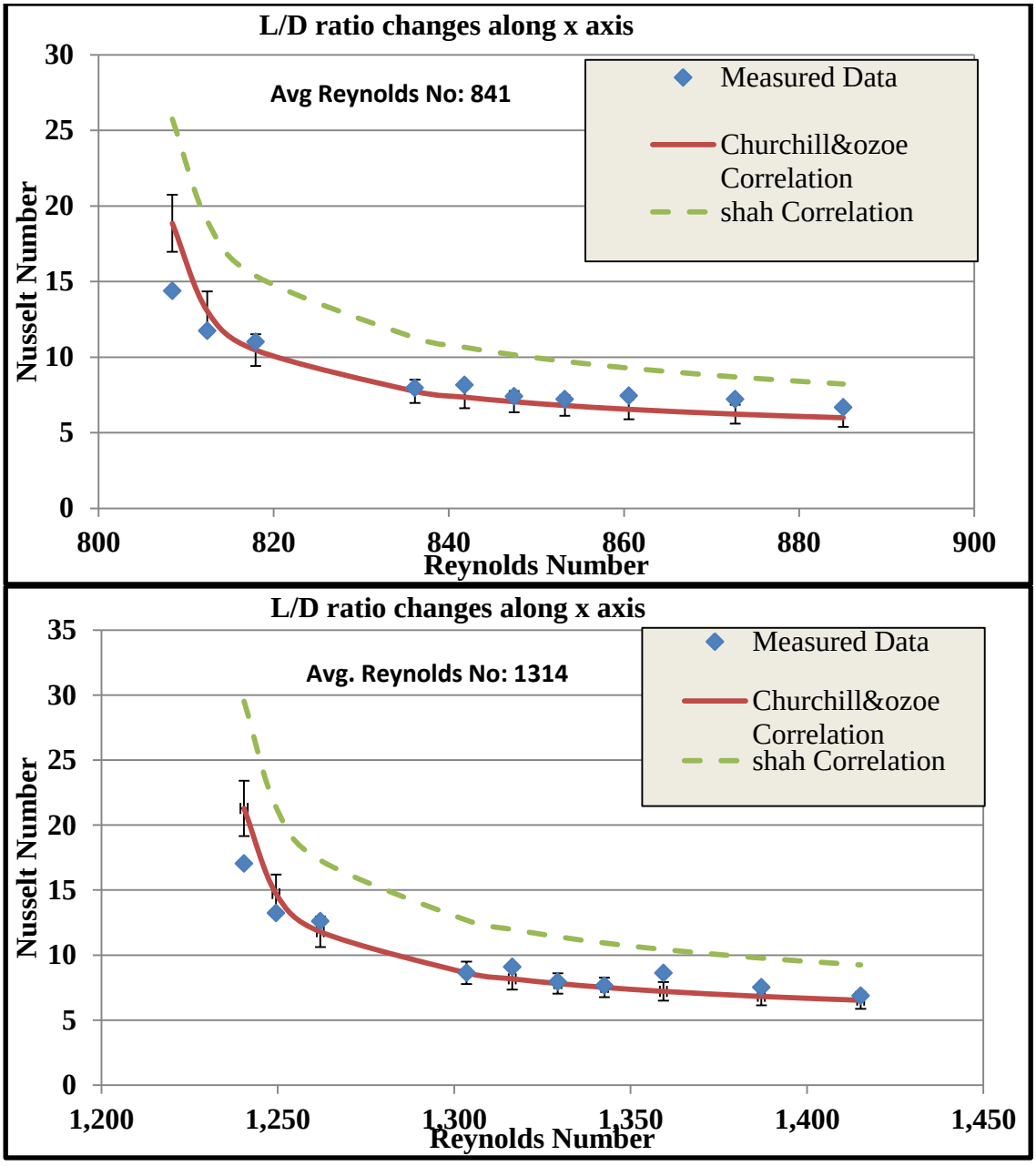

Figure 46: Nusselt number change along test section for 1.6% SiC nano-fluid
Error bar displayed in graph for Churchill & ozoe ±10%

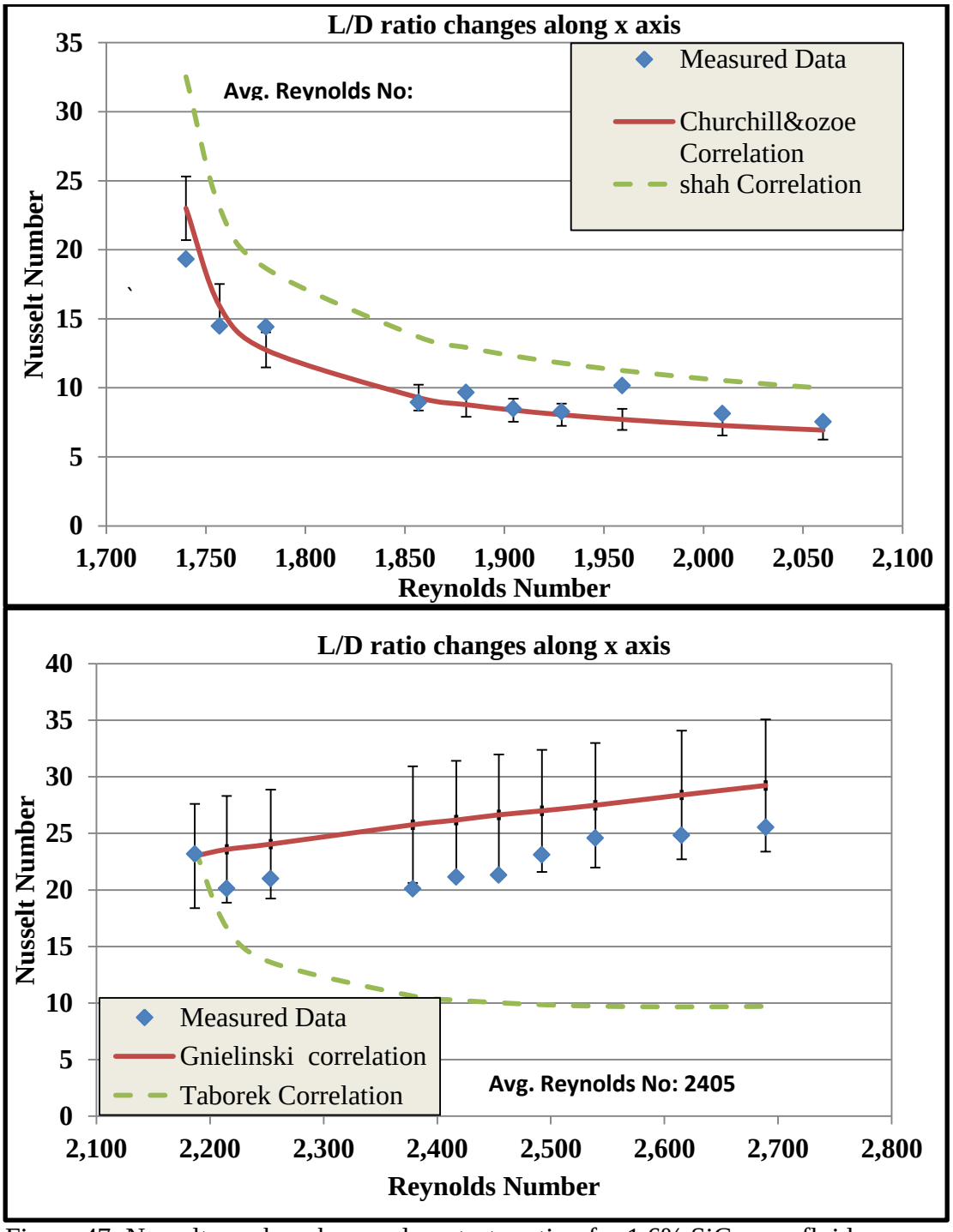

Figure 47: Nusselt number change along test section for 1.6% SiC nano-fluid
Error bar in displayed in graph for Gnielinski correlation is 20% [12]

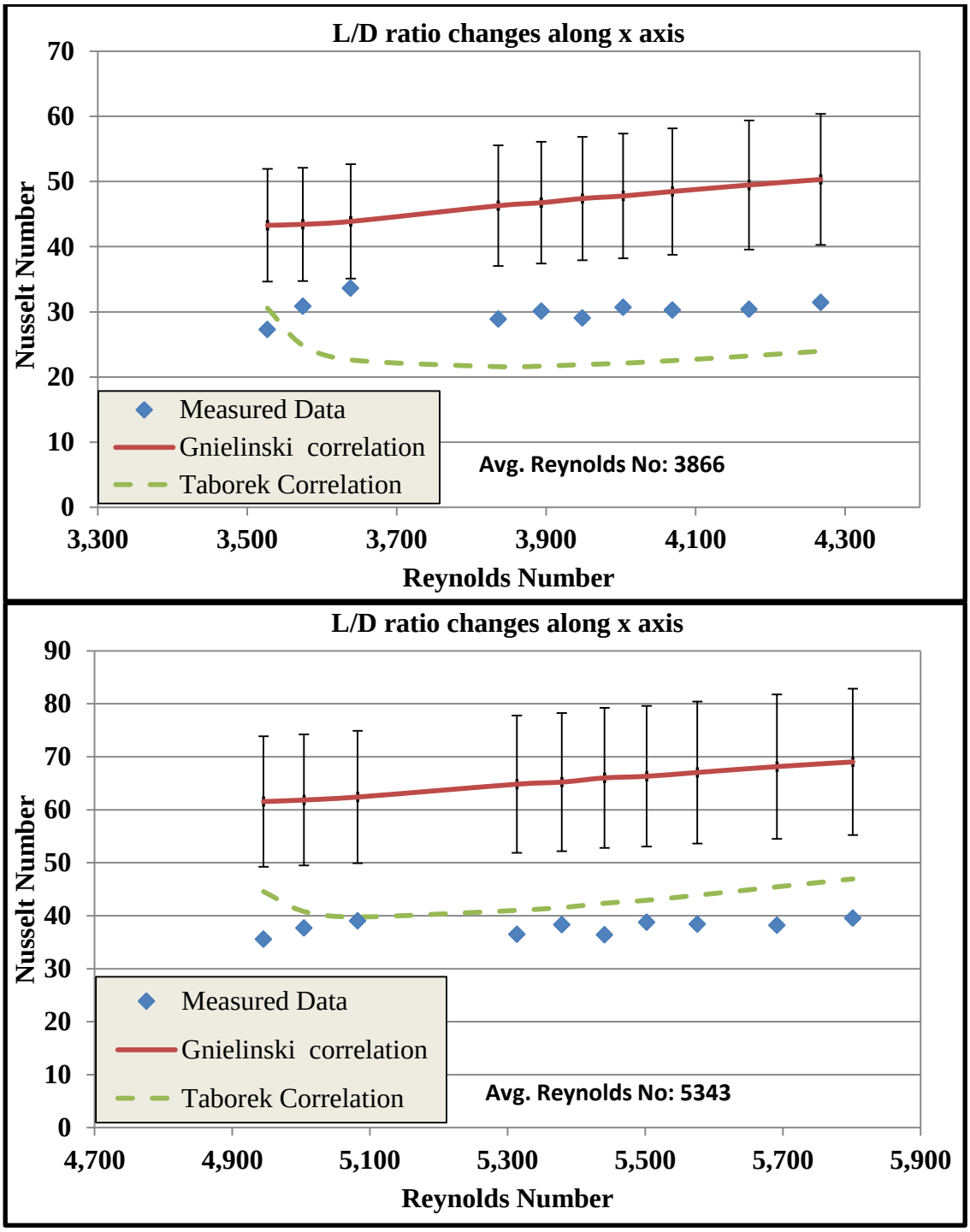

Figure 48: Nusselt number change along test section for 1.6% SiC nano-fluid

5.6. Deviation of experimental results from correlations

In the laminar flow regime, the average deviation of experimental Nusselt number data is about ±10% when compared with Churchill and Ozoe correlation. Deviation observed with Shah and London correlation was higher with an average deviation of -35%.

In the transition flow regime, the average deviation of experimental Nusselt number is -40% when compared with Gnielinski correlation. When the same is compared with Taborek correlation the deviation is very high at +60% for Reynolds number ranging from 2300 to 4000 and average deviation is ±25% for the Reynolds number ranging from 4000 to 6500.

The average deviation projected above is observed for base fluid as well as 0.55%, 1% and 1.6% volume concentration SiC nano-fluids.

While, experimental data in laminar region is well comparable with Churchill and Ozoe correlation, both correlations considered for transition region did not accurately predict the Nussult number.

Gnielinski correlation is considered to be not very accurate in the transition region [12, 16]. Ghajar [12] indicated that the majority of the Gnielinski's data falls in the fully turbulent regime, i.e. Reynolds number above 8000. Therefore, Ghajar [12] states that the Gnielinski considered his correlation is suitable for turbulent pipe and channel flows. Further, Gnielinski correlation relation as such has a deviation limit of ±20% [12].

Taborek correlation is just a linear proration of Nusslet number obtained from laminar correlation and turbulent correlation between 2000 to 8000 Reynold number [16]. This correlation is dependent on Gnielinski's values and moves towards the Gnielinski correlation as it approaches Reynolds number 8000. Hence, it may not be very accurate as the formulation is just a linear proration than experimental findings.

5.7. Nusselt number

From the experimental values, it is observed that there is little enhancement of heat transfer and Nusselt number for 0.55% and 1% volume concentrations of SiC nano-fluids compared to its base fluid. Enhancement is observed for 1.6% volume concentration. From the Figure 49 & **Figure 51,** we can observe that the difference in Nusselt value of base fluid and nano-fluid is decreasing as the percentage of the nano particles are increase and for 1.6% volume concentration SiC nano-fluid, the Nusselt number generated is greater than the base fluid. Based on the curve fitting equations obtained using the experimental Nusselt number, on an average, 0.55%, 1% SiC nano-fluids displayed Nusselt number -3.4%, -2.3% and for 1.6% SiC nano-fluid average enhancement of +6.8% is observed than that of base fluid respectively.

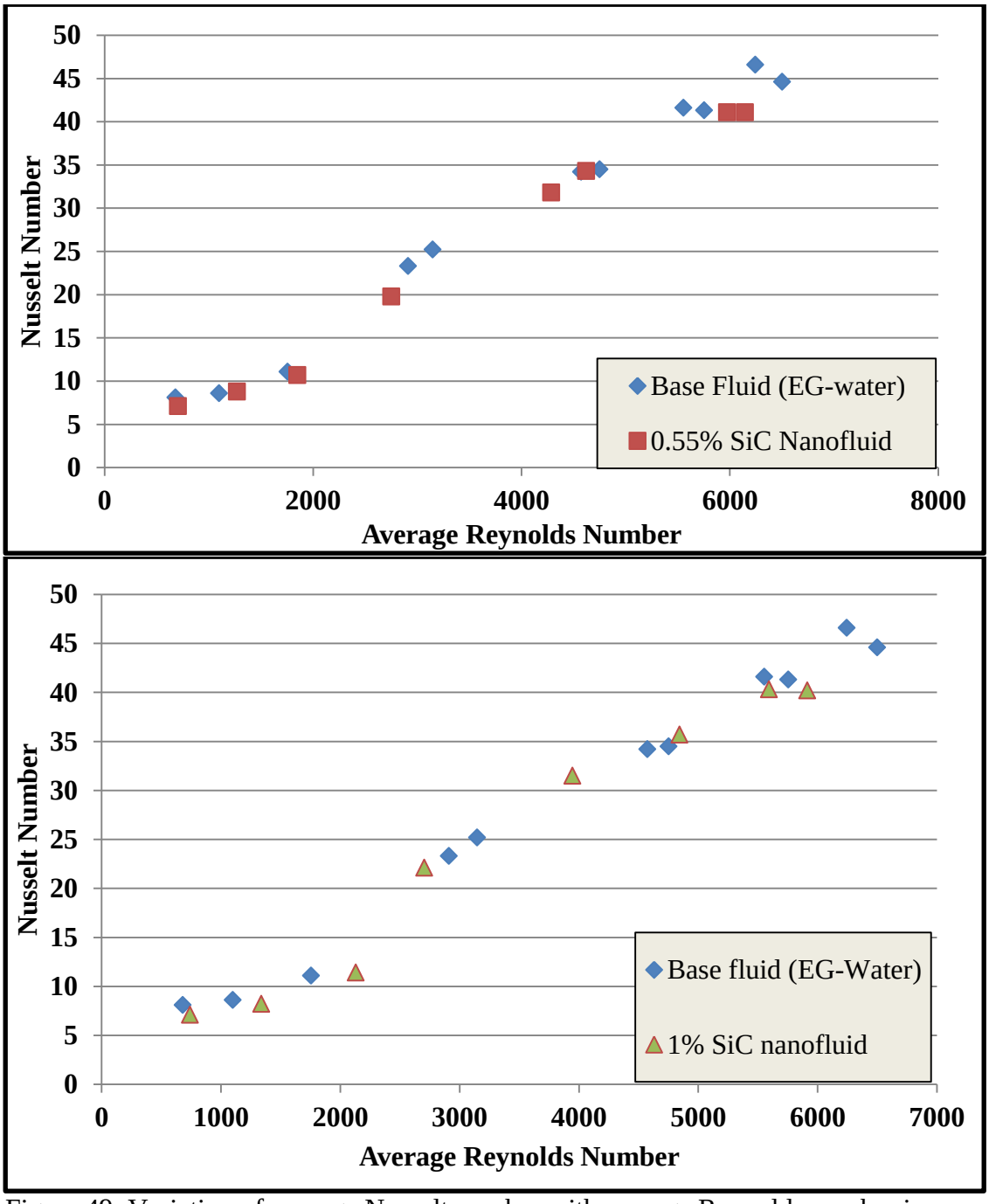

Figure 49: Variation of average Nusselt number with average Reynolds number is plotted for 0.55% SiC nano-fluid and compared with basefluid

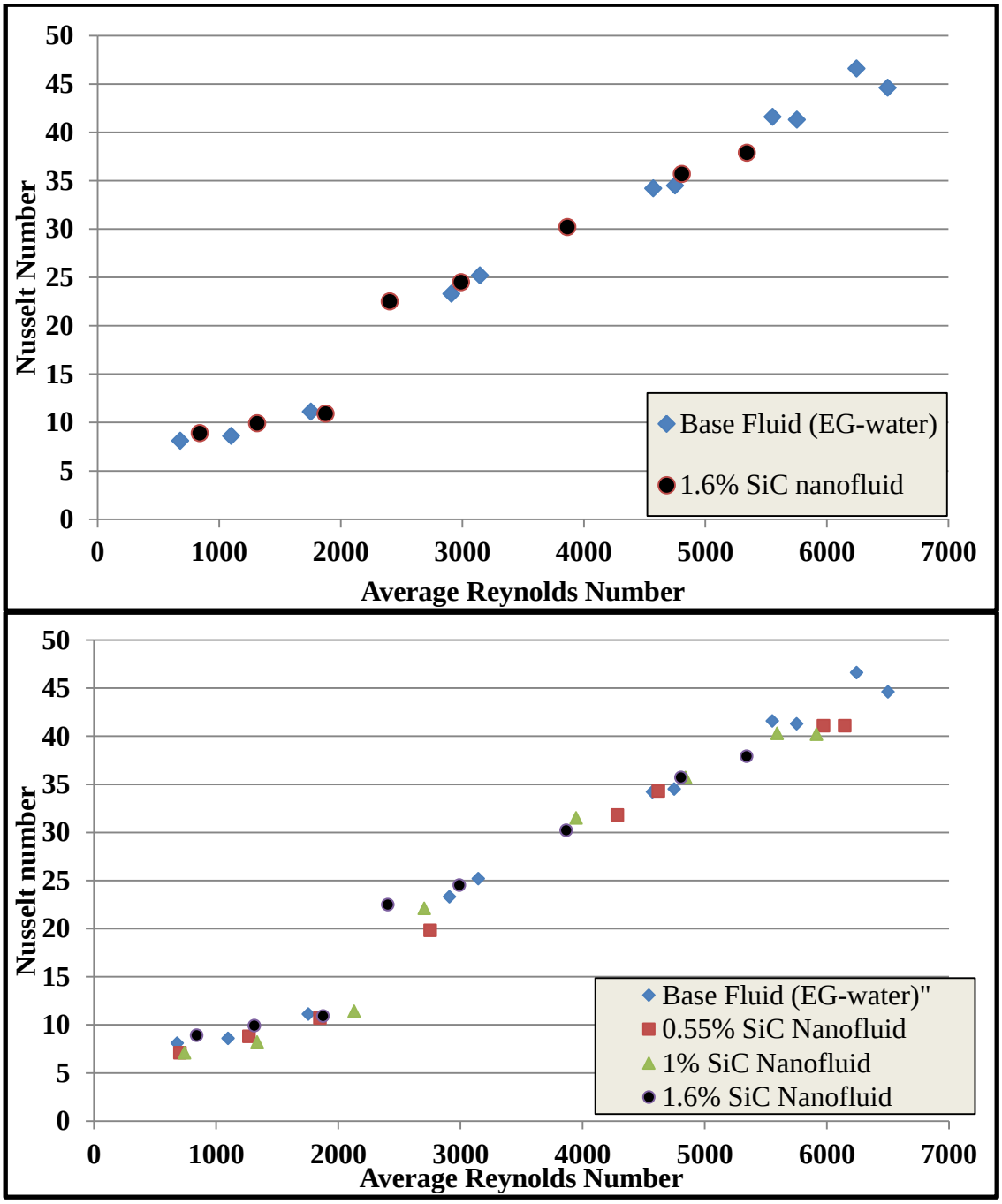

Figure 50: Variation of average Nusselt number with average Reynolds number is plotted

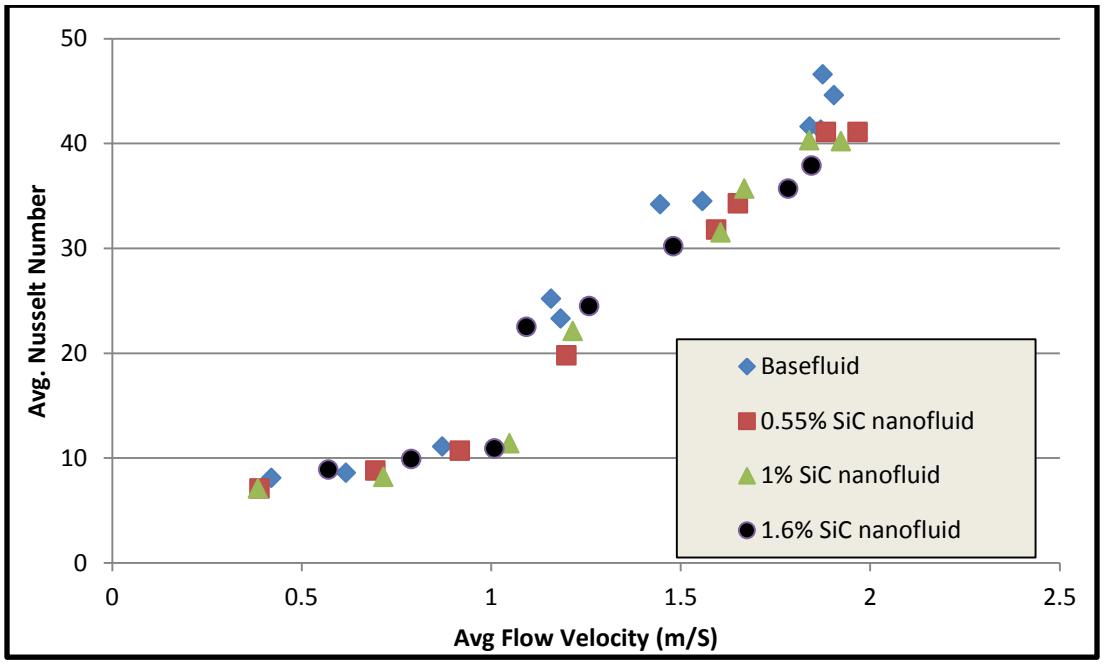

Figure 51: Variation of average Nusselt number with average flow velocity is plotted for all the three volume concentration and compared with base fluid

Nusselt number is directly proportional to heat transfer coefficient and inversely proportional to the thermal conductivity of the fluid in consideration. Since, the thermal conductivity value of the nano-fluids are higher than that of base fluid, we observe lower nusselt number values for nano-fluid when there is a marginal increase in heat transfer coefficient. Hence, comparing Nusselt number sometimes may be misleading when comparing heat transfer characteristic of nano-fluids [18], but this needs to take into account that the Reynolds number is also lower as the viscosity of the nano-fluid is larger.

5.8. Heat transfer coefficient

Since some of the data in the literature is presented in dimensional form, heat transfer coefficient values are presented for the experimental data at different volume concentrations of SiC nano-fluid and the base fluid. Heat transfer coefficient is plotted against Reynolds number and flow velocity.

Based on the curve fitting equations obtained from the experimental data points variation with Reynolds number, on an average, 0.55% volume concentration showed a decrease of 2.8% in heat transfer coefficient than it base fluid, 1% SiC nano-fluid displayed an increase of 4% percent increase on an average and for 1.6% there was an enhancement of 10.1% on an average. While enhancement of heat transfer coefficient is observed for 1% and 1.6% volume concentration SiC nano-fluid, there was marginal decrease (within experimental uncertainty) in heat transfer coefficient value of 0.55% SiC nano-fluid than its base fluid shown in the Figure 52 &Figure 53.

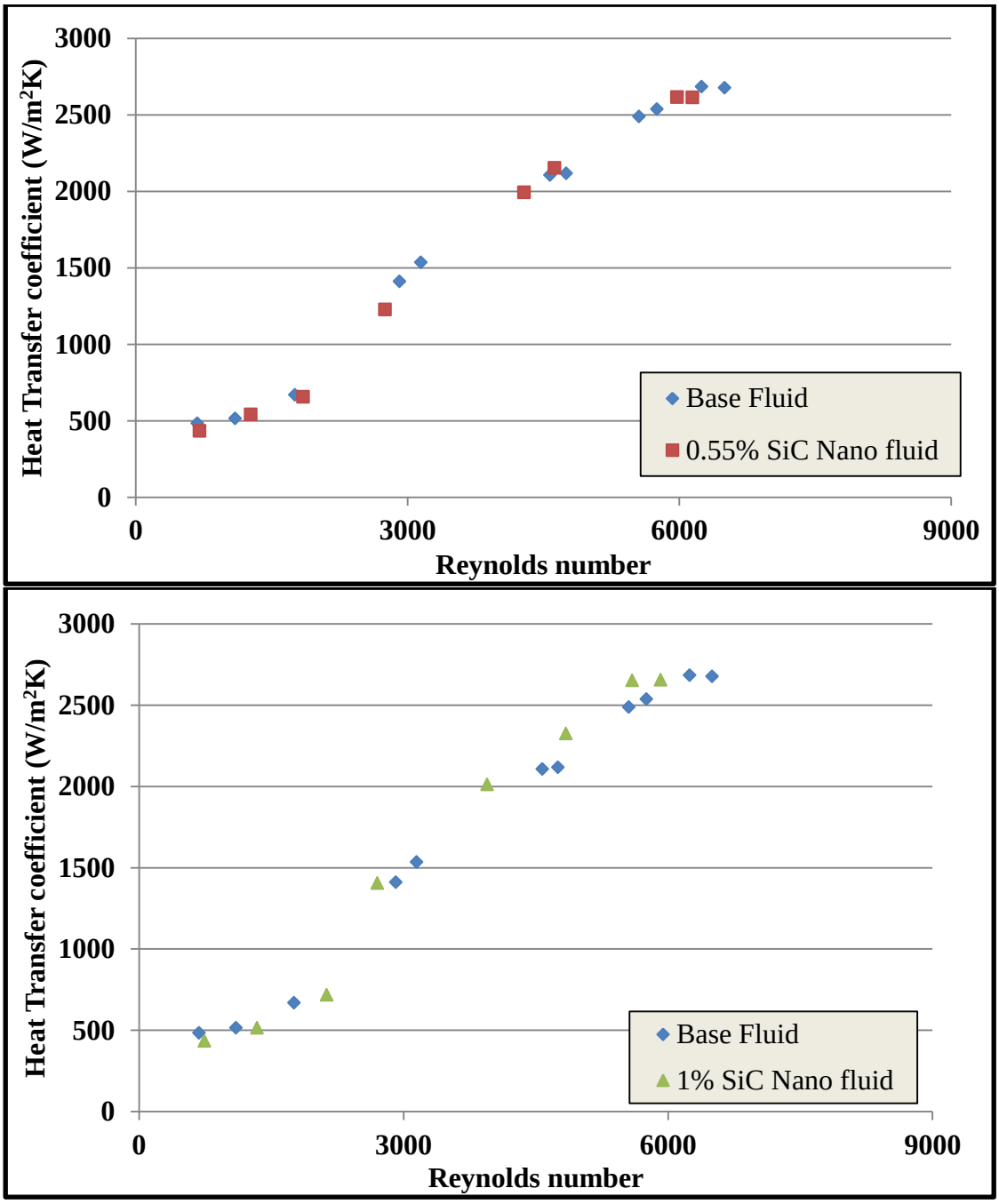

Figure 52: Heat transfer coefficient variation with Reynolds number for 0.55% and 1% volume concentration SiC nanofluid

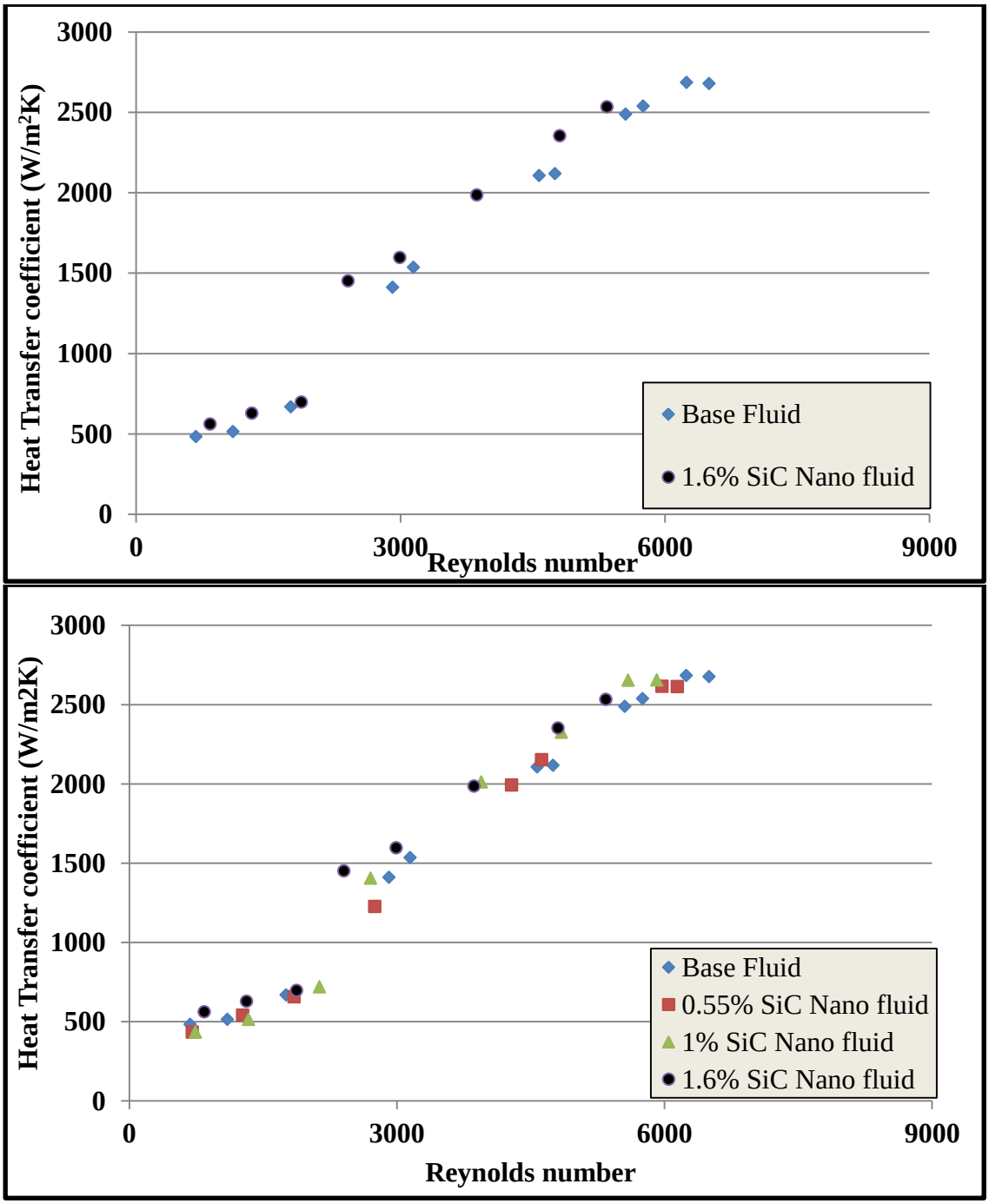

Figure 53: Heat transfer coefficient variation with Reynolds number for SiC nano-fluids

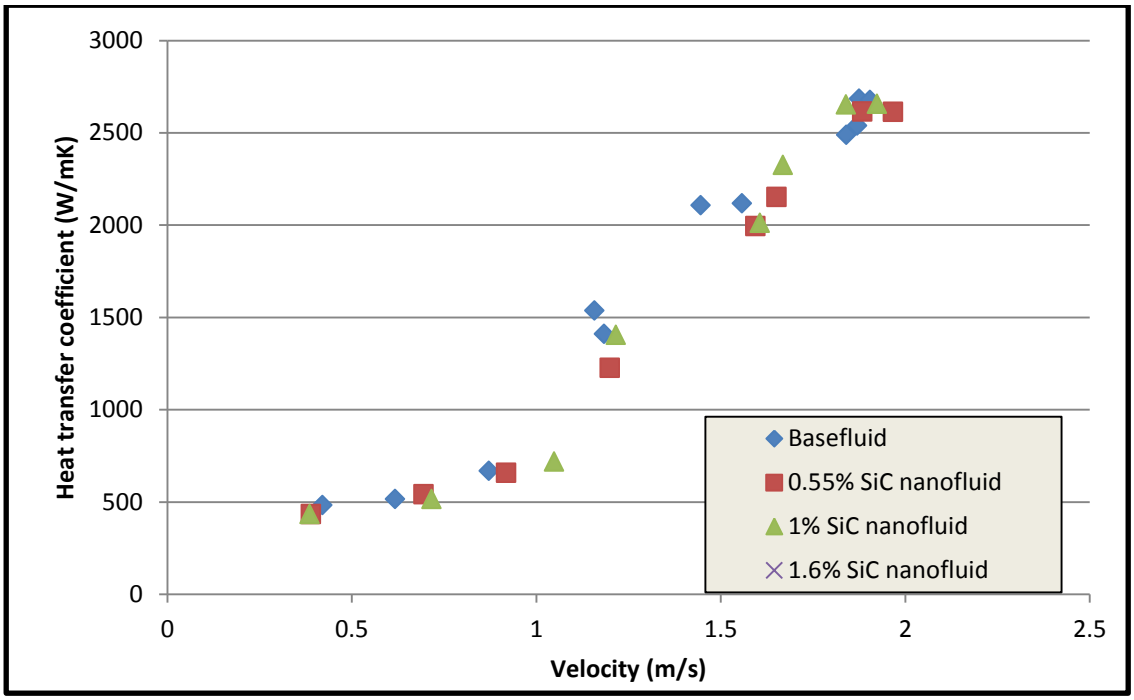

Figure 54: Heat transfer coefficient variation with average flow velocity for all three volume concentrations of SiC nano-fluids and base fluid

5.9. Pressure Drop

Pumping power and pressure drop are also important parameters in weighing the efficacy of nano-fluids in the context of heat transfer. Pressure drop is measured across the test section for all the experiments using a differential pressure meter. A comparison of obtained pressure drop values was made with the theoretical Darcy-Weisbach equation.

$$\Delta p = f_D \times \frac{L}{D} \times \frac{\rho \times u^2}{2} \qquad (20)$$

Δp= pressure Drop (Pa);

L/D = ratio of length to diameter of pipe;

ρ =density of fluid (kg/m3);

u=mean flow velocity (m/s);

f_D= Darcy Friction Factor (no units)

Measured pressure drop values obtained for base fluid are well in agreement with the theoretical predictions obtained from Darcy-Weisbach equation with an average deviation less than 10% shown in the Figure 55

We can observe from the figures 56 & 57 that the pressure drop is increasing with the increase in the percentage of SiC nano particles. This is due to higher viscosity values of SiC nano-fluid than its base fluid. There is an increase in average pressure drop of 6.9%, 22.8% and 38.5% for 0.55%, 1% and 1.6% volume concentrations SiC nano-fluid respectively when compare to its base fluid.

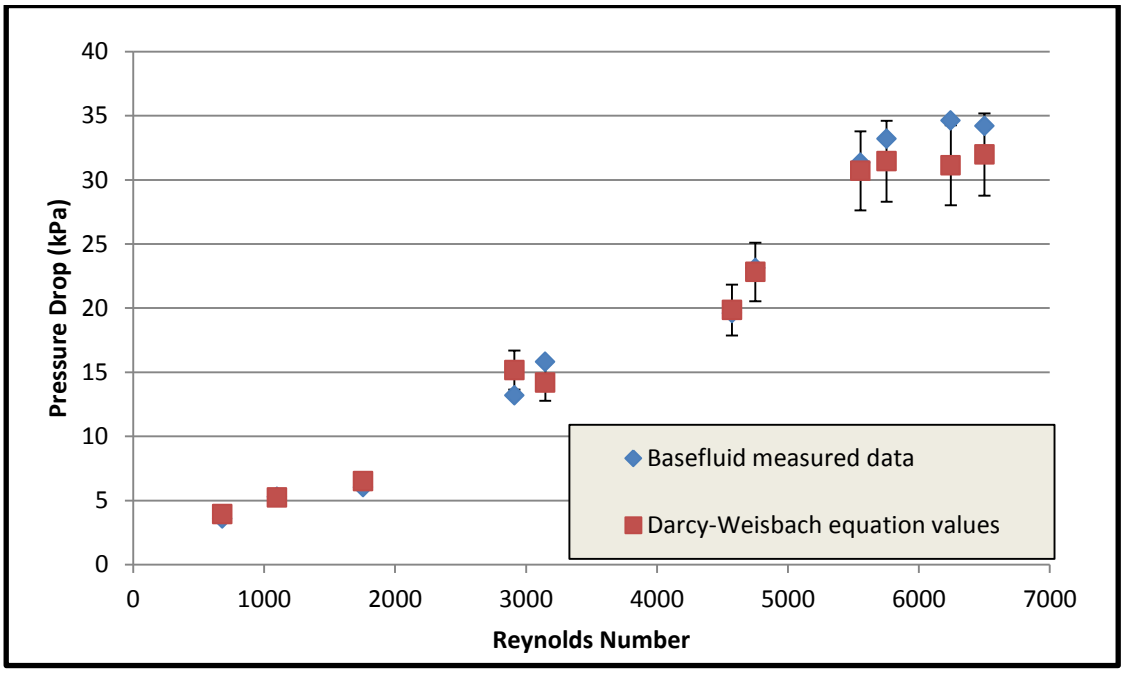

Figure 55: Variation of pressure drop with Reynolds number for base fluid and comparison of measured data with theoretical value from Darcy-Weisbach equation

Error bar for Darcy-Weisbach equation is ±10%

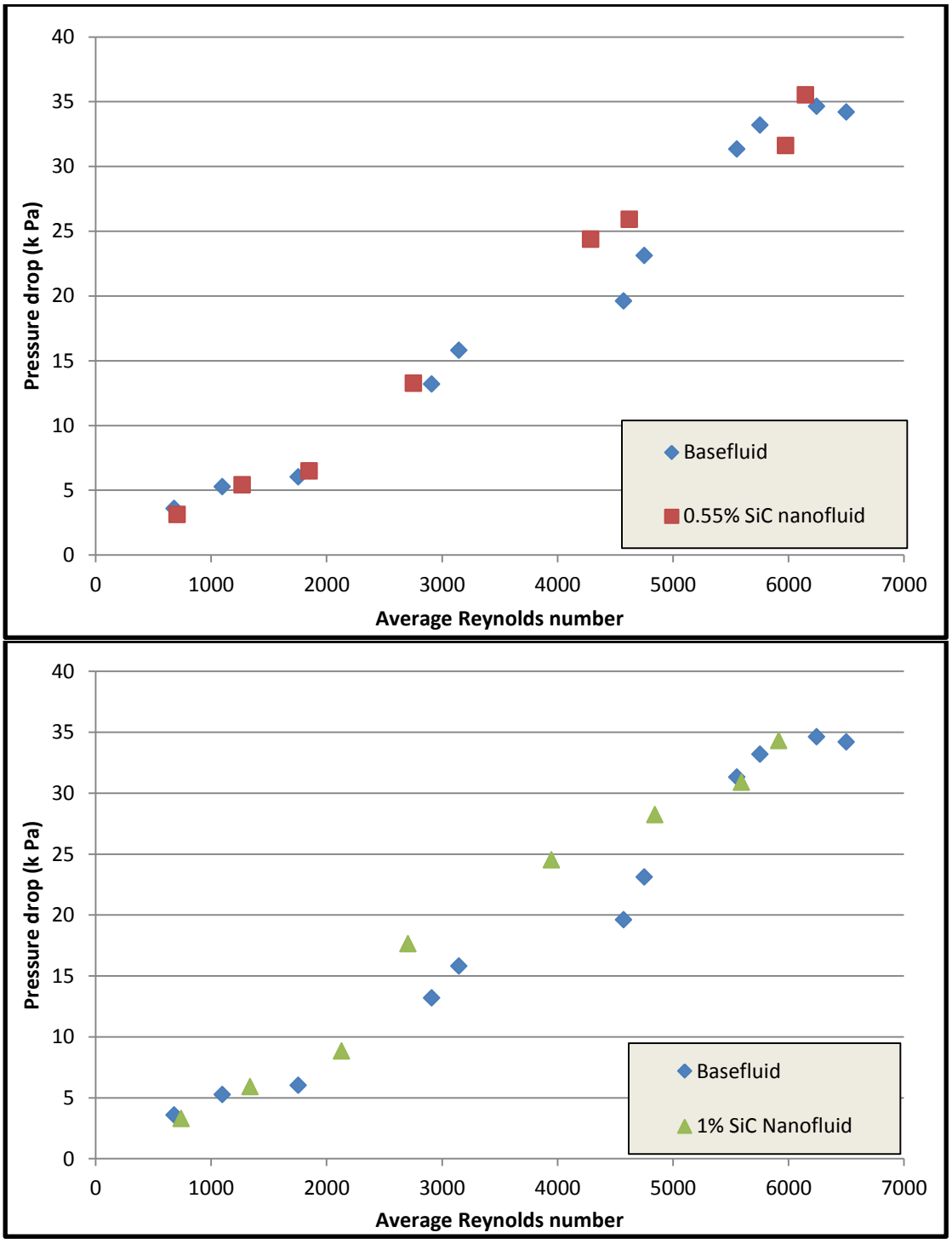

Figure 56: Pressure drop variation with Reynolds number for 0.55% and 1% volume concentration SiC nano-fluid

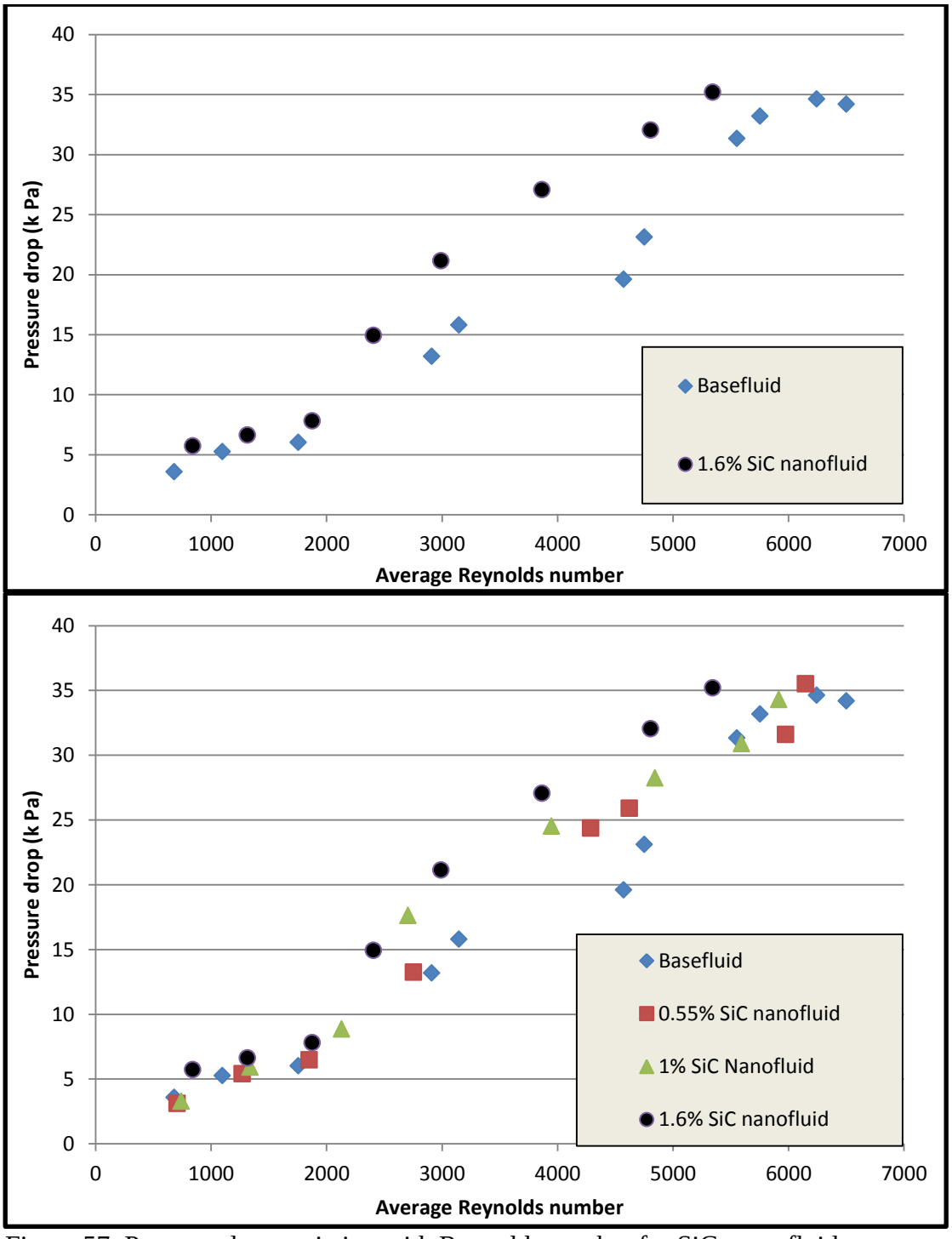

Figure 57: Pressure drop variation with Reynolds number for SiC nano-fluids

5.10. Effectiveness of Nano-fluids

Use of nano-fluids is expected to improve the heat transfer performance but it can also result in increases in the pressure drop in the system and corresponding increase in the pumping power requirements. Hence, to make nano-fluid feasible for use in heat exchangers, the increase in heat transfer properties of nano-fluids should be significantly high enough to compensate the increased energy requirement to pump the fluid. To compare the effectiveness of the nano-fluids, a thermal-hydraulic performance factor is formulated. In literature, the performance factor was defined in two ways, one based on Nusselt number [19] and other is based on heat transfer coefficient [17, 19]. Thermal-Hydraulic Performance factor is defined as:

$$\eta_{\mathrm{Re}} = \frac{\alpha}{\beta} \qquad (21)$$

Performance factor based on Nusselt number

$$\alpha = \frac{\text{avg. Nusselt number of nanofluid}}{\text{avg. Nusselt number of base fluid}}$$

$$\beta = \left(\frac{\text{Friction factor of nano} - \text{fluid}}{\text{Friction factor of base fluid}}\right)^{\frac{1}{3}}$$

Performance factor based on Heat transfer coefficient

$$\eta_{\mathrm{Re}} = \frac{\gamma}{\tau} \qquad (22)$$

$$\gamma = \frac{\text{avg. Heat transfer Coefficient of nanofluid}}{\text{avg. Heat transfer Coefficient of base fluid}}$$

$$\tau = \left(\frac{\text{Pressure drop of nano} - \text{fluid}}{\text{Pressure drop of base fluid}}\right)$$

It is clear that such a parameter has to be used with some caution since the Reynolds number changes as the viscosity of the nano-fluid changes with temperature and the addition of nanoparticles. Thus even for the same mass flow rate in the pipe, the Reynolds number is continuously changing along the test section length as the temperature increases. Additionally in these experiments only the overall pressure drop (for the whole straight pipe test section) is measured. Thus an average Reynolds number is used to present the data below though the Reynolds number is different at different points along the pipe. Thus though the viscosity of the nano-fluid is larger, the overall pressure can be lower since the viscosity is decreasing with temperature along the pipe length. Nonetheless this could a useful way of analyzing the data.

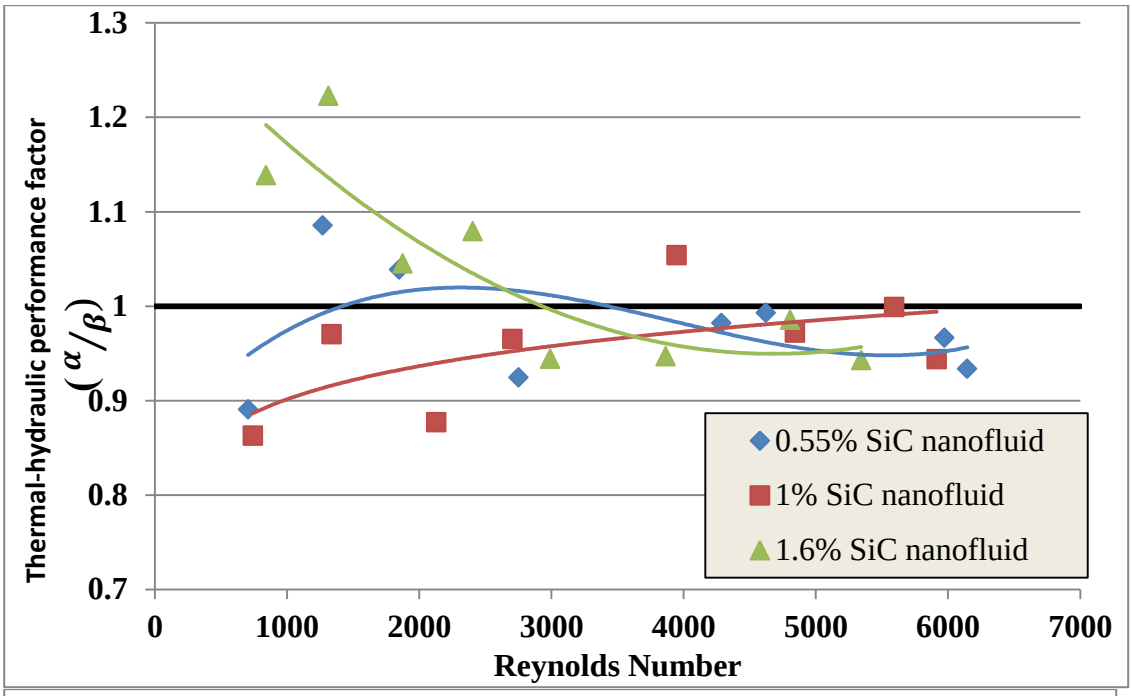

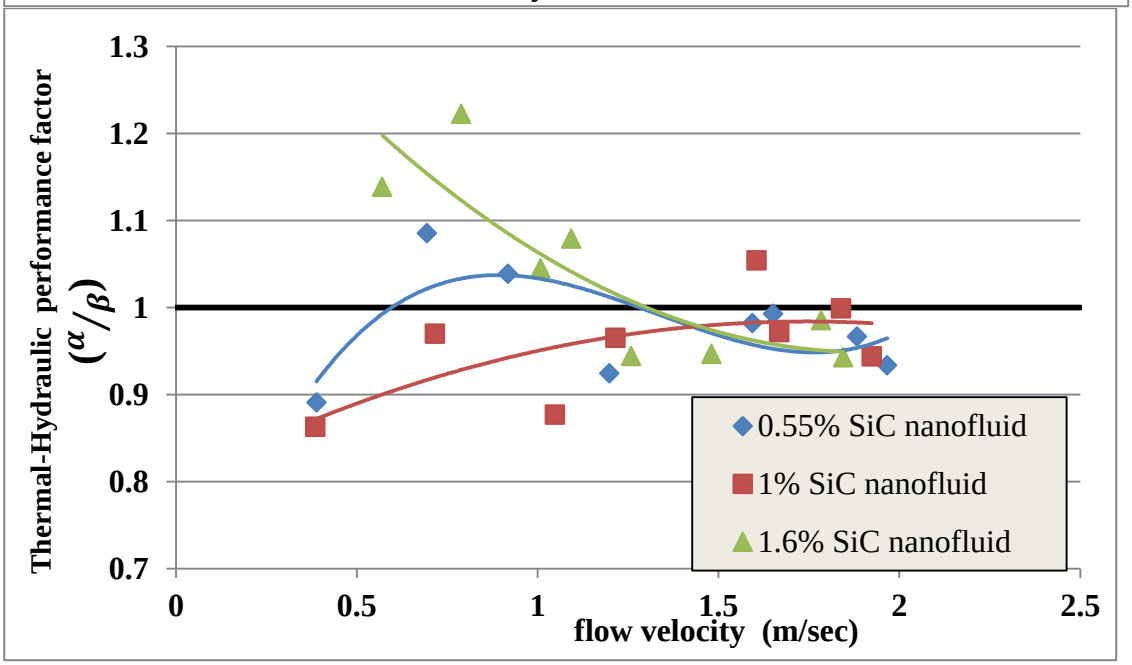

Figure 58: Nusselt number based Thermal-Hydraulic performance factor is plotted against Reynolds number and average flow velocity for 0.55%, 1% and 1.6% SiC nano-fluids. $\alpha = \frac{Nu_{nf}}{Nu_{bf}}$; $\beta = \left(\frac{friction\ factor_{nf}}{friction\ factor_{bf}}\right)^{1/3}$

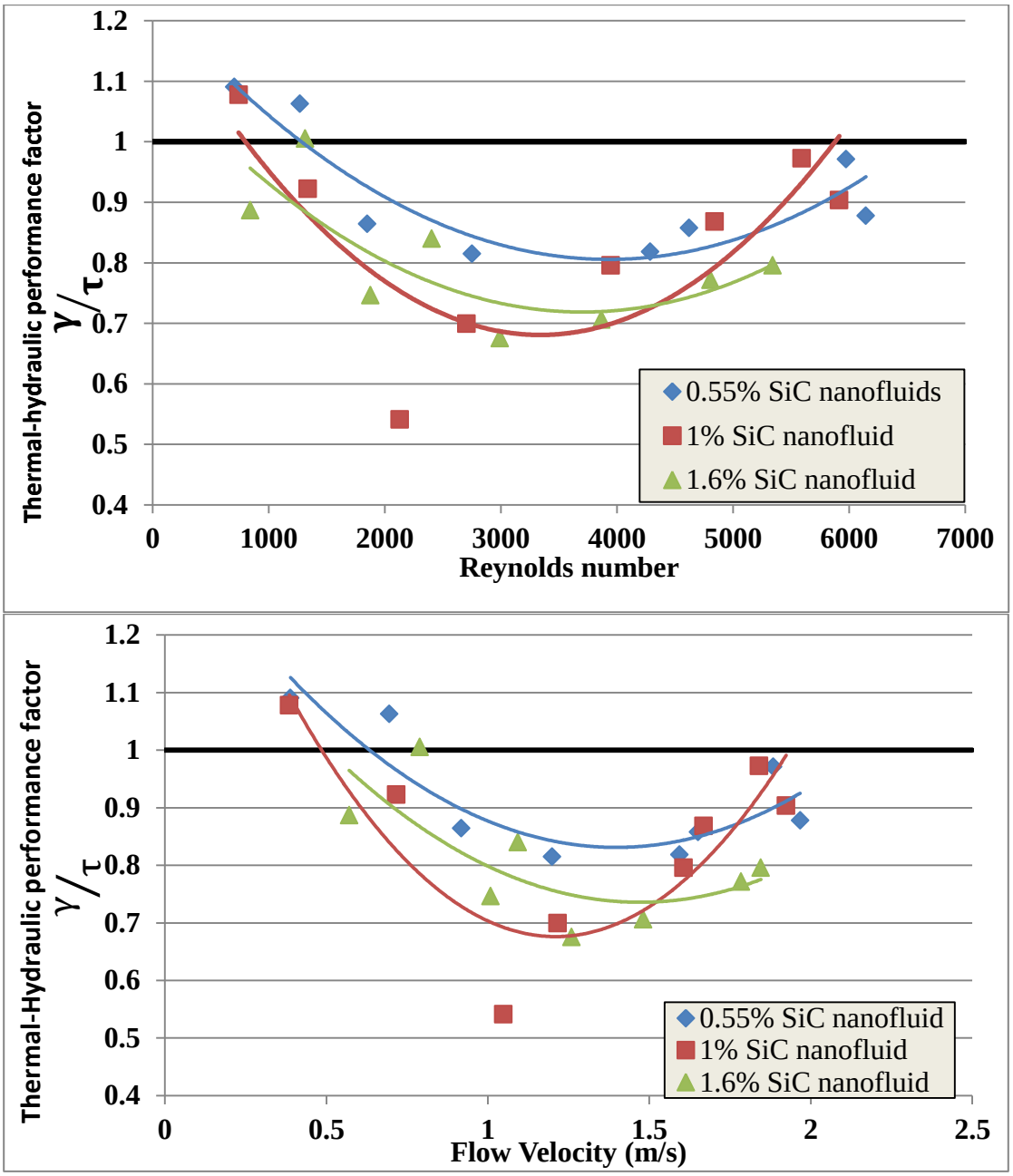

Figure 59: Heat transfer coefficient based Thermal-Hydraulic performance factor is plotted against Reynolds number and average flow velocity for 0.55%, 1% and 1.6% SiC nano-fluids. $\gamma = \frac{H_{nf}}{H_{bf}}$ $\tau = \left(\frac{\Delta P_{nf}}{\Delta P_{bf}}\right)$

Measured Performance factor based on Nusselt number

From the Figure 58 in which the Performance factor is plotted against Reynolds number, we can observe that the performance factor of 0.55% SiC nano-fluids is varying between the values 0.89 and 1.08 in laminar region and the values in transition region is varying from 0.92 to 0.99. From this graph we can infer that the majority of the region falls below 1. When we consider 1% SiC nano-fluid there is an increase of performance factor value from 0.85 at Reynolds number 741 to 0.94 at Reynolds number 5915. While 1.6% volume concentration displayed a superior performance factor values in the laminar region with an average performance factor of 1.13, but the value droped below 1 in the transition region.

Measured Performance factor based on Heat transfer coefficient

From the Figure 59, all the three volume concentrations Performance factor value tend to decrease with the increase in Reynolds number in laminar region and there is an increasing trend in the transition region.

For 0.55% SiC nano-fluid, the range observed is between 1.09 at Reynolds number 705 and 0.86 at Reynolds number 1849 in laminar region and in transition region, the value increased from 0.81 at Reynolds number 2752 to 0.97 at Reynolds number 5974.

Similarly, for 1% SiC nano-fluid, the range observed is between 1.07 at Reynolds number 741 and 0.73 at Reynolds number 1733 in laminar region and in transition region, the value increased from 0.69 at Reynolds number 2704 to 0.97 at Reynolds number 5593.

For 1.6% SiC nano-fluid, the range observed is between 0.89 at Reynolds number 841 and 0.75 at Reynolds number 1876 in laminar region and in transition region, the value observed at Reynolds number 2405 is 0.67 and increased to 0.79 at Reynolds number 5343.

5.11. Results and discussion

To check the results with Timofeeva [18], who also conducted experimentation on α-SiC based nano-fluids for different particle size and 4% volume concentration, we have plotted our data points against flow velocity. Timofeeva [18] data for 90nm SiC nano-fluid have no enhancement in Nusselt number and it is almost same as that of base fluid at all the flow velocities as shown in the Figure 60. From our measured data shown in the Figure 61, we can see that there is no enhancement of nusselt number for SiC nano-fluids with 90nm particle size. On contrary, there is a drop in Nusselt number with -10%, -12% and -6.7% drop is recorded for 0.55%,1% and 1.6% volume concentration SiC nano-fluids respectively. This drop can be contributed to the fact that volume concentration used by Timofeeva [18] is significantly larger (4% volume concentration) than currently used in the experimentation. The maximum volume concentration used in our experiment is 1.6%. Hence, we can conclude that the results obtained from our experiments are consistent with experimental data obtained by Timofeeva [18]. Note that though the velocity range is different in both the experiments, since the graph is linear it is expected to follow same trend even at low flow velocity.

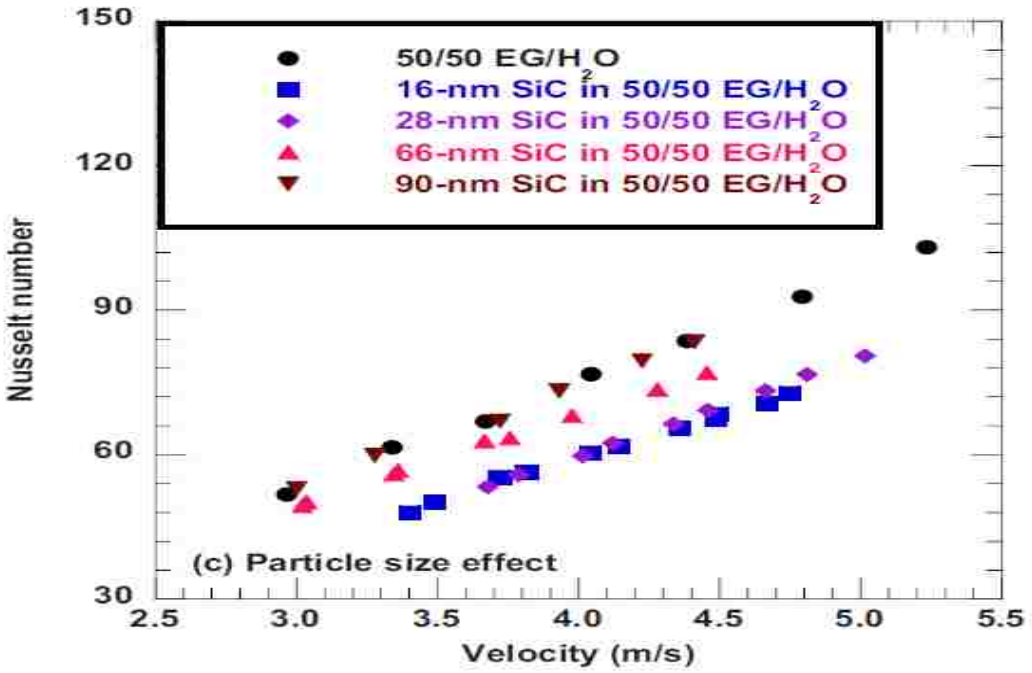

Figure 60: Timofeeva [18] data for SiC based nanofluids

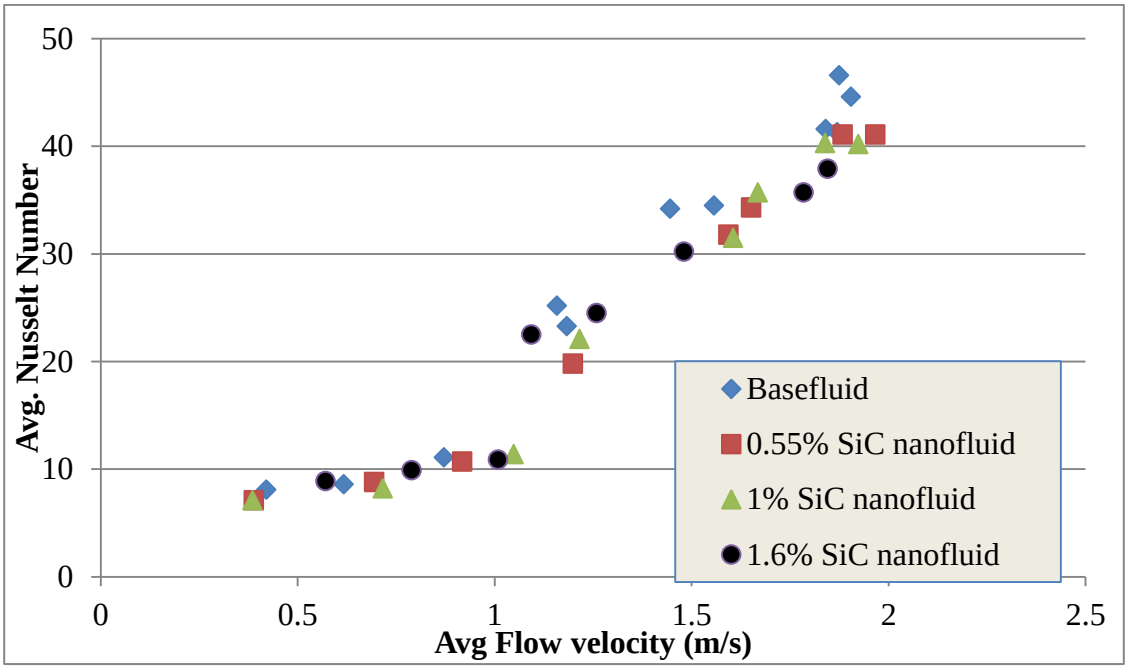

Figure 61: Variation of average Nusselt number with average flow velocity. Measured values obtained for this work

As expected there was an average enhancement of 4% and 6.5% heat transfer coefficient for 1% and 1.6% volume concentrations respectively. There is no improvement of heat transfer coefficient for 0.55% volume concentration. Though there are different theories which explain the enhancement of heat transfer coefficient of nano-fluids, disturbance of boundary layer by the Brownian motion of particles could be one of the mechanisms influencing higher heat transfer coefficient. Thermal diffusion of the particles due to thermal gradient may also lead to increase in heat transfer coefficient [35].

CHAPTER 6: SUMMARY AND CONCLUSIONS

6.1. Summary

After almost two decades of research on the nano-fluids, scientific community still work to engineer a very stable nano-fluid for heat transfer applications with good thermal properties. Among other things, high viscosity along with the stability issues are the primary concerns that are hindering the growth of nano-fluids into commercial products. Though the heat transfer properties for some nano-fluids tend to show satisfactory enhancement, the overall effectiveness drastically comes down due to poor rheological properties.

The present work is an effort to study a nano-fluid based on alpha-Silicon carbide particles. A detailed study was carried out to better appreciate thermal conductivity, viscosity and forced convention properties of SiC based nano-fluids. The base fluid considered here is an Ethylene glycol and water mixture with 50-50% volume concentration.

A heuristic static theoretical model has been formulated to calculate the effective thermal conduction of colloidal fluids. The present model compliments a number of theoretical models that have been used to predict the effective thermal conductivity (ETC) of colloidal fluids such as nano-fluid. The present model establishes the lower and upper bounds for the ETC. A MATLAB program has been generated to calculate ETC taking in to consideration the particle size, shape, thermal conductivities of base fluid and nano-particles, distribution pattern and volume concentration.

Based on the present model, effect of particle size on ETC is only experienced when the particle size is comparable to the system size and become independent when the particle size drops down below certain radius (This is the system containing more millions of particles).

The upper and lower bounds for effective thermal conductivity calculated were compared to the standard models such as Wiener bounds and H-S bounds. It is observed that the bounds are within the Wiener bounds which are considered to be the widest bounds possible.

The alpha-SiC used in the present work is manufactured by Saint Gobien and the current work started with 4 volume percent SiC nano-fluid obtained from Argonne National Laboratory. The SiC nano-fluid obtained from the Arogonne National Laboratory was diluted to 0.55%, 1% and 1.6% volume concentrations for the experiments here. Thermo-physical properties such as Thermal conductivity, viscosity, forced convection properties were measured using appropriate equipment and the details are given in this thesis.

Thermal conductivity of SiC nano-fluid was measured as a function of temperature for each nano-fluid. Thermal conductivity for all three volume concentrations of SiC nano-fluid showed an enhancement compared to the base fluid. On an average, 2.8%, 6%, and 7.5% enhancement was recorded for 0.55%, 1% and 1.6% SiC nano-fluids respectively.

ETC values obtained from experimental measurements were compared to the results of the current theoretical model (MATLAB calculations) and found to be close

to the lower bound with a deviation of 1.6%, 2.5% and 2.9% for 0.55%, 1% and 1.6% SiC volume concentration respectively.

As expected the viscosity of the nano-fluid is higher than the based fluid. Viscosity is also measured as a function of temperature and on an average, 7.9%, 14.49% and 24.37% increase was recorded for 0.55%, 1% and 1.6% SiC nano-fluids respectively.

Nusselt number was measured at different Reynolds numbers (Laminar as well as Transition regimes) and indicated no improvement for 0.55% and 1% volume concentration SiC nano-fluid and a marginal increase was observed for 1.6% SiC nano fluid. Based on the curve fitting equations obtained using the experimental Nusselt number, on an average, 0.55%, 1% 1.6% SiC nano-fluids displayed an enhancement of -3.4%, -2.3%, and +6.8% respectively when compared to its base fluid.

Heat transfer experiments showed enhancement of heat transfer coefficient at different Reynolds number for 1% and 1.6% volume concentration SiC nano-fluid and a decrease was noticed for 0.55% SiC nano-fluid compared to its base fluid. The latter could be within the uncertainty of the experiment. Based on the curve fitting equations obtained from the experimental data points, on an average, 0.55% volume concentration showed a decrease of 2.8% in heat transfer coefficient, 1% SiC nano-fluid displayed an average enhancement of 4% percent and for 1.6% volume % nano-fluid an average enhancement of 10% was observed when compared to the base fluid.
As a result of the increase in the viscosity, the pressure drop for the flow and related pumping power are increasing with the increase in the percentage of SiC nano

particles. There is an increase in average pressure drop of 6.9%, 22.8% and 38.5% for 0.55%, 1% and 1.6% volume concentrations SiC nano-fluid respectively when compared to its base fluid.

Nusselt number based 'performance factor' was evaluated for various Reynolds numbers. The performance factor is defined as the ratio of change in Nusselt number ($Nu_{nano\text{-}fluid}/Nu_{base\text{-}fluid}$) and the change in the Friction factor (friction $factor_{nanofluid}/\Delta$friction $factor_{base\text{-}fluid}$) $^{(1/3)}$. The performance factor for 0.55% SiC nano-fluids is varying between the values 0.89 and 1.08 in laminar region and the values in transition region varied from 0.92 to 0.99. The vast majority of the performance factor data was under unity for the 0.55% nano-fluid. For the 1% SiC nano-fluid there is an increase of performance factor value from 0.85 at Reynolds number 741 to 0.94 at a Reynolds number of 5915. While 1.6% volume concentration displayed a superior performance factor values in the laminar region with an average performance factor of 1.13, but the performance factor dropped under unity in the transition region.

In general, heat transfer coefficient based performance factor values tends to decrease with the increase in Reynolds number in laminar region and there is an increasing trend with Reynolds number in the transition region for all three concentrations. On the whole the performance of the nano-fluids studied here leaves much to be desired and lot more enhancements will be expected before these nano-fluids can be successful in the commercial market.

6.2. Conclusion

Theoretical Model for Effective Thermal conductivity of colloidal fluids

- Successfully able to predict Effective thermal Conductivity (ETC) based on K_p/K_f ratio and volumetric concentration solved using a MATLAB program.
- ETC is calculated based on distribution pattern of particles. Three different distribution patterns are considered in this study; pattern that gives highest enhancement possible (Upper bound), pattern that gives one of the lowest enhancements possible (Lower bound) and ETC for uniformly particle distribution.
- Particle size effect on the ETC was studied based on the proposed theoretical model.
- It is observed that the ETC was only affected by partial size when the particle size is comparable to the system size (this unlikely with nano-particles and nano-fluids). Once the particle size drops below a certain value (this value is dependents on the size of the system), the ETC tends to be constant irrespective of particle size (number of particles in the system) thereafter.
- The asymptotic value of ETC is more conveniently determined by the number of particles in the system than the radius of the particle. It is observed that the ETC becomes constant when the number of particle in the system is more than or equal to one million.
- The region where the ETC is influenced by the particle size is also the region where ETC is influenced by the dimensions of the system. It means changing

the dimensions of cuboid system would change the ETC value in this region for same volume concertation and $K_p/K_{f.}$

- To avoid this, ETC is considered only when particle number reaches 1 million or more or where ETC value reaches an asymptotic value.
- Upper and lower bounds are compared to the standard Wiener bounds and H-S bounds available in literature.

SiC Nano-fluid

- Enhancement is observed in the thermal conductivity of SiC nano-fluids over its base fluid for 0.55%, 1% and 1.6% volume concentrations.
- Thermal conductivity enhancement percentage was higher for higher volume concentration.
- Thermal conductivity was also measured as function of temperature and observed an increase in enhancement with temperature. Based on curve fit, when the temperature went up from 20 to 70 ^{o}C, the enhancement percentage increase from 2.28% to 3.96%, for 0.55% SiC nano-fluid, 4.21% to 10.22 % for 1% nano-fluid and for 1.6% enhancement percentage increased from 5.67% to 11.71%. This could be due to increased activity of Brownian motion of nano particles at higher temperature.
- Measured thermal conductivity is compared to the results obtained from theoretical derivation. It is found to be close to lower bound with an average deviation of 2.3%.

- Increase in the viscosity was observed for 0.55%, 1% and 1.6% volume concentration
- Viscosity was dependent both on volume concentration and the temperature.
- It is observed that as the particle volume concentration is increasing, there is an increase viscosity. On an average, 7.9%, 14.49% and 24.37% increase was recorded for 0.55%, 1% and 1.6% SiC nano-fluid respectively, Viscosity dependence on volume concentration is attributed to the fact that particle interaction increases with the increase in number of particles, thereby contributing to the effective viscosity of nano-fluid.
- Viscosity of nano-fluids tends to decrease with increase in temperature. This could be due to thinning of base fluid as the temperature increases.
- From the experimental values, it is observed that there is no significant enhancement of Nusselt number for 0.55% and 1% volume concentrations of SiC nano-fluids when compared to its base fluid. Enhancement is observed for 1.6% volume concentration
- On an average, 0.55%, 1% volume percent SiC nano-fluids displayed Nusselt number -3.4%, -2.3% and for 1.6% SiC nano-fluid average enhancement of +6.8% is observed than that of base fluid respectively.
- Decrease in Nusselt number for nano fluids can be explained by the fact that Nusselt number is inversely proportional to thermal conductivity and we know that thermal conductivity of nano-fluids is higher than the base fluids. Hence,

marginal increase in heat transfer coefficient would not result in any enhancement of nano-fluid.

- While enhancement of heat transfer coefficient is observed for 1% and 1.6% volume concentration SiC nano-fluid, there was marginal decrease in heat transfer coefficient value of 0.55% SiC nano-fluid than its base fluid.
- Pressure drop increases with the increase in volume concentration and this is due to increase in viscosity of higher volume concentration.
- Improvement in heat transfer properties was not very significant enough to offset the increased pumping losses.
- Based on the Performance factors considered, SiC nano-fluid with current volume concentration considered here will not have any additional advantage over its base fluid.

6.3. Suggested future work

To further enhance and expand on the modeling work presented here, results obtained from theoretical model can further be verified by solving a finite element analysis. Current model can be developed into a dynamic model where Brownian motion component can be incorporated. Since, the colloidal particles in practice are randomly distributed; it will be more realistic to develop a model for randomly distributed particles.

Though the stability of SiC nano-fluid studied here was in general acceptable for short periods of shelf life, serious consideration should be given to replace current additive Ammonium Hydroxide by other suitable bases with higher boiling points.

Forced convection study was carried out for Reynold number below 6,000 due to equipment limitations. Data for higher Reynolds numbers in the turbulent regime as well more data in Transition regime will be desirable. Higher volume concentrations of nano-particles, at least up to 5% should be studied to gage the effect of volume concentration on heat transfer properties. It would also be very interesting to study the effect of shape of the nano particles on heat transfer properties. Flat disk shaped particles are thought to have a great potential for success.

REFERENCES

1 Baby, Tessy Theres and Ramaprabhu, S., "Investigation of thermal and electrical conductivity of graphene based nanofluids," Journal of Applied Physics, 108, 124308 (2010)

2 Xiang-Qi Wang and Arun S. Mujumdar "A Review on Nanofluids - Part II : Experiments And Applications," Brazilian Journal of Chemical Engineering Vol. 25, No. 04, pp. 631 - 648, October - December, 2008

3 Ji-Hwan Lee1, Seung-Hyun Lee2, Chul Jin Choi1, Seok Pil Jang2, and Stephen U. S. Choi1, "A Review of Thermal Conductivity Data, Mechanisms and Models for Nanofluids," International Journal of Micro-Nano Scale Transport, Volume 1 · Number 4 · 2010

4 Sezer O¨ zerinc¸ • Sadık Kakac¸ • Almıla Gu¨venc¸ Yazıcıog˘lu, "Enhanced thermal conductivity of nanofluids: a state-of-the-art review," Microfluid Nanofluid (2010) 8:145–170, Springer.

5 Jing, FanLiqiu Wang, "Review of Heat Conduction in Nanofluids," Journal of Heat Transfer, April 2011, Vol. 133 / 040801-1

6 Ibrahim Palabiyik, Zenfira Musina*, Sanjeeva Witharana, Yulong Ding, "Dispersion Stability and Thermal Conductivity of Propylene Glycol-Based Nanofluids," Journal of Nanoparticle Research October 2011, Volume 13, Issue 10, pp 5049-5055

7 Todd R. Ferguson and Martin Z. Bazant, "Non-equilibrium Thermodynamics of Porous Electrodes," Journal of The Electrochemical Society, 2012, Volume 159, Issue 12, Pages A1967-A1985.

8 Bashir M. Suleiman, "Effective thermal cond1uction in composite materials," Applied Physics A, April 2010, Volume 99, Issue 1, pp 223-228.

9 Conway, J. H. and Sloane, N. J. A. Sphere Packings, Lattices, and Groups, 2nd ed. New York: Springer-Verlag, 1993.

10 Gnielinski, V., "New equations for heat and mass transfer in turbulent pipe and channel flow," International Chemical Engineering, vol. 16, pp. 359-368, 1976.

11 Shuichi TORII, “Advanced Energy Production, Exchange and Transport Technologies for Global-Warming,” International Journal of Energy Engineering (IJEE), Oct. 2013, Vol. 3 Iss. 5, PP. 202-208

12 Lap Mou Tam, Afshin J. Ghajar**, “**Transitional Heat Transfer In Plain Horizontal Tubes,” Heat Transfer Engineering, vol. 27 no. 5 2006 Page:23–38,

13 R. Lotfi , Y. Saboohi , A.M. Rashidi, “Numerical study of forced convective heat transfer of Nanofluids: Comparison of different approaches,” International Communications in Heat and Mass Transfer, 37 (2010) 74–78

14 S. W. Churchill and H. Ozoe, “Correlations for laminar forced convection with uniform heating in flow over a plate and in developing and fully developed flow in a tube,” Transactions of the ASME Journal of Heat Transfer, vol. 95, no. 1, pp. 78–84, 1973.

15 M.A.Ahmed, M.Z.Yusoff , K.C.Ng , N.H.Shuaib, “Effect of corrugation profile on the thermal–hydraulic performance of corrugated channels using CuO–water nanofluid,” Hindawi Publishing Corporation, Journal of Applied Mathematics, Volume 2012, Article ID 259284, 18 pages

16 Ramesh K. Shah and Dušan P. Sekulic, “Fundamentals of Heat Exchanger Design,”

17 Wenhua Yu, David M. France, David S. Smith, Dileep Singh, Elena V. Timofeeva, Jules L. Routbort, “Heat transfer to a silicon carbide/water nanofluid,” International Journal of Heat and Mass Transfer 52 (2009) 3606–3612

18 Elena V. Timofeeva, Wenhua Yu, David M. France, Dileep Singh, and Jules L. Routbort, “Base fluid and temperature effects on the heat transfer characteristics of SiC in ethylene glycol/H2O and H2O nanofluids,”

19 M. Khoshvaght-Aliabadi, A. Zamzamian, F. Hormozi, “Wavy Channel and Different Nanofluids Effects on Performance of Plate-Fin Heat Exchangers,” Journal Of Thermophysics And Heat Transfer, 03/2014; 28(3). DOI: 10.2514/1.T4209

20 Ibrahim Palabiyik, Zenfira Musina, Sanjeeva Witharana, Yulong Ding, Dispersion stability and thermal conductivity of propylene glycol-based nanofluids, 12 July 2011 Springer Science+Business Media B.V. 20 11

21 Ding Y, Chen H, Wang L, Yang C-Y, He Y, Yang W, Lee WP, Zhang L, Huo R (2007) Heat transfer intensification using nanofluids. KONA: Journal of Particle and Powder 25:23-38

22 Nielsen LE (1974) The thermal and electrical conductivity of two-phase systems. Ind Eng Chem Fundam 13:17–20

23 Gary L Harris , "Properties of Silicon Carbide," INSPEC, the Institution of Electrical Engineers, London, United Kingdom © 1995

24 Chapter 31 "Pysical Properties Of Secondary Coolants (Brines)," 2009 ASHRAE Handbook Fundamentals (SI)

25 Wei Li, Ping Chen, Mingyuan Gu, Yanping Jin, "Effect of TMAH on rheological behavior of SiC aqueous suspension," Journal of the European Ceramic Society 24 (2004) 3679–3684

26 Puliti G, Paolucci S, Sen M. "Nanofluids and their Properties,"ASME. Appl Mech. Rev. 2012; 64(3): 030803-030803-23 doi/; 10.1115/1.4005492.

27 Laura Fedele , Laura Colla , Sergio Bobbo1, Simona Barison and Filippo Agresti, "Experimental stability analysis of different waterbased nanofluids" Fedele et al. Nanoscale Research Letters 2011, 6:300

28 M. Chandra Sekhara Reddy, V. Vasudeva Rao, "Experimental studies on thermal conductivity of blends of ethylene glycol-water-based TiO2 nanofluids," International Communications in Heat and Mass Transfer 46 (2013) 31–36.

29 Elena V. Timofeeva, Jules L. Routbort, and Dileep Singh, "Particle shape effects on thermophysical properties of alumina nanofluids," Journal of Applied Physics 106, 014304 (2009)

30 Michael P. Beck, Yanhui Yuan, Pramod Warrier, Amyn S. Teja, "The effect of particle size on the thermal conductivity of alumina nanofluids," J Nanopart

Res (2009) 11:1129–1136.

31 M. Chopkar, S. Sudarshan, P.K. Das, And I. Manna, “Effect of Particle Size on Thermal Conductivity of Nanofluid,” Metallurgical and Materials Transactions a Volume 39a, July 2008—1535.

32 Purna Chandra Mishra, Sayantan Mukherjee, Santosh Kumar Nayak, Arabind Panda, “A brief review on viscosity of nanofluids,” Int Nano Lett (2014) 4:109–120.

33 Yurong He, Yi Jin, Haisheng Chen, Yulong Ding, Daqiang Cang, Huilin Lu, “Heat transfer and flow behaviour of aqueous suspensions of TiO2 nanoparticles (nanofluids) flowing upward through a vertical pipe,” International Journal of Heat and Mass Transfer 50 (2007) 2272–2281

34 I. Tavman, A. Turgut, M. Chirtoc, H.P. Schuchmann, S. Tavman, “Experimental investigation of viscosity and thermal conductivity of suspensions containing nanosized ceramic particles,” International Scientific Journal, Archivesof Materials Science and Engineering, Volume 34, Issue 2, December 2008, Pages 99-104.

35 J. Buongiorno “Convective Transport in Nanofluids,” Transactions of the ASME, Vol. 128, March 2006

36 P Keblinski., Phillpot, S. R., Choi S. U. S., and Eastman J. A., “Mechanisms of Heat Flow in Suspensions of Nano-Sized Particles _Nanofluids,” Int. J. Heat 2002, Mass Transfer, **45**, pp. 855–863.

37 Xiang-Qi Wang And Arun S. Mujumdar “A Review on Nano-fluids - Part I: Theoretical and Numerical Investigations,” Brazilian Journal of Chemical Engineering Vol. 25, No. 04, pp. 613 - 630, October - December, 2008

38 Hemar, Y., Lebreton, S., Xu, M., & Day, L. (2011). “Small-deformation rheology investigation of rehydrated cell wall particles-xanthan mixtures. Food Hydrocolloids,” 25(4), 668-676.

39 K. Hari Krishna, S. Neti, A. Oztekin, and S. Mohapatra “Modeling of particle agglomeration in nanofluids,” Journal of Applied Physics 117, 094304 (2015);

doi: 10.1063/1.4913874

40 Kanagala, Hari Krishna, "Modeling of Particle Agglomeration in Nanofluids" (2013). Lehigh University, Theses and Dissertations. Paper 1521.

41 YiJun Yang “Characterizations and Convective Heat Transfer Performance of Nanofluids,” Doctor of Philosophy Thesis, Lehigh University, January 2011

42 http://mathworld.wolfram.com/CirclePacking.html

VITA

Abhinay Soanker was born on April 5th, 1988 in Hyderabad, Telangana, India. He is the son of Ananda Kumar and Jaya Sree Soanker. He did his Bachelors of technology in Mechanical Engineering at Sreenidhi Institute of Science and Technology (SNIST), India and graduated in 2010. He worked with Hyundai Motors India Engineering, R&D center, India for a year and later joined SNIST as research assistant and worked on PEM Fuel cells and Nano-fluids under the guidance of Prof. V Vasudeva Rao. He currently is pursuing Masters of Science degree in Mechanical Engineering at Lehigh University en route to a PhD.